Published in final edited form as:
Chem Rev. 2012 December 12; 112(12): 6388–6430. doi:10.1021/cr300141q.

Obstructing toxin pathways by targeted pore blockage

Ekaterina M. Nestorovich[1,*] and **Sergey M. Bezrukov**[2,*]

[1]Department of Biology, The Catholic University of America, Washington, DC, U.S.A.

[2]Program in Physical Biology, Eunice Kennedy Shriver National Institute of Child Health and Human Development, National Institutes of Health, Bethesda, MD, U.S.A.

1. INTRODUCTION

The focus of this review is on the biophysical studies of the channel-forming bacterial toxins that shed light upon the mechanisms of their toxicity and propose new approaches to block their virulent action. Extensive data on the structural features of these toxins, the mechanisms of their secretion, proteolytic activation, extracellular receptors, enzymatic intracellular action, and cellular responses will be mostly omitted here. We refer our reader to several excellent specialized books and reviews that cover this material in the finest detail[1–15].

1.1. Channel-blocking and channel-forming toxins

In the course of evolution, Nature created numerous toxins, which selectively target ion channels of excitable cells[16–18]. Regardless of which version of Cleopatra's self-poisoning is true, the toxin-triggered modification of channel function was certainly involved. She either suffered from intoxication following blockage of her ligand-gated channels by the Egyptian cobra venom or from poisonous action of the chloride channel inhibitor extracted from cicuta. Numerous studies of the neurotoxins' biological functions allowed not only for deeper understanding of the structural and functional features of several channels of excitable membranes, but also for developing the pharmaceutical approaches to use these toxins for therapeutic purposes. Conversely, among the great variety of virulence factors secreted by different organisms, there is a significant group of toxins (mostly bacterial) that, *instead of blocking* channels, are able to *form ion-conductive pores* in membranes of the targeted cells. For most of them, there are no antidotes or antitoxins developed and approved for human use. At the same time, one of the possible ideas to target the bacterial exotoxins is quite simple. Following Nature, which created the channel-inhibiting toxins, it should be possible to design the potent antitoxins specifically blocking the conductive pathways of the channel-forming toxins with an ultimate goal to defend from the cytotoxic action of these agents. This idea is neither preposterous nor new. Indeed, amantadine, the small-molecule blocker of the tetrameric proton-selective M2 channel from the viral envelope of influenza A virus[19–21] had been approved for human use back in 1965. Interestingly, even though amantadine is no longer recommended by the CDC for use to treat seasonable influenza due to developed antidrug resistance, the exact mechanism of the amantadine interaction with the M2 channel is still a matter of debates[22–29]. Even so, the M2 channel is the main target for virtual screening for powerful channel blockers[30–34]. Therefore, the idea to design and develop the effective blockers of the channels formed by bacterial toxins in target membranes enjoys a well-appreciated attention. Not being able to use the evolutionary path,

[*]Address correspondence to: Sergey M. Bezrukov, Program in Physical Biology, NICHD, NIH, Bethesda, MD 20892 U.S.A.; Phone 301-402-4701, BEZRUKOS@mail.nih.gov; and Ekaterina M. Nestorovich, Department of Biology, The Catholic University of America, Washington, DC, U.S.A.; Phone 202-319-6723, NESTOROVICH@cua.edu.

we can employ the modern single-molecule biophysical approaches to study the pore-forming toxins and their potential inhibitors.

1.2. Classification of channel-forming toxins

All bacterial toxins can be divided into two functionally different groups: endotoxins and exotoxins[13]. The endotoxins are components of the outer membrane of Gram-negative bacteria (i.e. lipopolysaccharide). The exotoxins are proteins secreted by a number of Gram-positive and Gram-negative bacteria, which act on eukaryotic cells far off from the host bacterium. A crucial property of many exotoxins is their ability to exist in two states: a stable water-soluble conformation and an integral membrane pore[1]. There are several ways to classify the channel-forming proteins. The classifications are usually based on the nature of the toxin secreting organisms (e.g. clostridial toxins[14]), on the mechanism of their cytotoxicity (e.g. membrane-damaging toxins[35]; ADP-ribosylating toxins[36]), or on their structural types (e.g. α-helical and β-barrel pore-forming toxins[7, 35]). For the specific task of this review, we will use a combined structural/functional classification to discriminate between the following three groups of bacterial toxins (Figure 1).

Membrane-perforating bacterial toxins (Figure 1A)—Membrane-perforating bacterial toxins represent more than one third of the protein toxins identified so far[7, 35]. These toxins insert into target membranes and form aqueous ion-permeable pores. Subsequently, these pores can compromise the membrane barrier function and cause ion imbalance by allowing the flow of ions down their electrochemical gradient. In accordance with the mechanism of their action, they are often called the pore-forming toxins (PFT).

AB-type bacterial toxins (Figure 1B)—In contrast to the PFTs that damage the target cells membranes by forming ion-permeable pores, certain exotoxins act in the cytosol of mammalian cells enzymatically modifying specific intracellular substrates. Many of them are secreted in a so-called AB-type form, which contains at least two functionally distinct domains. The binding B-domain docks to a receptor on the surface of the target cells and mediates intracellular transport of the toxin, whereas the active/enzymatic A-domain modifies certain components in the cytosol[3].

Binary bacterial toxins (Figure 1C)—Several pathogenic species of *Bacillus* and *Clostridium* secrete binary exotoxins which consist of two (or three) individual *non-linked* proteins, an active/enzymatic A component and a binding/translocation B component[3, 13, 37, 38]. The B component of these toxins binds to a receptor on the surface of the target cells, self-assembles to form a ring-shaped oligomeric prepore able to bind the A components, and, after receptor-mediated endocytosis, is converted into an ion-conductive pore, which mediates A component translocation from acidified endosomal vesicles into the cytosol. Note that even though formally the binary toxins can be placed among the AB-type toxins, for the special purpose of this review we will describe these two groups separately.

This review aims to discuss the well-studied and/or intriguing channel-forming bacterial toxins, for which electrophysiological measurements coupled with X-ray crystallography provided important details of their structure and function. We do not intend to give comprehensive description of all membrane-perforating, AB-type, and binary toxins but prefer to focus on those examples of the channel-forming toxins that could serve as attractive candidates for the targeted design of effective channel-blocking agents.

1.3. Planar lipid bilayer technique

The planar lipid bilayer technique is a unique approach allowing incorporating purified bacterial protein toxins into artificial membranes formed across an aperture in a film (or

wall) separating two compartments (*cis* and *trans*) of a bilayer chamber (Figure 2). The alternative terms are “black lipid membrane” or “bilayer lipid membrane” (BLM) techniques. Two versions of the technique are routinely used by different groups. First, the bilayer membranes can be formed by brushing (or “painting”) a solution of lipid dissolved in an organic solvent (often in decane) across the aperture[39]. In time, a lipid bilayer membrane spontaneously forms across the aperture (for details see[40]). The second approach is often referred to as the “solvent-free” monolayer opposition technique[41]. In that case, lipid solution in an organic solvent (often in pentane) is applied on top of the bathing electrolyte solution in *cis* and *trans* compartments of the bilayer chamber. A pair of syringes is used to keep electrolyte solution level below the aperture. After pentane evaporates, lipid monolayers are formed on top of the *cis* and *trans* electrolyte solutions. The aperture is pretreated at this point with a small amount of a solution containing a less volatile component (often with 1% hexadecane in pentane) to insure better contact of the bilayer with the edges of the aperture[42]. Solution levels in the both compartments of the chamber are then raised above the aperture, and a bilayer lipid membrane forms across the aperture with both monolayers of lipid contributing. Each of the existing lipid bilayer techniques has its advantages and weaknesses. Thus, due to presence of the islets of organic solvent and larger sizes of the aperture (often 0.2–1 mm), channel incorporations is achieved easier with the brushed/painted bilayer technique. This is especially important for multichannel measurements, which often involve 100–1000 channels. On the other hand, the monolayer opposition technique allows one to minimize the membrane area by reducing the aperture size, so that a higher time resolution (e.g., 15 μs) of single-channel recordings can be often achieved. The measurements are regularly performed using specially prepared Teflon films with a diameter of the aperture not exceeding 50 μm. In many cases, these unique low-noise high-resolution conditions allow for recording of the short individual events of a single molecule metabolite and macromolecular transport across a channel reconstituted into the planar membrane. Importantly, this technique also allows formation of asymmetrical membranes in which *cis* and *trans* monolayers are formed from lipid mixtures of different compositions.

2. CHANNEL-FORMING BACTERIAL TOXINS

A unique ability of a number of bacterial toxins to exist both in a stable water-soluble conformation and in a membrane imbedded conformation allowed to perform numerous *in vitro* studies on the purified toxins. It turned out that the channel-forming toxins or their components are able to form stable ion-conductive structures in the bilayer lipid membranes lacking any extracellular receptors, which are normally required for their binding in cell assays or *in vivo*. The protein recombinant technology allowed for a large number of different mutants to be synthesized, in which the various amino acids were mutated in order to understand their possible role in the channel function. These studies not only provided the essential channels' properties, such as single channel conductance, ion selectivity, and current noise characteristics, but also allowed to reveal some interesting molecular details defining their complex behavior. One of the most fascinating examples is the binary (or tripartite) anthrax toxin where the meticulous biophysical studies yielded fine kinetics and structural details of the A component translocation through the channel formed by the B component[43–50]. Structure-based drug design approaches focused on single-channel single-molecule interactions had also allowed for designing a number of very efficient blockers, which act against several channel-forming toxins[51–62]. Moreover, a number of additional applications, which are not directly related to the toxicity of the channel-forming proteins, were developed. Perhaps one of the most notable applications involves the use of *Staphylococcus aureus* α-hemolysin channel as a sensor for different analytes[63–90].

The largest group of bacterial toxins, PFTs act at the cell surface level. They are secreted as water-soluble single proteins, which target eukaryotic cells by embedding into their cell membrane and forming large water-filled ion-permeable pores. These pores can significantly modulate one of the most important functions of the plasma membrane – its ability to maintain the membrane potential. The latter is determined by movement of ions across the cellular membrane, which is mostly regulated by a number of small highly ion-selective channels. The formation of the large and, to a certain extent, nonspecific pores results in a significant disturbance of the cell membrane integrity, which leads to a membrane depolarization due to fast inflow of Na^+ and efflux of Cl^- across cell walls[91]. Larger extraneous pores would also allow for the leakage of the intracellular macromolecules, essential for the cellular metabolic integrity, which eventually leads to cell death[91]. Structurally, the PFTs can be separated into two families: α-PFTs and β-PFTs[1, 10, 92]. α-PFTs cross the membrane as α-helices and β-PFTs as β-sheets, which form β-barrels[11]. Note that channel-forming domains or components of the bacterial AB-type or binary toxins can be also ascribed to one of these groups.

2.1. Colicins as α-helix membrane-perforating toxins

Colicins represent a class of antibiotics produced by many strains of *Escherichia coli* in times of stress. Colicins are lethal for other *E.coli* strains or closely related bacteria[93–95]. The first colicin was discovered in 1925[96] and later named "*colicine*" because its activity against *E.coli*. The host bacteria also produce small polypeptides, called immunity proteins, to defend themselves from their own toxins[95, 97]. After secretion, the water-soluble colicin molecules bind to specific outer membrane protein receptors of a target bacteria and are subsequently translocated across the outer membrane[98] into the intermembrane space using one of the two distinct bacterial transport systems, Tol or TonB[99]. Once in the periplasmic compartment, colicins cause bacterial cell death via variety of mechanisms[100–104]. Some colicins, such as colicins A, N, Ia, and E1, form pores in the cytoplasmic membranes[105], while others translocate into the cytoplasm. They degrade peptidoglycan, inhibit protein synthesis, or function as DNAse or RNAse (recently reviewed[95]). Regardless of the cytotoxic mechanism, all colicins need to insert or pass through the inner membrane of a bacterium they target[1]. Interestingly, several of them were shown to be able to mediate their own transport across the inner membrane[12, 106, 107]. Therefore, it is not surprising that different aspects of colicins' structure and function have been intensively investigated in the last decades. A comprehensive 70-page review covering all the details of this research published in 2007 contains more than 700 references[95], and the numerous papers published since then are reviewed in ref[98]. In particular, colicins were used as model systems for understanding the basic principles of protein incorporation into the lipid membranes as well as protein transmembrane transport[1, 93, 108, 109]. X-ray crystallography studies[101, 110–118] revealed a three-domain structure of the colicins with several characteristic features of the domain organization; each domain is involved in a certain step in its toxic activity such as receptor binding, translocation, and cell death[1] (Figure 3A). In pore-forming colicins, the cell death domain corresponds to a channel-forming part that is highly conserved among all pore-forming colicins. At that, no detectable sequence similarities were observed among the receptor binding and translocation domains of these molecules. This difference explains the narrow target range of each individual colicin that is usually able to bind only to specific receptors at the surface of a particular *E.coli* strain[95]. The striking similarities in amino acid sequence as well as the known crystal structures of colicin pore-forming domains suggest that all of the pore-forming colicins employ similar mechanisms of inserting into the inner membranes[95]. Interestingly, the pore-forming domains of the colicins[101, 110, 114, 118, 119] are able to embed into the bilayer membranes even in the absence of a transmembrane potential when isolated from the rest of the protein[1, 120, 121]. However, despite the fact that the structures of the pore-forming domains of colicins A, Ia, E1, N, and B were solved by

crystallography and extensively studied in bilayer lipid membranes, the mechanism of the transformation of a compact, water-soluble form of colicin into an ion channel in the inner membrane is far from being clear[95]. It is known that colicin membrane insertion is facilitated by an acidic pH, which may initiate a partial destabilization of the soluble colicin molecules resulting in rearrangement of the protein tertiary structure into a membrane-embedding configuration[1, 121, 122]. A single pore-forming colicin molecule is able to kill a bacterial cell by single-hit kinetics[1]; therefore, one molecule has to be sufficient to form a pore in the inner membrane or artificial bilayer. Formation of oligomeric transmembrane colicin pores has been also reported[123]. When inserted in the bilayer, membrane-perforating colicins form large stable voltage-gated ion pores[122] permeable to both cations and anions[124–126] and allowing for the passage of organic molecules of up to 9 Å diameter[1, 124, 127, 128]. Anomalous selectivity to protons over other cations (and anions) was reported for the pore-forming colicin A[129, 130].

Voltage-gated opening and closing of the colicin-formed pores is believed to be principally different from that of both the “classical” small ion-selective channels[94] and ion channels formed by the β-barrels[131, 132]. Gating of the classical ion channels, including many channel of excitable cells, is determined by a miniature conformational changes in the membrane spanning fragments of these channels[133]. The picture is entirely different for the voltage-gated colicin channels, where gating involves import of a large part of the protein molecule from the membrane surface. This is considered to be an essential part of their translocation across the membrane[134–136]. Structural organization and activity of pore-forming colicins (primarily of colicin Ia) were qualitatively described by Finkelstein and coworkers in a series of articles published in the last decades[129, 135–154]. Briefly, like many colicins studied so far, colicin Ia has three distinct domains: the middle receptor binding region, the N-terminal region which together with proteins on the target bacterial cells transports colicin inside the cell, and C-terminal region, which is the channel-forming domain made of 10 α-helices. All channel-forming domains carry a distinctive short hydrophobic segment near the C-terminus with 31–49 consecutive uncharged residues identified as a hydrophobic hairpin (helix 8 – helix 9, or H8–H9)[153]. The rest of the toxin is highly charged. Measurement with colicin Ia in planar lipid membranes led to an intriguing finding[135, 148]. It was demonstrated that a stretch of at least 31 amino acid residues (residues 474–541) of colicin Ia is translocated back and forth across the bilayer, which is accompanied by channel opening and closing. At the same time, residues 544–572 are moved in and out of the bilayer but not entirely across it[135, 148]. Measurements were performed in a series of experiments in planar lipid bilayers using *cis* and *trans* streptavidin trapping of biotin-labeled single-cysteine mutants of the C-terminal channel domain of colicin Ia[135]. Both the whole colicin Ia and its truncated C-domain are able to form voltage-gated ion channels with four membrane-spanning segments, all contributed by a single protein molecule[136]. At that, channel formation by colicin Ia in planar membranes was suggested to occur in several steps[153]. Once colicin is added to the *cis* side of the membrane, the hydrophobic hairpin H8–H9 inserts into the membrane in a voltage-dependent manner forming two transmembrane segments. Triggered by the positive voltage at the *cis* side, an additional part of the C-domain inserts, contributing two transmembrane segments (helices H1 and H6–H7). The helices H2–H5 are concurrently translocated across the membrane to the *trans* side (Figure 3B)[153]. This voltage-dependent insertion is recorded in the planar bilayer lipid membranes as a step-like opening of a conductive colicin Ia channel[136, 152, 153]. Interestingly, channel formation by the carboxyl-terminal colicin Ia fragment containing 345 residues is also similar to channel formation by the whole colicin or by the isolated C-domain[151, 152]. However, the portion of helix 1 is also translocated across the membrane and the channel is formed by three transmembrane segments only. The ability of the large transmembrane channel to be formed by only four (or even three) transmembrane segments created a fundamental problem in understanding the nature of the colicin Ia pore structure (see related

discussions in refs.[1, 93, 94, 153]). It is still hard to find an explanation for a paradox of forming a channel permeable for large, folded proteins (up to 26 Å in diameter) by a small protein[152]. Different models attempting to resolve this paradox either suggest that the channel wall can be partially lined by membrane lipids[155, 156] or advocate a possibility of oligomer formation[94]. Note that formation of multimeric colicin Ia channels was directly visualized recently with two-dimensional crystals of colicin Ia inserted into bilayer lipid membranes by electron crystallography[123]. However, the authors emphasize that despite their data indicate that colicin Ia channels exist as multimers, it does not imply that formation of an oligomer is required for the channel to function.

2.2. β-barrel membrane-perforating toxins

β-PFTs are secreted as water-soluble proteins that, in order to form a pore, need to oligomerize into multimeric complexes on the mammalian plasma membranes[2]. Each monomer of this oligomeric complex contributes one or two amphipathic β-hairpins to the pore thus forming a β-barrel. A hydrophobic outer surface of the β-hairpins favors insertion of these oligomeric pores into the lipid membrane[2, 92, 157]. The number of subunits composing the β-barrel can vary significantly ranging from 7 for α-hemolysin of *Staphylococcus aureus* to 50 for a family of cholesterol-dependent cytolysins. The variety in the subunit numbers results in a significant range of pore sizes[2], from 2 to 50 nm.

2.2.1. Staphylococcal toxins—Along with *Pseudomonas aeruginosa* and *Escherichia coli*, *Staphylococcus aureus* is the most frequently isolated bacteria in routine clinical laboratory hospital testing[1, 158]. In recent years, significant attention has been attracted to the toxins produced by *S. aureus* due to the wide spread of the multi-drug resistant type of the bacterium, the so-called methicillin resistant *Staphylococcus aureus*, or MRSA[159, 160], which is often associated with high mortality[161]. Among numerous virulence factors, *S. aureus* produces a number of pore-forming toxins (PFTs) that include α-hemolysin (sometimes referred as α-toxin or α-haemolysin), γ-hemolysin, and leukocidins. The cytolytic effect of these β-PFTs has been first described more than 100 years ago when the ability of Panton-Valentine leukocidin (PVL) of *S. aureus* to lyse leukocytes was demonstrated[162, 163]. The importance of each individual toxin secreted by *S. aureus* varies dramatically between different strains of the bacterium. For instance, a role of the pore-forming PVL in virulence of community associated MRSA (CA-MRSA) infection has been a subject of significant debates in recent years[159, 160, 164].

Staphylococcal α-hemolysin (α-HL) is released from bacteria as a water-soluble 293-amino acid monomeric polypeptide with molecular mass of 33 kDa. Upon binding to a cell membrane, it oligomerizes and forms heptameric complexes on the surface of a target cell[165–170]. Formation of hexameric α-hemolysin complexes has also been reported[171–173]. α-hemolysin oligomers demonstrate the ability to insert into lipid bilayers forming large water-filled pores that are slightly anion selective. Pioneering electrophysiological recordings on α-hemolysin pores in bilayer lipid membranes were reported by Krasilnikov and co-authors some thirty years ago[171, 174] followed by further intensive studies of the properties of the channel[175–180]. When inserted into a planar lipid bilayer, α-HL forms a stable channel of about 1 nS conductance in 1 M KCl at room temperature. The crystal structure of detergent-solubilized heptameric α-hemolysin has been solved to 1.9 Å resolution[167] showing a hollow 100 Å×100 Å heptamer. It was demonstrated that the heptamer has a mushroom-like shape consisting of the stem, cap, and rim domains (Fig. 1A). The stem part of the α-HL is a 14-stranded β-barrel made from 7 β-hairpins each contributed by an individual monomer. The cap, which together with the rim forms the core of the protein, is composed of a β-sandwich and has a diameter of ~ 100 Å[1]. The internal diameter of the α-HL pore ranges from ~ 6 to ~ 50 Å. Two apparent constrictions with radii

of 0.9 nm and 0.6 – 0.7 nm were reported to be present in the channel lumen, the larger one being closer to the *cis* side. Measurements were performed using an asymmetrical (one-sided) application of water-soluble polymers, polyethylene glycols (PEGs)[178] as first described in ref.[128] This approach explores the ability of polymers to partition into the channel lumen and reduce its conductance in a molecular weight-dependent way[69, 181–190], while reducing solution conductivity based only on their monomer concentration[191]. Channel dimensions and robustness determine the wide usage of this PFT in a variety of applications that are not directly related to the toxicity of this protein (see section 4).

The most interesting property of a family of *Staphylococcal* pore-forming cytolysins: γ-hemolysin (Hlg), leukocidin (Luk), and PVL is their bi-component structural organization. These toxins are formed as a result of interaction of two distinct polypeptides, so called class F component and class S component[192]. First crystal structure of a β-barrel transmembrane protein γ-hemolysin composed of two proteins was reported recently[193] (Figure 4), showing an octameric pore structure at 2.5 Å resolution. The measurements with planar lipid bilayers performed on another bi-component pore-forming octameric leukocidin, Luk showed a conductance of 2.5 nS in 1 M KCl, which is more than two-fold larger compared with that of α-hemolysin[72, 194, 195]. At the same time, the pore diameter was estimated as 28 Å indicating that geometrically an additional subunit contributes only slightly to the pore size and conductance increase[194].

2.2.2. Epsilon toxin of Clostridium perfringens—Epsilon toxin (ETX) is the major virulence factor secreted by Gram-positive, spore-forming anaerobic bacteria *Clostridium perfringens* types B and D[196]. In 2011, two excellent reviews discussing every known aspect of ETX's toxicity were published[197, 198]. ETX is responsible for a rapidly fatal enterotoxaemia in herbivores when their gastrointestinal tracts are colonized by this bacterium leading to *in situ* toxin production[14, 199, 200]. ETX is secreted in a poorly active form called prototoxin[201] and is activated into a highly potent toxin by proteolytic removal of 11 or 13 N-terminal and 29 C-terminal amino acid residues[202]. The activated ETX is one of the most potent bacterial toxins after botulinum and tetanus neurotoxins[203]; an estimated lethal human dose is 7 μg via the intravenous route[199]. Due to ETX's high potency and lethality, it has been classified as a CDC category B agent. The structure of the monomeric ETX[204] has a similarity to aerolysin, a 100-fold less potent pore-forming protein produced by the Gram-negative pathogen *Aeromonas hydrophila* (see section 2.2.3 below). ETX consists of three structural domains: N-terminal domain, which may participate in receptor binding, domain II, which is thought to contain a transmembrane stem involved in pore formation and, probably, also takes part in oligomer formation, and C-terminal domain, which likely helps to mediate ETX membrane insertion. ETX activation triggers its oligomerization in the synaptosomal membrane within the detergent-insoluble microdomains (lipid rafts) of MDCK cells[205, 206]. ETX was reported to form aerolysin-like[204] β-barrel heptameric[205–207] transmembrane pores that increase cell permeability to small molecules and ions[14, 208–210]. Surprisingly, *in vitro*, only a few cell lines such as MDCK, mouse kidney cells, and human renal leiomyoblastoma G-402 cells were found to retain susceptibility to ETX[207, 209] due to the presence of specific ETX-binding receptors. Moreover, several studies have reported that ETX was not cytotoxic for sensitive cell lines at 4°C[207, 208, 211–213]. This finding was recently extended to provide an evidence of a prepore stage in the channel formation by the ETX[213]. According to the suggested model, the toxin, when bound to an uncharacterized receptor, is first assembled into a heptameric prepore on the surface of the membrane. At 4°C, the process stops at this stage; however at 37°C, the heptameric prepore significantly changes its conformation and inserts into the membrane, forming an active pore that rapidly depolarizes the membrane[213]. The sequence of the assembly and membrane insertion steps represent one of the most significant problems in toxicology. For instance, clear evidence of prepore formation was provided for

the β-barrel channel-forming component of the anthrax toxin, PA_{63} and prepore's crystal structure was resolved[214]. However, no prepore step was identified for membrane insertion α-hemolysin, where the heptameric channel is believed to be assembled directly from the monomers inserted into the membrane.

No receptors are needed for ETX incorporation into artificial lipid bilayers[215, 216] or liposomes[217]. In bilayer lipid membranes, ETX forms wide, slightly anion-selective general diffusion pores with a single-channel conductance in the range of 440 – 640 pS in 1 M KCl[215, 216]. Based on the structural and functional similarities with oligomeric aerolysin of *Aeromonas hydrophila* and α-hemolysin of *Staphylococcus aureus*, ETX was supposed to be permeable to solutes up to a molecular mass of at least 1 kDa[215]. Recently a polymer partitioning study to access the ETX's pore functional shape and size has been conducted[58]. It was shown that PEG partitioning was highly asymmetric, as revealed by the dependence of ion current through the pore on the mode of asymmetric addition of polyethylene glycols to the membrane-bathing solutions (Figure 5). The *trans* opening of the ETX pore allowed for penetration of much larger polymer molecules than its *cis* opening (Figure 6A). Therefore, the partitioning data are suggestive of an asymmetrical, e.g., conical shape of the pore with the tentative radii of the openings of 0.4 nm and 1.0 nm on the *cis* and *trans* sides, respectively. In addition, the ionic selectivity of the ETX pore was explored by measuring reversal potentials in the oppositely directed gradients of potassium chloride aqueous solutions[58] (Figure 6B). As it was shown previously[218], such measurements allow one to judge upon the charge distribution along the channel pore. Interestingly, the asymmetry of the reversal potential in the salt gradient was found to be opposite to what is reported for the conical nanopores with a uniformly spread surface charge[219, 220]. In the case of the ETX pore, the selectivity is salted-out more easily from the wide *trans* opening of the channel. This suggests that the residues carrying the positive charge responsible for the anionic selectivity of the ETX pore[215, 216] are not localized at its *cis* opening but are shifted toward the *trans* side.

2.2.3. Aerolysin of Aeromonas hydrophila—*Aeromonads* are gram-negative bacteria frequently found in aqueous environments and mainly associated with gastrointestinal diseases[35]. Among the variety of virulent factors secreted by these bacteria, the aerolysin is one of the best-characterized pore-forming toxins. Aerolysin (for review see[221]) is produced by *Aeromonas hydrophila* as a water-soluble inactive precursor named proaerolysin, which can exist as a dimer or a monomer[92, 222]. It is known, that many toxins are synthesized by pathogenic organisms in an inactive form most likely to protect the host bacterial cells from self-destruction or to improve the efficiency of their delivery to the target cells[223]. Proaerolysin specifically binds to glycosylphosphatidylinositol-anchored receptors on the surface of target cells[224, 225]. Activation of the inactive aerolysin precursors involves proteolytic removal of a C-terminal peptide[226, 227]. The activated aerolysin then oligomerizes and incorporates into target cell membranes forming heptameric β-barrel channels. The structure of the proaerolysin was solved by X-ray crystallography at a 2.8-Å resolution[228] showing a structural similarly to the ETX monomer described above. When inserted into bilayer membranes, aerolysin makes stable, voltage-sensitive, slightly anion-selective channels[229–231]. Even though the pore structure of aerolysin heptamers is not yet well established, a statement about an α-HL-like organization of the aerolysin heptamer had been recently formulated[221]. However, the structure and effective charge of aerolysin and α-HL are significantly different (Figure 7). The electron microscopy studies of aerolysin channels demonstrated that they lack the vestibule domain[228, 232], resulting in a rivet-like model of the channel[92]. Despite anionic selectivity possessed both by aerolysin and α-HL channels, α-HL has a slightly positive global net charge ($Z = +7e$) whereas aerolysin is essentially negative ($Z = -52e$). The aerolysin pore diameter was also reported to be smaller compared with the α-HL, while their height is about the same[231, 233]. Due to the distinctive

properties of the aerolysin, this PFT had recently been suggested[232] as an alternative to α-HL, which is traditionally used as a biological nanopore sensor to study peptide translocation, peptide-pore interaction, and protein unfolding [75, 82, 234–236]. The electrical properties of the aerolysin channel in the presence of two different proteins, a wild-type maltose-binding protein (MalEwt) and its destabilized variant (MalE219), were probed in denaturing conditions in the presence of guanidium chloride[232] (Figure 8). While MalE219 is completely unfolded at 0.7 M Gdm-HCl, MalEwt required 1.5 M Gdm-HCl; at that, the aerolysin pore was proved to stay stable. After the addition of unfolded proteins, the authors detected two types of ionic current blockages with different ion current amplitudes and blockage duration. One was attributed to a situation when a protein chain diffuses close to the pore (bumping or straddling event) and another one to the protein chain transportation through the channel. The unfolded proteins were transported more slowly through the aerolysin channel compared with α-HL channel, thus making aerolysin a promising biological sensor for polymer analysis.

2.2.4. Vibrio cholerae cytolysin—Recently resolved 2.9-Å crystal structure of another member of PFTs family, heptameric[237] *Vibrio cholerae* cytolysin (VCC) boosted interest to this toxin (Figure 9)[238]. High degree of structural similarity with α-HL[167] was observed; at the same time, these two toxins display a rather weak sequence similarity (~15%). The oligomeric VCC was purified and crystallized in the presence of detergent, which allowed for determining the structure of the membrane-embedded oligomeric configuration of this toxin[238] – one of the main challenges in toxin's crystallography. Previously the same group resolved a 2.3-Å structure of the VCC water-soluble monomer[239]. As a result, VCC provides one of just a few examples of β-PFT for which both soluble and membrane-assembled structures are resolved[238, 239], which provides an excellent base for investigation of the intermediate steps of VCC oligomerization and membrane assembly[238]. X-ray crystallography revealed one interesting structural detail of the VCC pore – a narrow constriction region formed by an unexpected aromatic tryptophan W318 ring of residues within the pore that is rich in charged amino acid residues[238]. Authors compare this region with the famous phenylalanine clamp (φ-clamp) of the β-barrel PA_{63} component of anthrax toxin[240] (see section 2.4.1). However, in the case of binary toxins, such as anthrax and clostridial C2, the φ-clamp was shown to be essential in channel-mediated translocation of the enzymatic components of these toxins. So far, there is no evidence indicating that VCC serves as a transmembrane protein translocase[238]. The ability of VCC to form channels was probed with the planar lipid bilayers[241–246]. The most interesting feature observed was a superlinear dependence of the rate of VCC channel formation on the fraction of cholesterol in the both monolayers of the membrane[244, 246]. Remarkably, methyl-β-cyclodextrin (MβCD), which removes cholesterol from membranes, rapidly inhibited formation of the VCC pores, even when MβCD was added to the side opposite to VCC addition[244]. This cholesterol-dependence, however, was not observed in an earlier study[247], which may or may not be explained by the difference in the planar lipid membrane techniques used, namely, the monolayer opposition versus painted membrane techniques (see section 1.3).

Note that VCC is distinct from the main virulent factor of the human pathogen *Vibrio cholerae*, which is cholera toxin. The involvement of VCC in the pandemic of this devastating disease remains unclear[238]. However, keeping in mind that *Vibrio cholerae* is widespread in many parts of the globe and responsible for thousands of deaths every year[238, 248], it is important to focus on the secondary factors of virulence, such as the membrane-perforating toxin, VCC. It is not unusual when evolution brings bacterial toxins of secondary importance into the forefront. The binary CDT toxin secreted by hypervirulent *Clostridium difficile* pathogen is an excellent present-day example[249–253].

2.2.5. Cholesterol-dependent cytolysins—The cholesterol-dependent cytolysins (CDCs) (for review see refs.[9, 254–256]) belong to a large family of PFTs that have been identified in five different genera of Gram-positive bacteria including *Clostridium*, *Bacillus*, *Streptococcus*, *Listeria*, and *Arcanobacterium*[1, 256, 257]. Up to now, 20 members of the CDCs family have been discovered that include perfringolysin O (PFO) from *C. perfringens*, streptolysin O (SLO) from *Streptococcus pyogenes*, pneumolysin from *S. pneumonia*, and listeriolysin O (LLO) from *Listeria monocytogenes*. The so far identified CDCs share a high level of amino acid sequence homology (40–80%), which suggests a certain degree of similarity in their structural and functional properties[12, 256]. The pore-forming mechanism of the CDCs exhibits two unique features: an absolute requirement of the presence of cholesterol in a membrane and formation of very large multimeric transmembrane pores. Note that even though the rate of channel formation by *Vibrio cholerae* cytolysin (section 2.2.4) and by several other toxins in planar lipid bilayers was shown to be cholesterol-dependent, they do not belong to the CDC family of toxins. The CDC pores are currently the largest known toxin pores. CDCs associate with the cholesterol-enriched membrane domains[118,119]. It was initially suggested that cholesterol acted as a receptor for a CDC binding, however, eventually it was shown that the exact step at which cholesterol is required (cell surface binding, oligomerization or membrane insertion) can vary between CDCs[12]. Thus, perfringolysin O can indeed bind to cholesterol directly[258], however cholesterol is not a receptor for listeriolysin O and intermedilysin CDCs. Cholesterol is still required for pore formation by these two CDCs. The second hallmark CDC feature mentioned above is the ability to form extraordinary large pores. The CDC pores are composed of up to 50 monomers, though the number is somewhat variable[259] and more often ranges between 30 and 40 monomers[254], and can achieve about 480 Å in diameter[1, 12]. It is fascinating that the CDCs not only form oligomers with significantly larger number of identical subunits compared with the other β-PFTs, but also that each monomer contributes two β-hairpins to the transmembrane β-barrel channel[259, 260]. This structural arrangement leads to the unique β-barrels composed of up to 200 β-strands[261].

X-ray crystal structures of several monomeric CDCs in a water-soluble form are currently available[262–267]. As was predicted from the sequence similarity, the CDCs share a similar global structure[12]. CDCs are elongated molecules composed mostly of β-sheets and divided into 4 distinct domains where domain 3 provides the segments that form the two transmembrane β-hairpins. The numerous electron microscopy studies of CDC oligomers revealed pores of 240 to 480 Å in diameter (Figure 10)[268], that are big enough to allow the passage of large macromolecules. The pore-forming mechanism of the CDCs has been an object of intense studies and debates for the past two decades (recently reviewed in ref.[254]). The initial interaction of the CDC molecules with the membrane surface is mediated by hydrophobic loops on the tip of domain 4[269–274]. CDC membrane binding initiates changes in the monomeric CDC, leading to the formation of intermolecular contacts between different membrane-bound monomers[275]. The oligomeric complex continues to expand by incorporating multiple additional monomers up to the point when it is locked to a ring-shaped structure. This structure is usually referred to as a CDC “prepore complex” that has not yet embedded into the bilayer membrane as a β-barrel channel. Prepore to pore transition of CDC requires significant structural changes but proceeds in a cooperative and rapid manner as was visualized by electron microscopy[276]. *In vitro* electrophysiological measurements with CDCs are quite limited but those performed provide an interesting insight into the pore's physical properties[277–280]. In particular, perfringolysin O (PFO), one of the most studied members of the cholesterol-dependent cytolysin family, has been shown to form channels in planar bilayers[277]. PFO was found to increase the ion current through a lipid membrane by a number of discrete stepwise changes in current. These current steps were associated with the consecutive insertion of the large preassembled pore complexes into the bilayer. No small conductance patterns were ever recorded. At low PFO

concentrations, when only a small number of channels were present, the conductivity values did not show the insertion of small channels growing into larger channels[35]. This study allowed the authors to support one of the two existing models of the cytolysins pore formation (Figure 11), namely, oligomeric prepore to pore transition[263]*versus* a continuous growth model[281]. Electrophysiological properties of the pores formed by another member of the CDC family, pneumococcal toxin pneumolysin in the membranes of nucleated cells were evaluated using a patch clamp technique[278]. Both the wild type pneumolysin and the lytic-deficient pneumolysin mutant, W433F, were studied to investigate if the lytic deficiency correlates with the absence of pore-forming capability. In contrast to the PFO study discussed above, the authors reported that a spectrum of differently sized channels was observed both with the WT and W433F pneumolysin.

2.3. AB-type bacterial toxins

In contrast to the PFTs, a fundamental property of intracellularly active bacterial toxins, such as AB-type toxins, is that the enzymatic A domain or component has to be specifically delivered across the cell membrane into the cytosol of target cells[7]. AB toxins are secreted by a variety of bacterial pathogens in two forms. First, single-chain AB toxins can be comprised of two connected parts: part A, or an active enzymatic domain responsible for targeting the specific substrates in the cytosol, and part B, or a binding domain, which docks to certain cell surface receptors. The single-chain AB-type proteins will be reviewed in this section. The second form of AB-type toxins is represented by the binary toxins (reviewed in section 2.4) where the active and binding components are secreted as non-linked individual proteins. It is noteworthy that the B components of the binary toxins not only bind to the cell surface but also serve as receptors for the enzymatic A components. Moreover, following receptor-mediated endocytosis, B components form oligomeric transmembrane channels that facilitate translocation of the A components into cytosol of a target cell. The role of the B domain in transport of the single-chain AB-type toxins is not so obvious, namely it is not always clear if intracellular trafficking of these toxins involves formation of ion channels in target cell membranes. However, there are a number of single-chain AB-type toxins, such as botulinum neurotoxin, BoNT of *Clostridium botulinum* and diphtheria toxin, DT of *Corynebacterium diphtheriae*, for which channel formation was documented. Therefore, in this section of the review, we will focus on these two single-chain AB toxins. Investigation of the AB toxin intracellular transport is related to one of the most important problems in cell biology – understanding the mechanisms of protein transport across bilayer membranes. Insights into this process that constitutes a crucial intoxication step could provide the lacking knowledge needed for antidote/antitoxin discoveries[282].

2.3.1. Diphtheria toxins of Corynebacterium diphtheriae—Diphtheria toxin (DT) is a highly efficient toxin secreted by toxigenic strains of *Corynebacterium diphtheriae* bacterium as a single-chain protein[1, 283]. It is the major virulent factor of diphtheria. It was estimated that a single DT molecule is enough to kill a cell, which makes the diphtheria toxin one of the most toxic proteins identified[284]. DT destroys human and animal cells by inactivating elongation factor 2, EF-2, which is an essential protein of the translocation machinery[1]. As many other bacterial toxins, DT is secreted in an inactive form that needs to be activated by proteolysis to be able to cross the cellular membrane[285–287]. X-ray crystallography studies on DT demonstrated that this single-chain protein consists of three distinct domains, each domain responsible for a specific biological function (Fig. 1B)[288–294]. The N-terminal catalytic, or C-domain catalyzes the NAD^+-dependent ADP-ribosylation of EF-2, which completely shuts down protein synthesis and kills the cell[295]. The C-domain consists of both α-helices and β-sheets. The part of the protein corresponding to a fragment B of this AB-type toxin carries both the T- and R-domains[289, 296–298]. The A- and B-fragments of the DT toxin are connected by a disulfide bonds, and their reduction is

important for the C-domain transport across the membrane. The central translocational, or T-domain (entirely α-helical) mediates protein translocation across the cell membrane. The C-terminal receptor-binding, or R-domain is rich of the β-sheets, which allows it to adopt a β-barrel-like conformation. The R-domain acts as the receptor-binding domain to the toxin molecule interacting with a 20 kDa heparin-binding epidermal growth factor-like precursor hb-EGF[299]. As with many other intracellularly acting toxins, this binding triggers receptor-mediated endocytosis, the mechanism of which is not completely understood as of yet[300]. It is generally accepted, that the acidification of the early endosomes triggers the unfolding of the transmembrane translocation T-domain[283, 301, 302] followed by its incorporation into the endosomal membrane.

The precise mechanism for the catalytic domain translocation across the early endosomal membrane is still debated. The discussions mainly swing between two possible scenarios of C-domain transport. The first hypothesis suggests that the C-domain of DT is threaded through the channel by a process, which is mediated by the Cytosolic Translocation Factor complex[303, 304]. The second one assumes that the internal chaperone-like activity of the partially unfolded channel-forming T-domain facilities the transmembrane delivery of the C-domain[303, 305]. Somehow or other, it is widely accepted that the formation of the transmembrane channels by the T-domain of DT is a critical step mediating C-domain trafficking[283]. Furthermore, the transport of the catalytic domain is believed to be followed by the disulfide bond reduction (the famous “weak link” in biology) between fragments A (C-domain) and B (T- and R-domains), which leads to the release of the C-domain into the cytoplasm[283].

The first planar lipid bilayer measurements on DT channels suggested that a transmembrane pH gradient was required to facilitate C-domain transport[306–308]. The diameter of the pore was estimated to range between 18 and 22 Å. Studies with asolectin vesicles showed that no additional proteins or factors were needed for the C-domain transmembrane trafficking: DT was able to deliver its catalytic domain across the bilayer in a pH-dependent manner[309]. It is remarkable that not only the full-length toxin, but also the T-domain alone and a mutant lacking the receptor-binding R-domain were shown to form channels in planar membranes under conditions of low pH (below 6) at the side of protein addition[306, 307]. Moreover, the transmembrane channel formed by a T-domain in planar lipid bilayers was shown to be fully functional, mediating translocation of the entire catalytic domain along with about 70 residues of the N-terminus of the T-domain across the membrane (Figure 12)[305]. The study was performed using DT labeled with an N-terminal His (H6) tag in the presence of Ni^{2+} (which binds to polyhistidine) in the *trans* compartment (opposite to DT addition). Alternatively, the authors used *trans* streptavidin addition when a residue near the 6 histidines was biotinylated. Ni^{2+} or streptavidin addition inhibited the rapid closure of the DT channels. These results indicated that the H6 tag had been translocated from the *cis* to *trans* side of the membrane. Since no additional cellular components or even the R-domain of the toxin were used, this fascinating study clearly demonstrated that the T-domain contains all of the required translocation machinery. However, the autonomous *versus* the facilitated mechanisms of DT catalytic domain delivery to the cytosol are still under discussion (recently reviewed[283]). The main argument against the autonomous mechanism involves the notion regarding limitations of the planar bilayer technique, where influence of the numerous membrane-associated proteins, known to serve as mediators of endocytosis and vesicular trafficking, cannot be directly examined[283]. Still, we believe that the planar lipid membrane approach is a powerful technique, which enables direct evaluations of the intermolecular forces involved in translocation processes and interactions of proteins with small molecules and other proteins.

Indeed, several consecutive studies exploring the DT channel in planar bilayers contributed significantly to the current understanding of the catalytic domain intracellular transport[310--327]. One example includes an elegant study where a number of subunits of the T-domain of diphtheria toxin composing the channel were determined[328]. The paradigm addressed in that work dealt with the fact that the T-domain contributes only three transmembrane segments; however, the channel is permeable to ions as large as glucosamine^{+} and NAD^{-}. To determine if the T-domain can form oligomeric channels in planar membranes, mixtures of two T-domain constructs with distinct voltage-gating characteristics were tried (Figure 13). One of the constructs contained an N-terminal H6 tag that blocked the channel at positive voltages. The other one had an H6 tag at the C-terminal end. If the channels could be assembled from multiple T-domain subunits, the authors expected to see a population of single channels that are blocked both at positive and negative voltages. The possibility of oligomer formation was completely ruled out since the observed single channels were blocked at either negative or positive voltages but never at both.

2.3.2. Botulinum neurotoxin of Clostridium botulinum—Clostridial bacteria *C. botulinum* and *C. tetani* produce two very potent neurotoxins, BoNT and TeNT that cause serious neurological disorders, botulism and tetanus[2, 14]. Both toxins were reported to form similar ion channel in the planar lipid bilayer membranes. Here we focus on the better studied BoNT channels (recently reviewed[282, 329]). The BoNT is the most toxic protein identified so far, which is characterized as a category A agent by the CDC. Moreover, scientific interest to this toxin is explained by its wide use in cosmetic industry for facial esthetics[330, 331] and by the growing number of its applications in medicine[332, 333]. Just as the DT, BoNT is an AB-type single-chain protein with little proteolytic activity. It is activated to a dichain protein that is linked by a disulfide bond with AB structure-function properties[2, 334]. The N-terminal catalytic A-domain (light chain) is a ~ 50 kDa zinc metalloprotease[335]; the ~ 100 kDa C-terminal B domain (heavy chain) is made of two functional domains that are required for the receptor recognition and A-domain translocation across the endosomal membrane[2, 334]. As mentioned above, receptor-mediated endocytosis is an important step in intracellular trafficking of the AB toxins. While in cytosol, the BoNT proteases target their cytosolic SNARE (soluble NSF attachment protein receptor) substrates[336–338] that form a coil-coil, which underlies the assembly of the synaptic fusion core complex important for synaptic vesicle assembly[282]. Cleavage of the SNARE components by BoNT disrupts membrane fusion and neurotransmitter release[282]. The heavy chains of the toxins were shown to form tetramers[339] and to insert into the lipid membranes, forming cation-selective channels[340] permeable to small molecules (< 700 Da)[337]. The mechanism of BoNT translocation is still not completely understood[14]. However, the essential molecular details of the mechanism underlying BoNT translocation across endosomal membranes were obtained from single-molecule studies in planar lipid bilayers[340–348]. The nicked BoNT molecule is believed to act as a nanomachine[349–353] where the B-domain formed by the heavy-chain fragment acts as a specific protein-translocation chaperone for the light chain protease[282, 342–345, 351, 354, 355]. Translocation of the BoNT light-chain catalytic domain by the heavy chain was observed in real time using excised patches of BoNT-sensitive Neuro 2A[343, 345] neuroblastoma cells. It manifested itself by a progressive increase in membrane conductance: the channel formed by the B component of BoNT was transiently blocked by the catalytic domain and then unblocked after completion of translocation and release of the light chain fragment[282]. Maintaining the right condition, namely mimicking the pH gradient across the endosome (acidic inside and neutral in the cytosol) and inside-positive transmembrane potential was the central requirement triggering the translocation.

The suggested consequence of events underlying BoNT transport across the membrane is shown in Figure 14[282, 345]. Step 1 demonstrates free BoNT represented by its crystal

structure[351]. The catalytic light chain and translocation- and receptor-binding fragments of the heavy chain are shown in purple, orange, and red, respectively. Step 2 illustrates a schematic representation of BoNT inserted into the membrane during an event of entry where the enzymatic fragment (purple) is trapped within the channel formed by the heavy chain. A series of further steps of the light chain trafficking (3–4) and release (5) are shown. Remarkably, each step could be associated with the high-resolution real-time consecutive single channel recordings. Similarly to the DT transport, the disulfide bridge (shown in green) connecting the light and heavy chains of the toxin is stable at the low pH oxidizing environment of the *cis* compartment of the bilayer chamber that mimic the acidic endosomal pH. However, the disulfide bond is reduced by a reductant pH in the *trans* compartment (mimicking the pH of the cytosol), which promotes the release of the light chain. The authors observed the progressive stepwise increase in originally quite low single channel conductance (Fig. 14, current tracks from left to right). After the enzymatic fragment translocation is complete, the channel is free and shows a high (~66 pS) conductance value (step 5) typical for the heavy chain BoNT channel formed by the B-domain only[342, 343]. The half-time for the completion of one individual event of light chain translocation was found to be ~10 s. Numerous additional details of BoNT intracellular transport studied on a single channel level by Montal's group were recently reviewed and we address a zealous reader to these publications[282, 329].

It is clear that the planar lipid bilayer studies were able to provide an important insight into the AB toxins translocation mechanism contributing significantly to our understanding of the molecular events underlying protein-mediated protein transport. Several attempts to explore these processes using single-chained AB toxins were performed. One study reported measurements on a Pseudomonas exotoxin A secreted by *Pseudomonas aeruginosa*, where the burst-like single channel events were seen[356]. Other studies include planar lipid bilayer experiments with two major toxins of *Clostridium difficile*: Toxin A[357], and Toxin B[358]. Membrane insertion of the both toxins was shown to be facilitated by a low solution pH and in the case of Toxin A turned out to be cholesterol-dependent. Despite of the evident interaction with the lipid membrane manifested by the increased ion-current noise and membrane conductance, no well-defined conductance steps representing consequent insertion of the individual channels were recorded.

2.4. Binary toxins

Certain pathogenic species of *Bacillus* and *Clostridium* families employ a unique and refined way for targeting mammalian cells – they produce binary exotoxins, which are composed of two separate non-linked proteins, an active/enzymatic A component and a binding/translocation B component (for detailed reviews see refs.[3, 13, 37, 38]). In contrast to single-chain AB toxins, A and B components of the binary toxins are secreted as individual unbound proteins. Each component itself does not exhibit toxic effect; however, together the A and B components are cytotoxic. Note that as an exception from the rule, the binding/translocation B component of clostridial Iota toxins was shown to produce cytotoxic activity through necrosis with certain cell lines[359]. To gain access for their A components to the cytosol, all binary toxins rely on a similar cellular uptake mechanism (Figure 15). The B component of these toxins binds to a receptor on the surface of the target cells, self-assembles to form a ring-shaped oligomeric prepore (usually heptameric) able to bind the A components, and, after receptor-mediated endocytosis, is converted into an ion-conductive pore, which mediates A component translocation from acidified endosomal vesicles into the cytosol. Remarkably, the binding/translocation B components are structurally conserved between the *Bacillus* and *Clostridium* families. They share a high level of amino acid homology and numerous functional similarities [13], whereas the enzymatic A components of these toxins are quite distinct and target different cell functions.

2.4.1. Anthrax toxin of Bacillus anthracis—Recent progress made in understanding of anthrax toxin intracellular translocation is beyond any comparison. To the large extent, this was due to the well thought-out and elegant experiments performed with the planar lipid membranes, where protein translocation can be directly electrically monitored and managed, and the pH and transmembrane voltage can be precisely controlled (recently reviewed in refs.[37,50], see also the subsequent publications[46–49, 360–365]). Anthrax toxin, as a member of the bacterial AB exotoxin family, consists of three proteins that self-assemble at the surface of the cell. It is comprised of two enzymatic A components: Lethal Factor (LF), a Zn-metalloprotease that cleaves MAP kinase kinases and induces the cell death of macrophages, and Edema Factor (EF) (sometimes named Oedema Factor, or OF), which is a Ca^{2+}- and calmodulin-activated adenylyl cyclase[366–369], and one translocation/binding B-component (83 kDa Protective Antigen, or PA). Note that the name of "protective antigen" originates from its use as an active component of anthrax vaccine and does not refer to any protective properties of this protein in the course of anthrax toxin intoxication. Because instead of one A and one B component, *Bacillus anthracis* secretes three individual factors (two enzymatic and one binding), anthrax toxin, being a member of binary toxin family, is often referred to as a *tripartite* toxin. X-ray crystallography of the channel-forming B component of anthrax toxin shows that PA contains four distinct domains involved in cellular receptor binding, oligomerization, pore formation, and A component binding[214, 370]. Following proteolytic activation by a furin-like protease of the host cell[371, 372], the truncated B component, PA_{63}, forms ring-shaped oligomers, so called prepores, on the surface of eukaryotic cells or in solution (Figure 16). The population of oligomeric PA_{63} prepores for a long time was believed to be exclusively 7-fold symmetrical, or heptameric[214]; however, formation of 8-fold symmetrical, or octameric forms both in solution and on cell surfaces was recently discovered[373] and investigated[44, 364, 365]. Once assembled, the oligomeric $(PA_{63})_7$ and $(PA_{63})_8$ prepores can bind several copies of LF and EF[45, 374] and undergo endocytosis being transferred into an acidic compartment of the intracellular endosome. As discussed above, the last step is critical for the toxicity of anthrax toxin[375] as well as for several other intracellularly acting toxins. Under the acidic endosomal environment, the PA_{63} prepore endures substantial structural changes that allow it to embed into the endosomal membrane, forming an elongated mushroom-like cation-selective channel. The protein wall of the channel forms a single tunnel, a water-filled pore that connects solutions on both sides of the membrane. The mushroom-like (125 Å diameter and 70 Å long cap, and 100 Å long stem) membrane-spanning $(PA_{63})_7$ pores were seen by the negative-stain electron microscopy[376] (Fig. 1C, right). Instead of being a passive tunnel, PA then acts as an effective translocase, which, using the proton gradient across the endosomal membrane ($pH_{endosome} < pH_{cytosol}$), unfolds and translocates LF and EF into the cytosol of the target cell (Figure 17).

The peculiar molecular details of the PA_{63} channel acting as the translocase have emerged as result of its intense studies in bilayer membranes, where anthrax toxin intracellular transport was characterized as ΔpH-driven Brownian-ratchet mechanism[48, 49, 377, 378]. Briefly, LF transport across the PA channel was directly observed by monitoring the resumption of ion current, originally reduced by channel occlusion by LF, after LF was translocated[43, 44, 240, 377, 379, 380]. Moreover, the translocation of LF was proven to be initiated by entry of its N-terminus into the PA_{63} channel[380] and driven through by either transmembrane potential[379] or by proton gradient[377] across the membrane. Most importantly, the transport of LF through the PA_{63} channel, and, as a result, the anthrax toxin's toxicity was shown to be significantly suppressed by mutating phenylalanine residues at position 427[240]. In general, the seven F427 residues are believed to form a narrow constriction region inside the channel lumen (φ-clamp) that acts as a translocase active site crucial for the A components transport.

To address the fundamental question of the translocation driving force, a charge state-dependent Brownian-ratchet model was suggested[377]. The PA_{63} channel is known to be preferentially selective to cations. Therefore, acidic residues in the translocating polypeptide are expected to protonate when entering the channel to avoid being repulsed by negatively charged groups in the lumen of the channel cap[381]. Right after the protonated acidic groups reach the cytosolic part of the membrane (or *trans* side of the bilayer membrane, where higher pH value is intentionally maintained), they deprotonate becoming negatively charged again. As a result, the negatively charged LF chain, emerging from the channel into the cytosol, should be electrostatically repulsed from the cation-selective channel, which carries negatively charged residues in the lumen. The authors of the model suggest that this electrostatic repulsion in the presence of Brownian motion drives the translocation per se and enforces its directionality[50, 377]. Remarkably, recent experiments with planar lipid bilayers have imparted support to this model using semi-synthetic variant of LF_N(12–263), in which selected acidic residues were replaced with the unnatural amino acid, cysteic acid. This acid has a negatively charged side chain protonated only at pH values below the physiological range[362]. Depending on the number of acidic residues mutated, transport of these variants was either significantly suppressed or completely inhibited, whereas their binding and channel-blocking properties were comparable with those of WT LF_N. In another study, when an essentially non-titratable negatively charged SO_3^- group was introduced at most positions in LF_N, the voltage-driven LF_N translocation was drastically reduced[382].

To find out if the secondary structure of LF is preserved during the PA mediated transport, a method of trapping the polypeptide chain of a translocating protein within the channel was developed[47]. By attaching biotin to the N terminus of LF_N and using molecular stoppers at different positions, the authors determined the minimum number of residues that could traverse the channel. Streptavidin added to the *trans* side of the bilayer chamber was used as a probe. If the N terminus – stopper distance was long enough for LF_N to emerge from the channel, streptavidin was able to bind to the biotin. If the distance was not long enough, no biotin binding was recorded (Figure 18). The conclusion that the polypeptide chain can adopt a fully extended conformation as it translocates through the channel's stem was an instructive result of this elegant study. A kinetic analysis of protein transport via the PA_{63} channels, performed both in macroscopic and single-channel experiments, shows that the kinetics of channel-mediated translocation of a single LF_N protein molecule are S-shaped[49]. A simple drift-diffusion model of LF_N transport was also reported[49]. In this model, LF_N is considered as a charged rod that translocates through the channel being governed by the combined influence of random thermal motion and an applied transmembrane electrical field.

Two types of PA_{63} channels insertions with slightly different conductances were reported in several recent publications[57, 373]. The observation was explained by formation of both the heptameric and octameric channels in planar lipid membranes[44, 45, 364, 365, 373, 383]. However, the channels of lower conductance, when studied on a single-channel level, were noticed to exhibit the spontaneous reversible stepwise transitions to a substate of higher conductance (also observed in ref.[384]) that exactly corresponded to the conductance of the higher conductive channels[57]. Kinetic characteristics of blockage of these two types of channels by seven-fold positively charged cyclodextrins were indistinguishable. It is unclear if these apparent discrepancies were caused by the different PA samples used in the above studies. In addition to the two insertion types, two types of complex non-Markovian channel gating were also reported. We will discuss these features below together with the similar observations for clostridial binary toxins (see section 2.4.2). Nonelectrolyte polymers of poly-(ethylene glycol) successfully used before to determine the diameter of several channel-forming proteins incorporated into planar lipid membranes were also used to size the PA_{63}[189] giving the PEG molecular mass cutoff of ~1400 Da, which approximately

corresponds to the limiting diameter of the PA_{63} channel being less than 20 Å (Figure 19). This study is in a very close agreement with an all-atom model of the PA_{63} channel[385] (Fig. 1C, left) and with planar lipid membrane measurements where channel diameter was estimated with the tetraalkylammonium ions of different size[384, 386]. Interestingly, PEG molecules were shown to strongly interact with the channel giving a dissociation constant of 9 mM.

2.4.2. Clostridial binary toxins' B components are close analogs of the PA channel—Binary toxins secreted by a family of clostridial bacteria are closely related to anthrax toxin. They include C2 toxin of *Clostridium botulinum*, Iota toxin of *Clostridium perfringens*, CDT toxin of *Clostridium difficile* and CST toxin of *Clostridium spiroforme*, with C2 and Iota toxin showing well-defined stable ion channels when incorporated into planar bilayers. Therefore, here we will focus on these two binary toxins. In contrast to the anthrax toxin, which is a tripartite toxin formed by the two enzymatic and one binding/translocation components, clostridial C2 and Iota toxins are made of the two components only. Moreover, their A components (C2I and Ia) act through mono-ADP-ribosylation of G-actins, which causes a complete destruction of the actin cytoskeleton and caspase-dependent cell death[13, 387–395]. Just as with PA, X-ray crystallography of the B component of C2 toxin (C2II) has revealed four distinct domains involved in cellular receptor binding, oligomerization, pore formation, and A component binding[214, 370]. No crystal structure of the Iota toxin B component (Ib) is available, but there is a good reason to believe that the important structural details of PA and C2II, such as 4-domain organization, are also relevant for the Ib component. It has been shown that PA, C2II, and Ib share from 27% to 38% of amino acid homology. Remarkably, there is relatively little homology of domains 1 (A component binding) and 4 (cellular receptor binding) between PA, C2, and Ib, which is not surprising taking into account that these proteins are evolved to dock significantly different enzymatic A components and to bind to different cellular receptors. Thus, the amino acid sequence similarity of these three components is primarily localized within two central domains: domain 2, which participates in pore formation and A component translocation, and domain 3, which is important for the oligomerization of the monomers. Following proteolytic activation, the truncated B components of these toxins (C2IIa, and Ib) form ring-shaped heptamers – so called prepores on the surface of eukaryotic cells or in solution[396]. In contrast to the PA oligomer, formation of the 8-fold symmetrical C2IIa and Ib oligomers was not reported. A model structure of the $(C2IIa)_7$ prepore was constructed based on the corresponding structural assembly of the $(PA_{63})_7$ prepore[214, 370]. The cellular uptake mechanism of these two toxins is also similar to that of anthrax toxin (Fig. 15) with several distinctions reviewed elsewhere[3, 13]. Following the A component binding, the cell-bound C2I/C2IIa and Ia/Ib complexes are internalized by receptor-mediated endocytosis[397–400] and reach endosomal vesicles where C2I and Ia translocate across the endosomal membranes into the cytosol using the C2IIa and Ib pores as translocation corridors[396, 400–405]. Interestingly, *in vitro* planar bilayer measurements showed that PA_{63} is able to bind C2I, whereas C2II binds both EF and LF[406]. The authors also reported that PA, but not C2II, has the ability to transport the non-native enzymatic component into target cells, where it causes actin modification and cell rounding.

In mildly acidic conditions, the B components of C2 and Iota toxins form ion-permeable, cation-selective oligomeric channels in planar lipid membranes[401, 402, 407, 408]. It is unclear to what extend the C2IIa and Ib channels serve as the active translocase of the A components, similarly to the PA function discussed above. However, the preserved phenylalanine clamp (φ-clamp) in position 428 was found to catalyze the unfolding and translocation of the C2I component moieties across the membrane[409, 410]. The Phe residue at the corresponding position is also conserved in Ib[410], but the importance of the φ-clamp for the Iota toxin transport is not clear as of yet.

It is interesting to compare the salt concentration dependence of the PA, C2IIa, and Ib channel conductance because this dependence, together with ionic selectivity of the channel, may report on the sign and effective number of fixed charges inside the channel pore. Note that almost ideal cationic selectivity determined by the negative charges inside the PA_{63} channel lumen and, therefore, the requirements for the acidic residues of LF being protonated in order to pass through the channel, were persuasively used in the Brownian ratchet model of the PA-mediated LF transport (see discussion above)[37, 47, 48, 363, 377, 378, 382]. As shown in Figure 20A, conductances of the PA_{63} and C2IIa channels, in accordance with earlier studies[384, 401, 411], demonstrate non-linear dependence on salt concentration in the membrane-bathing solution, which is characteristic of charged pores, whereas the Ib channel exhibits close to linear behavior. The data on the reversal potential measurements for the three channels in changing KCl concentration gradients are shown in Figure 20B. Two features are clearly seen: (i) the channel cationic selectivity drops in the sequence PA_{63} < C2IIa < Ib, and (ii) all three channels exhibit similar asymmetry. The channel selectivity is "salted out"[218] more efficiently from the *trans* side of the channel, which corresponds to the neutral-pH cytosolic side. The channel selectivity is systematically smaller when the salt concentration is higher at the *trans* compartment of the reconstitution chamber. Interestingly, the ability of small molecules carrying one or two positive charges to block ion current through the PA_{63}, C2IIa, and Ib channels was shown earlier[240, 384, 386, 402, 407, 410, 411] (see section 3.2.1 below) with the equilibrium binding constants decreasing in the order PA_{63} > C2IIa >> Ib. The difference in the affinity of cationic blockers towards these channels was earlier attributed to the decreasing number of negatively charged amino acids in the lumens of these pores[407, 410]. The conductance salt dependence and selectivity measurements summarized in Fig. 20 strongly support this observation. The question that remains open is if the ΔpH-driven Brownian ratchet model is still relevant for the less cation-selective C2 and Ib toxins. Remarkably, the host cell chaperone Hsp90 and the peptidyl-prolyl *cis/trans* isomerase cyclophilin A were shown to be crucial for membrane translocation of the enzymatic components of clostridial C2, Iota, and CDT toxins but not for LF of anthrax toxin[412–415]. However, cyclophilin A and Hsp90 did facilitate translocation of the fusion protein LF_NDTA (where DTA is a catalytic domain of diphtheria toxins)[414]. These interesting observations introduce some new details in the long-lasting discussion about autonomous *versus* facilitated toxin intracellular delivery mechanisms.

The salt dependences of conductance and selectivity of PA_{63}, C2IIa, and Ib are quite different, however current noise characteristics are alike. Interestingly, the voltage-independent flickering of the channels between open and completely closed states was observed in high time-resolution recordings[57, 384, 401, 407, 416]. Typical ion currents through the three single channels, reconstituted into planar lipid membranes are presented in Figure 21. For all three channels, the flickering was described by the complex non-Markovian kinetics which are manifested by a 1/*f*-type shape of the current power spectra[57]. To the best of our knowledge, the 1/*f* fast flickering between the open and completely closed states is unique for the family of channel-forming B components of binary toxins. For instance, α-hemolysin (see section 2.2.1 of this review), which similarly to PA_{63}, C2IIa, and Ib forms heptameric channels, does not show this type of gating[417, 418] and neither do many other β-barrel pore-forming proteins.

In addition, PA_{63}, C2IIa, and Ib exhibited strong voltage-dependent gating that is observed with many β-barrel channels including artificial ones[131, 132, 419]. This type of gating is highly asymmetrical (more pronounced at *cis*-negative voltages)[420] and decreases in the order PA_{63} > C2IIa >> Ib. After the closure at negative voltages, the channels, especially PA_{63}, tended to stay in a low-conductive state for minutes, and in a number of cases reopening was not observed on a timescale of several hours even after the applied voltage

was reduced to zero. However, second-long pulses of voltages of −250 mV often made channel reopening possible. Interestingly, the voltage-dependent gating of cysteine-substituted PA_{63} channels was reported to be abolished by a reaction with a methanethiosulfonate reagent that catalyzes the formation of intersubunit disulfide bonds[421]. This perturbation was observed with cysteines substituted at sites all along the 100 Å length of the β-barrel stem region, which allowed the authors to draw a conclusion that the channel's entire β-barrel participates in the gating process. Moreover, the PA_{63} voltage gating was found to be lipid-dependent[57]. The channels were much more sensitive to the applied voltage if reconstituted in negatively charged PS membranes compared with zwitterionic PC membranes. The rate of PA_{63} channel insertions was also dramatically increased in the PS membranes.

3. INHIBITION OF CHANNEL-FORMING BACTERIAL TOXINS

Discovery and development of small-molecule antitoxins represent a high-priority task in modern drug design and medicinal chemistry[422, 423]. A number of bacterial toxins, such as BoNT of *Clostridium botulinum* can be aerosolized and directly used as biological weapons. With several bacterial diseases, such as anthrax, flu-like symptoms appear only after bacteria have multiplied inside the infected organism and started to produce the toxin that eventually causes death[424]. Even though aggressive antibiotic therapy inhibits *Bacillus anthracis* bacterium growth, patients can still die because of intoxication[425]. Moreover, engineered strains of *Bacillus anthracis* resistant to the existing antibacterial agents had been already developed[422, 426]. Besides the formation of the native toxic complexes, several binary toxins are able to cross-react interchanging their A and B components, which creates a danger of their potential misuse[406, 427].

Most importantly, a number of existing and emergent multi-drug resistant bacteria, so-called “superbugs”, such as *Pseudomonas aeruginosa*, *Clostridium difficile*, *Staphylococcus aureus*, and *Escherichia coli* secrete a variety of highly potent exotoxins with no antitoxins currently available on the market. Vaccination, clearly being one of the most significant medical achievements of 20th century, is not always available, sometimes reactogenic[428], or economically unpractical. Therefore, to combat the emergent infectious diseases and to counter a terrorist's deployment of bacteria whose pathogenicity relies upon secreted toxins, stable broad-spectrum antitoxins must be stockpiled. Small molecules are especially attractive as antitoxins, since their room temperature shelf-life far exceeds that of the current solution, antisera to toxins. We will focus here on the existing efforts to design the antitoxins counteracting the channel-forming bacterial toxins.

3.1. Role of interactions in channel-facilitated transport

Theoretical modeling of ion channels has long been recognized as an important tool in the studies of channel-facilitated transport[133]. Progress in this direction, quite substantial already, is being currently accelerated by the newly revealed three-dimensional structures of many channels. The availability of the high-resolution structures allows researchers to address and understand the structure-function relationships in channel functioning at the atomic level[429, 430]. One of the most successful approaches is all-atom molecular dynamics simulations, in which not only the molecules comprising the channel structure but also ions and water are explicitly taken into account[431–437]. Though this methodology has brought a number of important insights in ion channel functioning, in the present review, for the sake of clarity, we will restrict ourselves to a simple model of channel-facilitated transport, namely, the continuum diffusion model[438–443]. This model allows for analytical consideration of the problem, leading, in a number of cases, to simple algebraic expressions for the main transport characteristics. It does not involve any sofisticated state-of-the-art molecular dynamics simulations or complex numerical solutions of electrodiffusion

equations and, for this reason, is very transparent in what regards the assumptions and approximations used in its formulation.

Interactions between particular solute molecules and the channel that define its major transport characteristics can be separated into different types not only by the nature of the underlying physical forces but also by their functional role. Perhaps the simplest one is related to steric limitations. The straightforward sieving principle is that solute molecules, which are smaller than the narrowest aperture of the channel pore, are able to partition into the channel and use it as a pathway from one side of the membrane to the other. The molecules that are too big are excluded from either any part of the pore or its constriction region. However, in reality, even this simple picture is complicated by at least two factors: (i) the dynamic structure of some pores whose aperture dimensions fluctuate and are able to adjust to the solute size and (ii) the entropic cost of molecule partitioning into the pore. For a hypothetical case of a regular cylinder of radius R_{ch} and a spherical particle of radius r the entropic cost can be described by the following potential of mean force

$$U_{ent} = -2k_B T \ln\left(1 - r/R_{ch}\right), \quad r \le R_{ch}, \quad (1)$$

where k_B and T have their usual meaning of the Boltzmann constant and absolute temperature. To enter the channel, the particle has to climb up this potential barrier, which could be quite substantial. For example, for a molecule whose radius is 10% smaller that the radius of the channel, Eq. (1) gives a barrier height of 4.6 k_BT or 2.7 kcal/mol. Such a potential will deplete molecule concentration in the channel compared with its concentration in the bulk by two orders of magnitude, rendering the channel inefficient.

To overcome this limitation, channels exhibit a significant affinity to the molecules they evolved to transport. A straightforward strategy is to create some kind of attractive interactions that would extend to the aqueous solutions at the channel entrances to increase the effective concentration of the molecules. This kind of attraction was recently demonstrated with the major β-barrel channel of mitochondria – voltage dependent anion channel (VDAC) of the outer mitochondrial membrane – in the light of its interaction with dimeric tubulin[444]. It was shown that phosphorylation of VDAC's cytosolic loops increases the on-rate of VDAC blockage by tubulin by orders of magnitude. It is clear, however, that the strength of such transport-facilitating interactions has an optimal value. When the attraction between the molecule and the channel is too strong, the molecule stays in the channel for too long, thus blocking translocation of other molecules.

Analytical considerations of the problem in the case when the attractive interaction is limited to the channel interior was given in a series of publications based on the continuum diffusion model of particle interaction with the channel[438,439–443]. The model describes particle motion in the channel as one-dimensional diffusion with the position-dependent diffusion coefficient $D(x)$, where x is the particle coordinate measured along the channel axis, and the position-dependent interaction potential $U(x)$ of mean force. The nature of the physical forces that could be responsible for the interaction potential is briefly discussed in Section 3.2.2. Motion of the particle in the channel is characterized by the Green's function $G(x,t;x_0)$which is the probability density of finding the particle at point x at time t on condition that it was at x_0 at $t = 0$ and it has not escaped from the channel during time t. The Green's function satisfies the Smoluchowski equation

$$\frac{\partial G(x,t;x_0)}{\partial t} = \frac{\partial}{\partial x}\left\{D(x)\exp\left(-\frac{U(x)}{k_B T}\right)\frac{\partial}{\partial x}\left[\exp\left(\frac{U(x)}{k_B T}\right)G(x,t;x_0)\right]\right\} \quad (2)$$

with the initial condition $G(x,0;x_0) = \delta(x-x_0)$ and radiation boundary conditions at the cylindrical channel ends, $x = 0$ and,$x=L$ that take care of the three-dimensional nature of the problem

$$\left.\begin{array}{l} D(0)\frac{\partial}{\partial x}\left[G(x,t;x_0)\exp\left(\frac{U(x)}{k_BT}\right)\right]\Big|_{x=0}=\frac{4D_b}{\pi R_{eff}}\exp\left(\frac{U(0)}{k_BT}\right)G(0,t;x_0) \\ -D(L)\frac{\partial}{\partial x}\left[G(x,t;x_0)\exp\left(\frac{U(x)}{k_BT}\right)\right]\Big|_{x=L}=\frac{4D_b}{\pi R_{eff}}\exp\left(\frac{U(0)}{k_BT}\right)G(L,t;x_0) \end{array}\right\}, \quad (3)$$

where D_b is the particle diffusion coefficient in the bulk. Introduction of the effective pore radius, $R_{eff}=R_{ch}-r$, accounts for the entropic contribution discussed above. Analysis can be easily extended to non-cylindrical, e.g., conical channels by including the position-dependent entropic potential into $U(x)$[445, 446].

This model has been used to derive general expressions for the particle translocation probability[439],P_{tr}, and the mean time of particle residence in the channel, τ. For the case of zero external field,$U(0)=U(L)$ (Figure 22A), we have

$$P_{tr}=\frac{1}{2+\frac{4D_b}{\pi R_{eff}}\int_0^L\exp\left(\frac{U(x)}{k_BT}\right)\frac{dx}{D(x)}}. \quad (4)$$

The general expression for the mean time of particle residence in the channel can be found in refs.[440, 447]. In the case of a deep rectangular potential well of depth ΔU occupying the entire length of a cylindrical channel (Figure 22B) and a position-independent diffusion coefficient in the channel,$D(x)=D_{ch}$, the expression simplifies to the following

$$\tau_r=\frac{\pi R_{eff}L}{8D_b}\exp\left(\frac{\Delta U}{k_BT}\right). \quad (5)$$

Then, assuming that the channel occupied by one molecule is blocked for other molecules, for the unbiased diffusion we can write down the flux of molecules in a simple algebraic form[441, 442]

$$J=\frac{2D_bR_{eff}\ c_{cis}-c_{trans}}{\left[1+\frac{\pi R_{eff}^2L\ c_{cis}+c_{tr}}{2}\exp\left(\frac{\Delta U}{k_BT}\right)\right]\left[1+\frac{2D_bL}{\pi D_{ch}R_{eff}}\exp\left(-\frac{\Delta U}{k_BT}\right)\right]}. \quad (6)$$

The flux in Eq. (6) is driven by the difference in molecule concentrations on the *cis* and *trans* sides of the membrane, $c_{cis}-c_{trans}$. It is seen that the flux depends not only on the geometric parameters of the channel,R_{eff} and L, but also on the strength of the molecule-channel attraction, ΔU, and on the molecule diffusion coefficients both in the bulk and in the channel, D_b and D_{ch}. It is important that the flux is a non-monotonic function of the interaction strength. The depth of the potential well that maximizes the flux at $C_{trans}= 0$ is

$$\Delta U_{opt}=\frac{k_BT}{2}\ln\left[\frac{4D_b}{\pi^2D_{ch}R_{eff}^3C_{cis}}\right]. \quad (7)$$

This value of ΔU provides a compromise between sufficiently high translocation probability and not too long blockage of the channel, Eqs. (4) and (5).

The non-monotonic behavior of the flux is shown in Figure 23[441, 442]. The parameters are: L = 5 nm, to put it close to the thickness of a lipid bilayer, R_{eff}= 0.2 nm, to account for the fact

that many solutes exhibit a tight fit to the channel pore, and $D_b=2D_{ch}=3\times10^{-10}$ m^2/s, to follow the idea that a molecule in the channel moves slower than in bulk.

Though the analysis reviewed above pertains to translocating molecules, the results can be easily extended to the channel blockage by non-penetrating molecules. The dynamics of the molecules, whose trajectories in the channel are limited to length$_B$, can be described by assuming the reflecting boundary condition at $x=L_B$, so that the mean residence time of the molecule in the channel is twice the time given by Eq. (5) with the integration range limited to L_B. Assuming a square-well potential of depth ΔU occupying the entire blocker-accessible length of the channel, we arrive at

$$\tau_r=\frac{\pi R_{eff} L_B}{4D_b}\exp\left(\frac{\Delta U}{k_B T}\right). \quad (8)$$

The characteristic on-rate time τ_{on}, that is, the time between successive blockages, is given by

$$\tau_{on}=\frac{1}{k_{on}c}=\frac{1}{4D_b R_{eff} c}, \quad (9)$$

where c is the blocker concentration in the bulk. It is reasonable to assume that the channel is closed for translocation of any molecules of interest while it is occupied by a blocker. Then for the efficiency of blockage, defined as an inverse probability to find the channel open, $P_O=\tau_{on}/(\tau_{on}+\tau_r)$, minus one, one can write

$$\gamma=\frac{\tau_{on}+\tau_r}{\tau_{on}}-1=\pi R_{eff}^2 L_B\, c\exp\left(\frac{\Delta U}{k_B T}\right). \quad (10)$$

Defined this way, the efficiency of blockage changes from zero to infinity, grows linearly with the bulk blocker concentration, and is exponential in the well depth.

Blockage by non-translocating molecules can be considered as an equilibrium process in which distribution of the blocker molecules between the bulk and the channel is characterized by equilibrium constants and thermodynamic potentials, which generally are the functions of the transmembrane voltage, temperature, and salt concentration. The equilibrium dissociation constant of the blockage is

$$K_D=\frac{\tau_{on}c}{\tau_r}, \quad (11)$$

which, using Eqs. (8) and (9), leads to

$$\ln K_D=-\frac{\Delta U}{k_B}\frac{1}{T}+\ln\left(\frac{1}{\pi R_{eff}^2 L_B}\right). \quad (12)$$

In the hypothetical case of the temperature-independent depth of the potential well, the first term of the right-hand side of Eq. (12) allows evaluation of the enthalpy change ΔH, while the second term – of the entropy change ΔS of the reaction, according to the main equation of thermodynamic analysis of binding reactions used in the van't Hoff plots[448]

$$\ln K_D=-\frac{\Delta H}{R}\frac{1}{T}+\frac{\Delta S}{R}, \quad (13)$$

where R is the molar gas constant.

3.2. Targeting bacterial binary toxins

With the binary anthrax toxin being an exception, no extensive studies searching for effective therapies against the binary toxins have been reported. The similarities between the channel-forming B components (see section 2.4 of this review) suggest that these channels can be a specific universal target in the search for new broad-spectrum antitoxins against the *Bacillus* and *Clostridium* pathogenic species.

3.2.1. Small cationic blockers—Nearly any tested compound, which is positively charged at mildly acidic pH, was shown to interact with PA_{63} channels incorporated into planar bilayers. Moreover, cells were shown to be protected from lethal and edema toxin action by weak bases such as ammonium chloride or antimalarial drug chloroquine[375, 420, 449]. The PA_{63} channel is permeable for and interacting with symmetrical tetraalkylammonium ions (Table 1, compounds 1–6)[384, 386, 450]. The ability of tetraalkylammonium ions to reversibly block the K^+ current was used to determine the physical size of the PA_{63} channel lumen – the value that was later confirmed with several independent approaches[189, 376, 385] and used for the rational design of anthrax toxin blockers[51]. It was shown that the tetraalkylammonium binding site was accessible from either *cis* or *trans* compartments of a bilayer chamber, showing the ability of these ions to permeate through the channel. The tetraalkylammonium residence time as a function of transmembrane voltage had a pronounced maximum, which is typical for the permeable *versus* impermeable blocking compounds[451–454]. It was also determined that an ion as large as tetraheptylammonium, which has a diameter of ~12 Å, could translocate through the channel; there was an impetuous fall in the entry rate from tetrahexylammonium to tetraheptylammonium ions[420, 450]. The interaction of tetraalkylammonium ions was described as a diffusion-controlled binding reaction[450].

The ability of small molecules carrying one or two positive charges to block ion conductance through the channel-forming B components of the anthrax, C2, and Iota toxins was reported in several publications[240, 402, 407, 410, 411, 416]. Moreover, antimalarial drug chloroquine not only inhibited PA_{63} (K_D^{PA} = 0.51 μM in 0.1 M KCl) and C2IIa (K_D^{C2IIa} = 10 μM in 0.15 M KCl) channels *in vitro* but also prevented translocation of enzymatic component of C2 toxin, C2I across the cell membrane when studied with intact cultured cells. However, only a weak binding was reported for chloroquine with Iota toxin's channel forming component, Ib in planar lipid bilayers (K_D^{Ib} = 0.22 μM in 0.1 M KCl) and, correspondingly, chloroquine did not efficiently protect cells from Iota toxin intoxication[407]. Parameters of the binding kinetics of chloroquine and related compounds (Figure 24) to the PA_{63} and C2II channels were obtained from the ligand-induced current noise on a multi-channel level using the planar bilayer technique[410, 411, 416]. The measurements showed that the spectral density of the open PA_{63} and C2IIa channels in the ligand-free solutions could be described by $1/f$ noise at low frequencies not exceeding about 100 Hz. As described above, this finding was later confirmed for the single PA_{63}, C2IIa, and Ib channels (see Fig. 21), thus demonstrating that the origin of $1/f$ noise in the present systems is not related to channel-channel interactions. Rather, it is an inherent property of individual channels[455–457]. Analysis of the single-channel currents clearly shows that $1/f$ current noise of PA_{63}, C2IIa, and Ib channels is caused by voltage-independent flickering between their open and completely closed states, which was never observed with β-barrel proteins of bacterial outer membranes. It would be interesting to see if high-resolution single-channel recording of the φ-clamp mutants of PA_{63}, C2IIa, and Ib channels possess this type of fast flickering. The addition of interacting ligands led to the current noise increase with the spectral density of the Lorentzian type, characteristic of a single binding-site model[411, 416]. Strong dependence of the binding reaction on-rate, characterizing the frequency of blockage events, on the ionic strength was attributed to the involvement of ion-ion electrostatic interactions responsible

for blocker binding. At that, the reaction off-rate, characterizing the residence time of the blocker in the channel, was dependent on the structural properties of the blocker. Interestingly, binding of chloroquine both to the PA_{63} and C2IIa channels was highly asymmetrical when the ligand was added either to *cis* or *trans* side of the bilayer chamber. Addition of chloroquine to the *trans* side of the membranes resulted in a significantly diminished binding affinity. However, fluphenazine binding was quite symmetrical. Note that the insertion of the channel into the planar lipid membranes is usually highly unidirectional, so it is expected that the “cap” region of the channels (assuming a mushroom-like shape for both PA_{63} and C2IIa) faces the *cis* side solution, the side of protein addition, and the membrane-inserted β-barrel stem emerges on the *trans* side. Generally, binding affinity of the cationic compounds decreases in the order PA_{63} > C2IIa >> Ib, which was explained by a decreasing number of the binding sites formed by negatively charged amino acid residues in the *cis* entry region of these channels.

An alternative explanation of the binding of positively charged compounds to the PA_{63} pore was introduced in a study where the importance of the φ-clamp in PA_{63} translocase activity was first described[240]. A library of 35 cationic quaternary ammonium and phosphonium ion compounds was examined to compare their blocking activity towards the PA_{63} channel. Several interesting observations were made. First, mutations in the φ-clamp were shown to significantly affect binding affinity of hydrophobic cations, such as tetrabutylammonium (TBA). For instance, TBA's affinity to F427A channels was greatly reduced from that of the wild type (about 4000 times). Considering the hydrophobicity of the φ-clamp, authors hypothesized that this site may also be a binding site for the hydrophobic cations such as TBA. At that, the TBA blocking mechanism includes cation-π interactions between aromatic residues interacting with cations through their delocalized negative π-electron cloud. Second, it was shown that among the 35 compounds studied, the more hydrophobic ones possessed higher binding affinity towards the PA_{63} channel. For instance, introduction of the hydrophilic amide and ester groups to a TBA analog of a similar size, led to a 140-fold reduction in the binding affinity of this molecule (Table 1, compound 7). At the same time, the wild type PA_{63} channels preferred tetraphenylphosphonium to TBA by 160-fold (Table 1, compound 8). Across the studied library of compounds, the φ-clamp preferred aromatic moieties by 0.7 kcal/mol per aromatic ring. Table 1 (compounds 8–13) illustrates examples of the most effective (K_D < 1 μM) small cationic blockers selected from the library of tested 35 compounds (for the full data see Table S1, supplemental material in ref.[240]). Several compounds with multiple aromatic rings (3 or 4) were the ones that showed the nM-range binding affinity towards the channel. Again, this activity was reduced drastically with the F427A mutants. The authors made an interesting suggestion that the φ-clamp can be exploited in the development of channel-blocking drugs as a binding site responsible for nonspecific hydrophobic interactions, although its negative π-clouds could also contribute through aromatic-aromatic π-π and cation-π interactions.

Amino acid residues involved in binding of cationic chloroquine to the C2IIa channel were also investigated[410]. It turned out that mutation of the negatively charged amino acids leads to a dramatic decrease in their affinity for binding chloroquine and its analogs, as well as the φ-clamp mutations (F428A, F428D, F428Y, and F428W) do. Note that the φ-clamp is preserved within the C2II as F428. The authors showed that residues Glu399, Asp426 (probably localized in the vestibule near the channel entrance), and Phe428, but not Glu272, Glu280, Asp341, or Glu346 are important for biding of chloroquine and 4-aminoquinolones, which act as C2IIa channel blockers. However the F428A mutation effect was the strongest, increasing K_D values by a factor of almost 400, which emphasized once again the important role of the φ-clamp in binding of cationic compounds.

3.2.2. Cationic cyclodextrin derivatives—A substantial progress in disabling anthrax lethal toxin by the high-affinity blockage of the PA_{63} pore with cationic molecules was achieved using a rational drug design approach[51]. The idea was to block the oligomeric pore by a low-molecular non-peptide compound of the same symmetry as the target pore. In particular, it was shown that tailor-made 7-fold symmetrical 7-positively charged derivatives of β-cyclodextrin (7+ βCD) blocked the pore of anthrax's PA_{63} in planar bilayers (K_D = 0.13 ± 0.1 nM) and protected cultured macrophage-like cells from intoxication with anthrax lethal toxin (PA + LF) (IC_{50} = 0.5 ± 0.2 μM)[52, 62]. As far as we are aware, these blockage and inhibition parameters are the best among the published data for the small-molecule blockers. Moreover, the most effective 7+βCD, per-6-S-(3-aminomethyl)benzylthio-β-cyclodextrin (AMBnTβCD) completely protected Fisher F344 rats from intoxication with lethal toxin and, in combination with the antibiotic ciprofloxacin, significantly increased the survival of mice in an infection model of anthrax[56]. These findings demonstrate a value of the 7+βCD as a potential scaffold for designing drugs against anthrax toxins, especially when an appropriate lead optimization and pharmacokinetic studies are conducted. Interestingly, about 2/3 of over 100 custom-synthesized 7+βCD compounds were protective against the lethal toxins with cell assays and nearly all tested so far showed strong or moderate channel blocking in planar lipid membranes. This finding once again showed an advantage of the rational drug design approach over the traditional time- and money-consuming high-throughput screening of libraries of thousands of compounds, which often produces a hit rate lower than 1%.

The idea to use 7+βCD cationic derivatives as inhibitors of anthrax was based on the wealth of earlier research[51]. First, as described in the Introduction, the high-affinity blockage of transmembrane channels formed by infectious agents with the anti-influenza M2 channel-blocking drug amantadine is the most prominent example[19–21, 28]. Second, in the particular case of heptameric pores, it was shown that the pore of β-barrel PFT α-hemolysin of *S. aureus* (see section 2.2.1) can be partially blocked by β-cyclodextrins[65]. Third, the positively charged tetraalkylammonium ions were reported to block PA_{63} channels[384, 386, 450] interacting with the negative charges on the channel walls. Finally, the PA_{63} prepore internal diameter was estimated to be between 20 – 35 Å[214] with the channel's constriction region not exceeding 12 Å[384, 386, 450]. These findings guided the choice of the ~15 Å βCD molecule carrying seven positive charges covalently linked to a cyclodextrin's core by a hydrocarbon links of the different length and nature (Figure 25A). From the point of view of medicinal chemistry, it is important to emphasize that cyclodextrins, a cyclic oligomers of glucose that can form water-soluble inclusion complexes with small molecules and portions of large molecules, have a long history of usage in pharmaceutical, agrochemical, environmental, cosmetic, and food industries[458]. The cyclodextrins do not elicit immune response and have low toxicity in animals and humans. There are thousands of variations of the CDs with different ring sizes and random or specific chemical modifications; as a result, reliable methods for cyclodextrin syntheses and selective modifications have been developed[459].

Several 7-positively charged βCD derivatives as candidate antitoxins were custom-synthesized[53] and tested[51] (see Figure 25B for two examples). As Figure 25C shows, the addition of per-6-(3-aminopropylthio)- β-cyclodextrin (AmPrβCD, Fig. 25B, left) to the *cis* side of a membrane containing about 60 PA_{63} channels in 0.1 M KCl inhibits the ion channel activity in a step-like manner with a step amplitude of 87 ± 13 pS. This amplitude coincides with the PA_{63} single-channel conductance in 0.1 M KCl, implying that AmPrβCD acts on individual channels[51]. To identify more potent inhibitors of anthrax toxin compared with the reported AmPrβCD, the effect of the positively charged pendant groups and the length and nature of alkyl spacers on the activity of βCDs was estimated[52, 60, 62] (Table 2). β-cyclodextrin is a naturally occurring cyclooligosaccharide containing seven α-(1,4)-D-

glucopyranose subunits linked through α-(1,4) glucosidic bonds[460]. The primary (C-6) and secondary (C-2 and C-3) hydroxyl groups may be used as points of functionalization. The hydroxyl groups at positions 2 and 3 form hydrogen bonds and are required to keep the molecule rigid, making the 6-OH group a favorable site for modifications. First, a group of hepta-6-thioaminoalkyl derivatives with alkyl spacers of various lengths was tested for their ability to inhibit the cytotoxicity of lethal toxin and to block ion conductance through PA_{63} channels in planar lipid membranes (Table 2, compounds 1–11). From a combination of measurements with planar lipid membranes and cell assays, it was shown that there is some optimal length of the alkyl spacers (3–8 CH_2-linkers) connecting an amino-group with the cyclodextrin core. Shorter spacers were less effective in inhibition of the channels and longer ones exhibited higher toxicity to the RAW cells, which was probably related to derivative-induced instability of the membranes observed in the bilayer measurements[52]. In order to check if the nature of the positively charged groups carried by the βCDs is an important factor in compound's efficiency, a group of hepta-6-guanidine β-cyclodextrin derivatives, in which positive charges were distributed between the nitrogens of the guanidine moiety was tested (Table 2, compounds 11, 12). The activity of these compounds was slightly decreased compared to their aminoalkyl analogs. Remarkably, hepta-6-arylamine βCD derivatives, which in addition to the pendant positively charged amino-groups contained one phenyl group carried by each thio-hydrocarbon linker, possessed significantly enhanced binding affinity both *in vitro* and with cell assays. One of the derivatives, per-6-S-(3-aminomethyl)benzylthio-β-cyclodextrin (AMBnTβCD) was chosen for the further development. In most of the experiments performed on planar membranes either AmPrβCD (Fig. 25B, left and Table 2, compound 3) or AMBnTβCD (Fig. 25B, right and Table 2, compound 13) or both were used as model molecules to study physico-chemical parameters of the blockage.

It was shown that in addition to inhibition of anthrax toxin, cationic β-cyclodextrin derivatives were also effective against clostridial binary toxins. In particular, AMBnTβCD efficiently protected cultured epithelial cells from intoxication with two clostridial binary toxins (C2 and Iota) and blocked the ion current through heptameric channels formed by C2IIa and Ib in planar lipid membranes *in vitro*[61]. The compound acted by inhibiting the membrane translocation of C2 and Iota toxin A components (C2I and Ia) into the cytosol of intact cultured cells showing that it might serve as a universal pharmacological inhibitor against binary pore-forming toxins produced by pathogenic bacteria. To examine the nature of the physical forces involved in the blocker interactions, the voltage and salt dependence of the rate constants of binding and dissociation reactions for the two structurally different β-cyclodextrins (AmPrβCD and AMBnTβCD) (Fig. 25B) and the PA_{63}, C2IIa, and Ib channels were recently investigated (submitted to Biophysical Journal). It turned out that with all three channels, AMBnTβCD, carrying extra hydrophobic aromatic groups on the thio-alkyl linkers of positively charged amino groups, showed significantly stronger binding compared with AmPrβCD. This finding is in a good agreement with the data reported earlier on a group of positively charged blockers. The blocking efficiency directly correlated with the number of aromatic groups carried by the molecules[240] (section 3.2.1). The effect of increased affinity of the AMBnTβCD blocker to the channel is manifested by an increase in the residence time of the blocker in the channels, whereas the time between blockages (Figure 26A), which characterizes the binding reaction on-rate, stays practically unchanged. This result indicated that the capture rate of the blocker molecules by the channels did not significantly depend on the chemical structure of the blocker and probably was only determined by the relative size of the blocker and the channel. However, the time the blocker spends in the channel is significantly influenced by the structural changes in the blocker molecule.

Interestingly, the voltage sensitivity turned out to be practically the same for all six cases studied. The logarithm of the blocker residence time plotted as a function of transmembrane voltage, Figure 26B, displays practically identical slopes for both blockers and all three channels. Note that in contrast to tetraalkylammonium studies[384, 386, 450], the residence times as functions of voltage lack any maxima, the circumstance that was used as a proof of the "blockage without translocation" mechanism of ion channel inhibiting[57]. It was also shown that the more effective AMBnTβCD blocker demonstrates weaker salt dependence of the binding and dissociation rate constants compared with AmPrβCD. Moreover, PA_{63} channel behavior was explored under conditions in which the blocker was added only to the *trans* side of the membrane[57]. Since the insertion of PA_{63} is always directional, the *cis* side application of the blocker is the physiologically relevant one. The *trans* addition was shown to irreversibly bring the channel to a low-conductance sub-state. This may indicate that the blocker is able to enter the channel from either side, but binds to different sets of amino acid residues without translocating through.

At moderate and low salts, the dependence of blockers' residence times on KCl concentration (Figure 26C) revealed the contribution of long-range Coulomb interactions. Particularly, at physiological salts, these interactions increase the binding efficiency by orders of magnitude. At salt concentrations lower than 0.5 M, the AmPrβCD residence time increases in the order Ib < C2IIa < PA_{63} (Fig. 26C), and so does the cationic selectivity of the channels (Fig. 20B). This pattern is Ib ≈ C2IIa < PA_{63} for the AMBnTβCD binding. The difference in the affinity of positively charged blockers towards the PA_{63}, C2IIa, and Ib channels was earlier attributed to the different number of negatively charged amino acids on the lumen of these pores[407, 410, 411]. The preservation of the affinity pattern for the 7+βCD binding may indicate that the positive charges of the βCD blockers interact with the negatively charged amino acids in the channel lumen. At high salt concentrations, interpolation of the residence time to zero voltage allowed for an estimation of the salt-concentration-independent short-range interactions which predominate in all six cases studied.

In the case of the more effective AMBnTβCD blocker, its binding to the PA_{63}, C2IIa, and Ib pores is further enhanced by the presence of the aromatic groups presumably interacting with a certain conserved group of residues (for instance with the φ-clamp[240]) in the lumen of these channels. Alternatively, the presence of aromatic groups could change the conformation of the linkers creating additional stabilizing interactions. The blocker's pharmacophoric pattern (three-dimensional arrangements of the several functional groups) is most probably involved in a number of Coulomb and salt-concentration-independent short-range interactions acting simultaneously within a single binding pocket of the channels. Clearly, the strong short-range interactions, added to the relatively weak Coulomb ones, determine enhanced affinity of the AMBnTβCD compound towards the Ib channel as well as the inhibitory properties of this compound against Iota toxin in cell assays[61].

To summarize, analysis of voltage- and salt-dependence of the blockage demonstrated that even though both long-range Coulomb forces and interactions of the blocker charge with the transmembrane field are able to significantly increase the residence time of the blocker in the channel, the leading interactions are determined by salt-concentration-independent short-range forces for both AmPrβCD and AMBnTβCD blockers. As for the particular origin of these forces, the answer to this question will require further experimental and theoretical effort. Many factors complicate quantitative interpretation of blocker-channel interactions. Among them are the hydration state of the blocker molecule[461], a sophisticated interplay between the hydrophobic effects and different electrostatic components, as, for example, in the case of polyamines binding to kainate subtype glutamate receptor channels[462], and the uncertainties in the interaction-induced changes in the blocker and channel structures. At

this moment, guided by the structural features of the efficient cyclodextrin-based blockers of Table 2, we can only speculate that in addition to hydrophobic interactions many others such as aromatic-aromatic π-π and cation-π interactions, hydrogen bonding, van der Waals interactions, etc. might be involved. We hope that careful Monte-Carlo and molecular dynamics simulations and multi-scale modeling combined with the results of existing and future experiments will shed light on the relative importance of different contributions.

The analysis given above accounts only for the reversible blockage obeying a two-state Markov process. It was also reported that the presence of blockers enhanced voltage gating (described in section 2.4.2) of these channels by making their closed state more favorable[57]. The closed state of the channel possessed the characteristic properties of a typical voltage-induced closed state of a β-barrel channel. For instance, it was hard to reopen the channel by keeping it at 0 mV, but application of −250 mV pulses often allowed channel reopening. Among the studied channels, the blocker-enhanced gating was minimal for Ib and maximal for PA_{63}. Moreover, with all three channels studied, the voltage gating increase was more obvious with the more effective AMBnTβCD blocker. Thus with measurements on multi-channel membranes, which did not discriminate between the two modes of action, for AMBnTβCD this resulted in IC_{50} = (0.13 ± 0.1) nM for PA_{63}, IC_{50} = (1.5 ± 0.5) nM for C2IIa, and IC_{50} = (23 ± 10) nM for Ib channels in “physiological” 0.1 M KCl at +20 mV of applied voltage. For the reason that the very nature of the voltage gating of β-barrel channels remains vague, it is unclear to what extent this second type of 7+βCD action could influence the blocker activity *in vivo*.

Finally, it was demonstrated that even though the 7-fold symmetry of the blocker molecules complementing heptameric structure of binary toxins' translocation components was important, it was not an absolute requirement for the effective blockage. Both 6-fold symmetrical αCD carrying 6 positive charges and 8-fold symmetrical γCD carrying 8 positive charges were able to block the PA_{63} channel in planar lipid membranes[62] (Table 2, compounds 14–17). Note that 6- and 8-fold symmetrical compounds 14 and 15 are analogs of the 7-fold symmetrical compound 1, whereas compounds 16 and 17 are αCD and γCD analogs of the AMBnTβCD (compound 13). The activity of the 8+γCDs tested with cell assays was equal or even higher compared with their 7+βCD analogs, whereas binding of 6+αCD was not strong enough to make these compounds protective against anthrax toxin. Supposedly, the pronounced activity of the 8-fold symmetrical γCDs could be related to the recently reported observation of PA_{63} octameric pores[373]: however, both positively charged βCDs and γCDs were able to block any single PA_{63} channel incorporated into the planar lipid bilayers. The cyclodextrin molecules serve as ring-shaped platforms carrying multiple positive charges and aromatic groups that are able to interact with hydrophobic and negatively charged groups provided by the seven subunits of the PA_{63} channel. The less active derivative of αCD contributes only six substituents to the blocker-channel binding reaction. Moreover, its 13.7 Å external diameter compared to the 15.3 Å βCD diameter may not be large enough to allow for the strong interactions with the residues located in the channel lumen. The situation is different for the 8+γCDs, the compounds showing similar activity as their 7+βCDs analogs. The external diameter of γCD is 16.9 Å, which may limit the flexibility of the blocker inside the channel. However, the presence of an additional linker carrying the functional groups may increase the resultant strength of the channel-blocker interactions. Recently, several new groups of potential βCD-based inhibitors differing in the number, arrangement, and face location of the cationic elements were reported and tested using cell assays (Table 2, compounds 18–29)[60]. The results indicated that the development of new blocking agents couldn't rely exclusively on the symmetry and the putative electrostatic interactions. First of all, the cationic compounds synthesized based upon the symmetry complementarity concept alone did not provide an increased affinity towards the PA_{63} pore[60]. Second, introduction of additional positive charges (14+βCD) did

not lead to more potent compounds (IC_{50} > 100 μM), however significantly increased their cytotoxicity (compounds # 19, 21, 23, 27)[60]. Interestingly, several derivatives, where positively charged groups were introduced in the (C-2) and (C-3) positions of the each α-(1,4)-d-glucopyranose subunit, turned out to be highly efficient as antitoxin agents (Table 2, compounds 28, 29).

In contrast to the cyclodextrin-based neutral derivatives interacting with the α-HL pores in planar lipid bilayers[65], reversible blockages of the binary toxins' translocation components by cationic cyclodextrins were always complete, that is, they showed fluctuations between the current of the open state and zero. In the case of α-HL, the residual conductance that was observed in the reconstitution experiments was explained by the ability of ions to pass through the cyclodextrin cavity. This is obviously not the case for the blockage of the PA_{63}, C2IIa, and Ib pores by the cationic CD derivatives. It is not clear what the reason for such a difference is. One tentative explanation would be that, in contrast to the α-HL – cyclodextrin complex, the cationic cyclodextrins are oriented in the channel in a way that prevents the ionic flow through their internal cavity. There is however no real evidence that would support this explanation.

3.2.3. Other agents against anthrax toxin—The current situation, when a vaccine is not available to the general public and only a limited number of antibiotics are approved by the FDA for the treatment of inhalational anthrax, had stimulated intense search for potent and selective antitoxins (see resent reviews)[463, 464]. Most of the efforts are focused on neutralizing and inhibiting the different basic steps in a multi-stage cell journey of the lethal and edema anthrax toxins (Fig. 15). In addition to the small molecule blockers directly obstructing the translocation channel-forming component of the toxin reviewed above, the therapies under development include employing toxin-neutralizing antibodies[465–470], receptor decoy-based antitoxins[471, 472], blockers of PA cleavage and oligomerization[473], and inhibitors of LF and EF association with the PA_{63} prepore[422, 474]. Several interesting approaches utilize targeting of the channel-forming component of the anthrax toxin by means other than occluding it. PA as a potential target for the antitoxin therapy can be inhibited in a number of ways; several promising anti-PA strategies had been reviewed recently[463, 464, 475, 476]. For instance, a polyvalent peptide inhibitor that binds to the PA prepore preventing its interaction with LF has been reported[477]. The screening of a phage display library of mutant peptides able to interact with the heptameric component of anthrax toxin revealed a novel peptide that can block toxin assembly[478]. A series of mutant peptides were attached to polymer backbones to estimate their *in vitro* inhibitory activity. This approach allowed for identification of a minimal peptide sequence, TYWWLD, that can be used in developing of polyvalent anthrax toxin inhibitors. PA oligomer formation was shown to be inhibited by the one of the most effective chemotherapeutic anticancer agent, cisplatin that modifies PA in a reversible manner[479]. Dominant-negative mutants of protective antigen that co-assemble with the wild-type PA_{63} protein and block its ability to translocate the LF and EF components have also been developed[474, 480–482]. Interestingly, a single dominant-negative subunit with the key amino acid residues mutated was sufficient to block the translocase function of the PA_{63} heptamers. Moreover, dominant negative mutants of anthrax toxin potentially can be used both as an anthrax vaccine and in therapy[463]. In another study, the mouse monoclonal anti-PA antibody 1G3 was demonstrated to severely perturb the receptor-bound heptameric PA_{63} complex creating a PA supercomplex, which was directly visualized by electron microscopy[483]. *De novo* computer-aided drug design of small molecule inhibitors of the PA heptamerization had been recently reported[484]. Two molecular scaffolds were first identified using the CAVEAT molecular design package, and then seven candidate inhibitors were synthesized based on the discovered scaffolds and tested for their ability to inhibit anthrax toxin. Three of the designed agents demonstrated modest inhibition of the anthrax toxin in murine J774A.1 macrophage cells.

3.2.4. Polyvalent inhibitors of anthrax toxin—The idea of attaching multiple interacting ligands onto a suitable scaffold, similarly to the one realized with cyclodextrin-based molecules carrying 7 functional group clusters[51, 52] or with the peptide-based inhibitors[477, 478, 485], seems to be very helpful for the drug design objectives. These multi-ligand structures often possess an affinity toward multiple binding sites or receptors that is significantly higher than that of a single functional group interacting with a single receptor (recently reviewed in refs.[486, 487]). Different strategies exploring this approach had been suggested[488–497]. The first strategy is based on neutralization of PA_{63} heptameric complexes by peptide-functionalized liposomes of ~50 nm in size (Figure 27)[489]. The liposomes were allowed to interact with a cysteine-derivatized version of a heptameric PA_{63} binding peptide[477], which acts by inhibiting lethal factor binding. Remarkably, peptide-functionalized liposomes inhibited the intoxication of murine macrophage RAW264.7 cells by the lethal toxins at extremely low concentrations (IC_{50} = 20 nM on a per-peptide basis), whereas the monovalent peptide did not inhibit lethal toxin activity at concentrations as high as 250 μM. Moreover, the peptide-functionalized liposomes were active *in vivo* protecting rats from the lethal toxin intoxication. Because several liposome-based drug formulations had already received an approval as vaccines adjuvants[498] and the nanoparticles for drug delivery[499–501], liposome-based scaffolds represent a promising application in search for polyvalent inhibitors including antitoxins. Furthermore, the liposome-based inhibitor study[489] also indicated the several important aspects of the biophysics of polyvalent recognition, such as the influence of the density of the ligand and the membrane fluidity and heterogeneity on polyvalent inhibition (reviewed in ref.[486]).

Another strategy used guided synthesis of polyvalent inhibitors of the controlled molecular weight and ligand density and placement along an inert polymeric scaffold[491, 495]. Such control was achieved by using reversible addition-fragmentation chain transfer polymerization (so called RAFT technique)[493–495]. The advantage of designing polyvalent inhibitors with the control over molecular weight and ligand spacing is illustrated in Figure 28. It is seen that the spacing between peptides on the inert linear framework is either too short (left panel) or is sufficient (right panel) to allow for polyvalent inhibitors to bind at the peptide-binding sites of the PA_{63} heptamer[495].

In rational drug design of polyvalent inhibitors, once a biospecific ligand is identified, the next important step is a search for a suitable and inert scaffold to attach the ligands[486]. Recently, the idea about advantage of matching the symmetry of the target with the symmetry of the interacting polyvalent molecule[51] was developed further with β-cyclodextrin chosen as the core for the inhibitor scaffold[497] (Figure 29). However, in contrast to the previous βCD-based studies, where the substituents consisted of positively charged groups linked to the core via hydrocarbon and aromatic linkers, seven copies of inhibitory peptide were linked to the cyclodextrin scaffold via polyethylene glycol linkers. A linker length was manipulated to insure an optimal fit of the polyvalent inhibitor to the heptameric PA_{63}. The important objective of the study was to design the effective polyvalent ligands by matching the pattern of binding sites on the heptameric PA_{63}. To achieve this goal, experimental mutagenic studies were accompanied by computational docking experiments searching for a suitable binding site for the inhibitory peptide on the heptameric component. The root-mean square distance from the center of cyclodextrin core to the end of the PEG_{11} linker was estimated as 30 Å, which matched the distance from the center of the PA_{63} oligomer to the identified peptide-binding residues. Note that unlike in the previous studies on cyclodextrin-based blockers, in this application the heptavalent inhibitors were designed to target lethal factor binding sites on the PA_{63} complex rather than to block the channel translocation pathway[497]. Again, the idea of a 7-fold symmetrical functional group placement allowed reaching the IC_{50} values as low as 10 nM on a per-peptide basis *in vitro* by incubating RAW264.7 cells with lethal toxin. Most importantly, the

heptameric inhibitor provided a more than 100,000-fold increase in the activity compared with the monomeric peptide. At the same time, it did not show any major decline in activity over a three-day period and was also effective *in vivo* protecting rats from intoxication by the lethal toxin.

To summarize, several studies to design PA-based anthrax toxin inhibitors showed the value of polyvalent interactions. These cooperative interactions can be significantly stronger than the corresponding monovalent interactions of the same ligands[486]. The examples include potent biospecific peptide-based or small-molecule ligands (or functional groups) attached to a variety of scaffolds formed by the liposomes[489], polymers[491] or cyclodextrins[51, 52, 497]. Note that the idea of using the polyvalent interactions was also explored in the design of potent inhibitors for other bacterial toxins[502–506].

Meanwhile a thermodynamic analysis of multivalent interactions aiming to clarify the theoretical basis for the large enhancement in avidity as a result of multivalency had been recently published[507]. In particular, the author investigates the influence of a linker – the structural element that connects the binding fragments with the inert scaffold – on the activity of a resulting multivalent compound to address the existing controversy about the extent to which the loss of conformational entropy of the linker may influence the increase in binding. The simple thermodynamic analysis of a heterodivalent ligand-receptor interaction demonstrated that even if the loss in conformational entropy of the linker on binding is extremely unfavorable, the dependence of the free energy of multivalent binding on linker length can still be weak[507]. Most importantly, the predicted weak dependence of the free energy is consistent with other studies showing that flexible linkers of different length can be successfully used to design effective multivalent inhibitors.

3.3. Targeting membrane-perforating bacterial toxins

Surprisingly, the number of molecules under development that specifically target the pore-forming toxins is relatively low. At the same time, experimental studies of these toxins, particularly in the planar lipid bilayers, are significantly simplified by the fact that PFT's biological action is based on permeabilization of the target cell membranes. As a result, the complex multi-stage transport of enzymatic domains and components described above does not apply to these toxins. For this reason, their disabling could simply imply a physical obstruction of the “virulent” ion conductive pores formed by these toxins as opposed to the more elaborate approaches to either single-chain AB (diphtheria toxin and botulinum neurotoxins) or binary (anthrax) toxins.

3.3.1. Small molecule blockers of α–hemolysin and epsilon toxins—Currently used approaches to prevent the toxic effects of α–hemolysin and epsilon toxin include polyclonal and monoclonal antibodies[508–517]. Several compounds were shown to inhibit α–HL production[518, 519]. Dominant-negative inhibitors of ETX were also reported[520]. However, the studies searching for small-molecule channel-blocking inhibitors are very limited.

As described above (section 2.2.1), α–HL is a heptameric pore-forming cytotoxin secreted by gram-positive *S. aureus* bacterium, which is essential in the pathogenesis of pneumonia[521]. The high-resolution crystal structure of the membrane form of α–HL (Fig. 1A) revealed a mushroom-like heptameric channel with a radius changing from 7 Å to 23 Å in the cap diameter and about 100 Å in the total height[167]. Recently, the idea of enhancing the blocking ability of compounds by having the same symmetry as the target pore was extended to the design of βCD-based inhibitors of α–HL[55]. Interestingly, several unsubstituted cyclodextrins were earlier used as molecular adapters docking into the β-barrel of the α–HL[65, 522]. The approach allowed designing a new hepta-6-substituted β-

cyclodextrin derivative, named IB201 (compound 31, Table 2), which was able to protect rabbit red blood cells from α–HL-induced hemolysis in the low micromolar range[55], prevented α–HL-mediated alveolar epithelial cell lysis and mortality associated with *S. aureus* pneumonia in a murine model of infection[59]. IB201 was assayed for its ability to block ion conductance through the pores formed in artificial membranes by α–HL[55]. In contrast to 7+βCD binding to the PA_{63}, the α–HL interaction with IB201 was irreversible within the limit of the time period of the experiment. Addition of this compound caused the channel to switch to a weakly conductive sub-state (Figure 30). The residual conductance of the closed state was between 1% and 15% of the open channel conductance and displayed a current noise typical for the voltage-gated closed state seen commonly with α–HL at high voltages. Thus, introduction of positive charges to the cyclodextrin molecule led to its ability to block this anion-selective channel from the physiologically relevant *cis* side, not from the *trans* side as in the case of molecular adapters[65, 522]. Since only a very limited number of compounds from the available library of 7+βCDs acted similarly to IB201, it is unclear what particular interactions are involved in the α–HL blocking. Remarkably, in contrast to PA_{63}, α–HL was selectively blocked only by β-cyclodextrin derivatives, whereas αCDs and γCDs carrying the same substituents groups were not effective with cells assays and showed no interaction with the channel in planar membranes[62] (Table 2, compounds 30–32).

A different approach was used to search for the small-molecule inhibitors of epsilon toxin. A cell-based high-throughput screening of a 151,616-compound library led to identification of three compounds inhibiting ETX[523]. Those were N-cycloalkylbenzamide, furo[2,3-b]quinoline, and 6H- anthra[1,9-cd]isoxazol. It appeared that none of these three compounds inhibited ETX cell binding or oligomerization, making the authors to suggest that they might act by blocking the ETX pores.

3.4. Blockage of ion-selective channels of neurophysiology: a comparison

It is interesting to compare the affinity of the blockers of the channel-forming toxins discussed above with a wealth of data on the blockage of ion-selective channels of neurophysiology. The well-being of a multi-cellular organism involves significant coordination of the functions of many organs, which, in its own turn, relies on efficient transmission of information between the various cells in different parts of the body. In vertebrates, transduction of electrical signals and the corresponding calcium transients are the major mechanisms of processing information in the brain and environment sensing. They are also responsible for delivering signals from the brain to peripheral organs including controlling muscle contraction and release of hormones. Unsurprisingly, the ion-selective channels of neurophysiology, which are vital for the information transfer function, represent the most extensively studied membrane proteins, in both functional and structural aspect[133].

Impressive advances in the structure-inspired design of new drugs that modulate properties of the ion-selective channels are reviewed in a number of recent instructive publications[524–535], which discuss a variety of blockers and activators of different channel species. Most of the modulators discovered up to date are used as versatile research tools, but quite a remarkable number have found their way into pharmacology for treating a broad spectrum of diseases such as epilepsy, chronic pain, cardiac arrhythmia, ischemia, memory disorders, hypertension, type 2 diabetes, and many others. For example, in the case of potassium channels, the effect of the blocker is to increase cell excitability, which may facilitate signal transduction. On the contrary, channel activation leads to a decreased excitability, which could help in certain disorders. In the light of the present review, we are mostly interested in the channel blockers. Moreover, among the modulators of different nature we will restrict ourselves to the non-peptide “small-molecule” blockers only.

The comprehensive list of available IC_{50} values for blockers of potassium, sodium, and calcium channels is quite lengthy, even if restricted to non-peptide compounds. Because of this, in Table 3 we give only representative examples of the blockers, which, however, are intended to include the most efficient ones. It is seen that the IC_{50} values for the small-molecule blockers of ion-selective channels of neurophysiology are higher than that for compound #13 interaction with the anthrax PA_{63} channel (Table 2), characterized by IC_{50} = 0.13 ± 0.10 nM. The hepta-6-arylamine β-cyclodextrin derivative has nearly an order-of-magnitude stronger affinity to the PA_{63} channel than the most potent small-molecule blockers in Table 3 to their corresponding channels with only one exception of UCL1684 interaction with the calcium-activated potassium channel $K_{Ca}2.2$, which is characterized by about the same affinity.

4. DOUBLE LIFE OF CHANNEL-FORMING BACTERIAL TOXINS

Unique intrinsic properties inherent to the channel-forming bacterial toxins, such as their ability to respond to electrical, chemical, or mechanical stimuli[536], were utilized in several nanobiotechnological applications (recently reviewed in ref.[537]). The potential applications range from molecular sensing and detection, DNA sequencing, monitoring chemical and biochemical reactions, and development of biocompatible nanotransistors to drug delivery and targeted killing of cancer cells[537]. It is remarkable that most applications are not necessarily based on toxic pathways these pores are involved in, but rather benefit from their unique electrical properties. These applications truly bring about “second life” for these biological toxins, where genetic engineering and covalent attachments or non-covalent adapters are often used to generate desired novel features.

4.1. Bacterial toxins as biosensors

Without any doubt, of all the PFTs, α-hemolysin of *S. aureus*, suggested to serve as a “nanoscopic cuvette” to study reaction dynamics some 20 years ago[417, 418], is an absolute leader in this field. The crystal structure of this heptameric pore resolved more than 15 years ago,[167] as well as its ability to form large stable ion channels in bilayers[174, 538] contributed to the wide usage of this toxin in the various biotechnological applications under development. Wild type or genetically engineered α-HL serves as a molecular sensor for the detection of ionic species and organic molecules including divalent metal ion[64, 539], phosphate anions[73], trinitrotoluene[74], styryl dyes[87], proteins[78, 81, 90] and nitrogen mustards, which are chemical warfare agents[80].

In another remarkable application, β-cyclodextrin-based molecular adapters were shown to reversibly interact with the β-barrel of the α-HL channel[65, 522, 540]. As a result, modification of the channel by βCD created a binding site for a number of small organic molecules. Transient formation of the host-guest complexes of small organic compounds with the cyclodextrin (Figure 31) by embedding into its internal cavity could be registered through conductance fluctuations. In particular, the α-HL channel – βCD complex allowed for stochastic sensing of adamantane derivatives and other small therapeutic molecules[65, 541]. This approach also allowed studying the changes in preferential solvation during association reactions at the singe-molecule level[542, 543]. Cyclodextrin adapters within the modified α-HL pores were used to discriminate between the *S*- and *R*-enantiomers of the ibuprofen and thalidomide drug molecules[77]. The enantiomers of these small chiral molecules generated distinctly different current signals upon their reversible binding to the α-HL-βCD complex. Keeping in mind that thalidomide, which is responsible for one of the most tragic medical failures of the 20th century, is now brought back to market for the treatment of leprosy and certain types of cancer[544], the ability to rapidly distinguish between the chiral forms of the drug molecules is very important. Note that teratogenic and antitumor properties of this compound are sometimes attributed to the thalidomide *S*-enantiomer[545]. Novel α-HL-βCD

based adapter systems with the asymmetrical cavity have been suggested recently[88]. Besides, α-HL was engineered to accommodate two different cyclodextrin molecules (βCD and hepta-6-sulfato βCD) simultaneously at the different binding sites[541]. As a result, the space between these adapters formed a nanocavity able to trap organic molecules, which shuttled back and forth between the adapters for hundreds of milliseconds.

Figure 32 illustrates the use of the cyclodextrin-based molecular adapters to study the dynamic aspects of the Hofmeister effect[542]. The thermodynamic and kinetic parameters of the adamantane binding to a cyclodextrin molecule residing in the β-barrel of the α-HL channel were explored as functions of addition of different salts to the initial membrane-bathing solution of 1.0 M KCl (or NaCl). The linearity of the changes in the free energy of the adamantane-cyclodextrin complexation with solution osmolarity (Fig. 32B) allowed the authors to characterize the reaction by a constant preferential hydration coefficient Δn_{water}, shown in the uppermost Table on the right. Similar formal procedure was applied to describe the sensitivity of the kinetic parameters to the added salts (Figs. 32C, D). It was found that not only the off-rate, characterized by the residence time of adamantane in cyclodextrin (τ_r), but also the on-rate, characterized by the times between consecutive complexations when channel is open (τ_o), are changed by salt addition. The change in the on-rate induced by KBr is small and might be well within the measurement error, but the effect of KCl and, especially, of Na_2SO_4 is clear. Thus, the change in the free energy of the complexation is due to both the change in the complex stability, as quantified by the off-rate, and the change in the accessibility of the complexation site, as quantified by the on-rate.

Sensing with biological nanopores was also exploited to detect the DNA and RNA biopolymers with an ultimate goal of ultrafast sequencing (reviewed in refs.[536, 537, 546–550]). Since first electrical recording of polynucleotides passing through the α-HL pore were pioneered more than 15 years ago[63], this application had been significantly advanced[66–68, 70, 71, 76, 79, 83–85, 89, 551–555] mostly focusing on overcoming serious challenges related to the ability of α-HL (and other biological and engineered nanopores) to detect current signals generated by individual nucleotides. While α-HL undoubtedly bears the palm, pore-forming bacterial toxin aerolysin of *Aeromonas hydrophila* (see section 2.2.3 of this review) and heptameric channel-forming component of anthrax toxin, PA_{63} had been suggested for use as molecular biosensors[232, 234, 556]. The use of biological nanopores as molecular biosensors has been challenged by the emergent technology of synthetic solid-state nanopores, including the first demonstration of DNA sensing[557] (recently reviewed in ref.[536, 549]). At the same time, biological nanopores, including bacterial toxins, bring several important advantages to the biosensing field. Among those is an atomic level of similarity between individual molecules of the same protein that often can be investigated with X-ray crystallography. Besides, modern genetic tools, such as site-directed mutagenesis, allow for specific modification of physico-chemical properties of the channel-forming proteins. On the other hand, the lipid bilayers are mechanically less stable compared to the solid-state nanopores. An interesting new approach that combines the advantages of two techniques (so called “hybrid biological-solid state nanopores) suggested incorporating a genetically engineered α-HL channel into a small nanopore fabricated within a thin SiN membrane [85].

4.2. Bacterial toxins for cancer treatment

Many existing cancer therapies have significant limitations because of the side effects on the fast-growing healthy cells. Several therapeutic agents, which specifically target cancer cells, are under development[558]. One of the novel emergent approaches involves the application of channel-forming bacterial toxins, rationally modified to selectively destroy cancer cells (reviewed in refs.[537, 559]). The later can be achieved by either genetic engineering or chemical modification of the bacterial toxins to provide these proteins with the cell-selective

ligands or domains allowing them to effectively recognize certain membrane receptors or antigens that are typically overexpressed by malignant cells[560]. For this reason, many bacterial toxins for cancer cell targeting were designed as the fusion proteins composed of several parts with different functions. In a way, AB-type bacterial toxins are naturally made "fusion" proteins, where membrane binding domain translocates enzymatic domain into the cytosol. The same idea is exploited with the engineered "tailor-made" fusion therapeutic proteins[13], where the cell specificity of one fragment can be successfully combined with the toxicity of another. Naturally, the mechanism of self-mediated delivery of the foreign proteins into the cytosol of mammalian cells is sometimes compared with the famous Trojan Horse[5, 13]. There are several strategies to generate fusion proteins, also termed "chimeras" (recently reviewed in refs.[13, 561–565]). One approach presumes integration of the enzymatic and binding components of different bacterial toxins, which allows for generation of the novel fusion proteins with a desired property being enhanced. The very first fusion protein that effectively destroyed cancer cells was generated from diphtheria toxins of *Corynebacterium diphtheriae* and exotoxin A of *Pseudomonas aeruginosa*[566]. Alternative (and often less toxic to the healthy cells) approach involves substitution of toxin's binding and/or enzymatic domains with eukaryotic proteins. Thus, the B-domain is intended to be replaced by a specific cell-binding protein that selectively targets the malignant cells only. Alternatively, specific antibodies are sometimes fused into the A-domains creating the chimeras referred as "immunotoxins"[562, 563, 565]. In several studies, epidermal growth factors or interleukin 2 as binding domains were conjugated with diphtheria toxin; a number of these chimeras are very effective for the treatment of hematopoietic malignancies[567–570].

A series of interesting anthrax fusion toxins for targeting cancer or intracellular delivery of macromolecules were generated[571–574, 574–577]. Clostridial binary ADP-ribosylating toxins, which share many structural and functional similarities with the anthrax toxin (mostly at the stages of their cell binding and intracellular trafficking), represent another ideal system for transporting foreign molecules into the cell (recently reviewed in ref.[13]). In particular, the chimera toxin, based on the clostridial C2 toxin delivery system and enzymatic activity of C3 transferase from *C. limosum*, $C2I_{1–255}$-C3lim + C2IIa, effectively delivers the C3 transferase into all targeted vertebrate cells, making this chimeric toxin 300-fold more active compared to C3lim transferase alone[578, 579]. Moreover, the binary Iota toxin of *C. perfringens* was also used to transport the *C. botulinum* C3 enzyme[580]. Besides AB and binary toxins, PFTs are also considered as functional components of the chimeric toxins. For instance, certain mutations of the pore-forming α-HL made this protein sensitive to activation by the tumor-specific protease, cathepsin B, which triggered the pore formation selectively in the cancer cells[581]. Recently, aerolysin of *Aeromonas hydrophila* was coupled as an inactive precursor of this protein to a peptide that could be cleaved by a prostate cancer cells protease[582].

Detailed description of various chimeric toxins made of the enzymatic, binding, or channel-forming domains or components of bacterial toxins is beyond the scope of this review. The additional applications not mentioned above include targeted drug delivery, for instance to generate protective antiviral immunity[583–585]. Besides biomedical applications, chimeric proteins are of significant scientific interest, for instance the clostridial C2 toxin fused with the virulence factor SpvB of *Salmonella enterica*, $C2I_{1–255}$ − C/SpvB is used to study the consequences of actin-ADP-ribosylation by SpvB in mammalian cells[36, 564, 586, 587].

5. CONCLUDING REMARKS

For the last several decades, the structure-inspired drug design has been successfully used to develop small-molecule modulators of classical ion-selective channels of neurophysiology[524–535]. The emerging structural details of potassium, sodium, chloride, and

various ligand-gated channels are crucially important in the virtual screening of molecular libraries and creating new compounds. Relatively recently[51], the structure-inspired drug design was extended to include the pores of “virulence” – those of the channel-forming bacterial toxins. The newly synthesized compounds, which mimic the symmetry of the pores and are complementary to their structures in charge, size, and hydrophobicity, are quite effective in channel-blocking activity; by the potency (Table 2) several of these compounds compare well with the blockers of classical channels of electrophysiology (Table 3).

At the same time, the general approach to the development of efficient blockers of toxin pores is considerably different. Indeed, while one of the main goals of designing blockers of ion-selective channels of excitable cells is to achieve high specificity, with only one type of the channels targeted, the toxin pore blockers are expected to be universal. The first successful steps in the search for such wide-spectrum blockers have been reported recently in a study where cationic βCD-based compounds were shown to be protective against the cytotoxicity induced by the anthrax, C2, and Iota toxins[61]. The universality requirement is easy to appreciate, because a potent wide-spectrum antidote would be expected to be active against a number of different toxic agents. In the search for such a compound, researchers rely on the knowledge of the structure and function of bacterial toxins, focusing on the mechanisms of those shared intoxication steps that could be directionally targeted. For instance, formation of the β-barrel transmembrane pores by the membrane-perforating (section 2.2 and 3.3) and binary toxins (section 2.4 and 3.2) can be considered as a targetable universal property. On the other hand, such an ideal antidote is expected to be harmless against mammalian channels, including the β-barrel voltage dependent anion channel (VDAC)[588–590] of the outer mitochondrial membrane, based on the fundamental differences in their structural organization. According to numerous studies, VDAC is a wide monomeric channel[591], which does not possess the symmetry features characteristic of the oligomeric toxin channels discussed above. VDAC's functional properties can be modulated by a number of factors, including the membrane lipid composition and cytosolic proteins[444, 592–596], but the effect of the cyclodextrin blockers on VDAC is negligible (Philip Gurnev, private communication). This leaves us with a hope that the inhibitive action of the advanced, wide-spectrum antidotes of the future will be mostly limited to toxin channels, thus paving the way for the eventual use of these drugs in clinical settings.

Acknowledgments

EMN research is supported by startup funds from The Catholic University of America. SMB research is supported by the Intramural Research Program of the NIH, *Eunice Kennedy Shriver* National Institute of Child Health and Human Development.

Biographies

Nestorovich's Biosketch: Ekaterina M. Nestorovich earned her Ph.D. in electrochemistry from St. Petersburg State University, Russia under supervision of Prof. Valery Malev. She performed a postdoctoral research in biophysics with Dr. Sergey Bezrukov at the National Institutes of Health. While at the NIH, she mastered the art of ion channel reconstitution into

planar lipid bilayers (the models of biological membranes) and modern methods of statistical analysis of ionic currents – powerful tools which allowed her to study kinetic and transport properties of channel-forming proteins at the single-molecule level. In January 2011, she joined the faculty in the Department of Biology at The Catholic University of America as Assistant Professor of the new Biotechnology program. Her teaching interests include Biotechnology Project Managements and Rational Drug Design. She also holds a professional certificate in Advanced Project Management from Stanford University. The direction of her research is best described as medical biotechnology and biophysics. From the biomedical science perspective, she searches for novel effective approaches to make good use of ion-conducting nanostructures in a variety of medical, chemical, and biotechnological applications. From the biophysical perspective, she pursues a new level of understanding of biological structures through the physical forces that animate them. By learning the physics and chemistry of biological structures' functioning, Dr. Nestorovich strives to determine how to design new agents that effectively correct the deviant interactions associated with diseases.

Bezrukov's Biosketch: Sergey M. Bezrukov is a Senior Investigator and chief of the Section on Molecular Transport, Program in Physical Biology, NICHD/NIH, a position he has held since October 2002. In order to address fundamental questions of membrane transport, Dr. Bezrukov's section combines physical theory with experiments on bacterial, mitochondrial, and toxin-induced membrane channels, reconstituted in planar lipid bilayers. This line of research serves as the basis for the development of new approaches to treatment of many diseases where regulation of transport through ion channels plays the key role. Dr. Bezrukov received his M.S. in Physics from St. Petersburg Polytechnic University, Russia, Ph.D. in Biophysics from Moscow State University, and D.Sci. in Condensed Matter Physics from the St. Petersburg Nuclear Physics Institute of the Russian Academy of Sciences. He started his career as a researcher in Russia and moved to United States in 1990, first as a visiting research professor at the University of Maryland. In 1992, he joined the National Institutes of Health as a visiting scientist. He was awarded NIH tenure in 2002. Dr. Bezrukov has authored numerous scientific papers, five of them published in Nature (London). He has organized and chaired many international meetings and workshops. Dr. Bezrukov's recent honors include election to Fellowship in the American Physical Society (2009), the NIH Director's Award in Science and Medicine (2010), and appointment to the Senior Biomedical Researcher Service (2011).

References

(1). Parker MW, Feil SC. Prog. Biophys. Mol. Biol. 2005; 88:91. [PubMed: 15561302]

(2). Henkel JS, Baldwin MR, Barbieri JT. EXS. 2010; 100:1. [PubMed: 20358680]

(3). Barth H, Aktories K, Popoff MR, Stiles BG. Microbiol. Mol. Biol. Rev. 2004; 68:373. [PubMed: 15353562]

(4). Menetrey J, Gillet D, Menez A. Toxicon. 2005; 45:129. [PubMed: 15626361]

(5). Trujillo C, Ratts R, Tamayo A, Harrison R, Murphy JR. Neurotox Res. 2006; 9:63. [PubMed: 16785102]

(6). Rádis-BaptistaI G, Kerkis A, Prieto-Silva A, Hayashi M, Kerkis I, Yamane T. J. Braz. Chem. Soc. 2008; 19:221.

(7). Geny B, Popoff MR. Biol. Cell. 2006; 98:667. [PubMed: 17042742]

(8). Gilbert RJ. Cell Mol. Life Sci. 2002; 59:832. [PubMed: 12088283]

(9). Gilbert RJ. Adv. Exp. Med. Biol. 2010; 677:56. [PubMed: 20687480]

(10). Gouaux E. Curr. Opin. Struct. Biol. 1997; 7:566. [PubMed: 9266180]

(11). Gonzalez MR, Bischofberger M, Pernot L, van der Goot FG, Freche B. Cell Mol. Life Sci. 2008; 65:493. [PubMed: 17989920]

(12). Iacovache I, van der Goot FG, Pernot L. Biochim. Biophys. Acta. 2008; 1778:1611. [PubMed: 18298943]

(13). Barth H, Stiles BG. Curr. Med. Chem. 2008; 15:459. [PubMed: 18289001]

(14). Popoff MR, Bouvet P. Future Microbiol. 2009; 4:1021. [PubMed: 19824793]

(15). Alouf, JE.; Popoff, MR., editors. Bacterial Protein Toxins. Third Edition. Academic Press; San-Diego, California: 2006.

(16). Karalliedde L. Br. J. Anaesth. 1995; 74:319. [PubMed: 7718380]

(17). Mouhat S, Jouirou B, Mosbah A, De Waard M, Sabatier JM. Biochem. J. 2004; 378:717. [PubMed: 14674883]

(18). Dutertre S, Lewis RJ. J. Biol. Chem. 2010; 285:13315. [PubMed: 20189991]

(19). Sugrue RJ, Hay AJ. Virology. 1991; 180:617. [PubMed: 1989386]

(20). Pinto LH, Holsinger LJ, Lamb RA. Cell. 1992; 69:517. [PubMed: 1374685]

(21). Wang C, Takeuchi K, Pinto LH, Lamb RA. J. Virol. 1993; 67:5585. [PubMed: 7688826]

(22). Leonov H, Astrahan P, Krugliak M, Arkin IT. J. Am. Chem. Soc. 2011; 133:9903. [PubMed: 21534619]

(23). Pielak RM, Chou JJ. Protein Cell. 2010; 1:246. [PubMed: 21203971]

(24). Rosenberg MR, Casarotto MG. Proc. Natl. Acad. Sci. U. S. A. 2010; 107:13866. [PubMed: 20643947]

(25). Boltz DA, Aldridge JRJ, Webster RG, Govorkova EA. Drugs. 2010; 70:1349. [PubMed: 20614944]

(26). Kozakov D, Chuang GY, Beglov D, Vajda S. Trends Biochem. Sci. 2010; 35:471. [PubMed: 20382026]

(27). Cady SD, Schmidt-Rohr K, Wang J, Soto CS, DeGrado WF, Hong M. Nature. 2010; 463:689. [PubMed: 20130653]

(28). Chuang GY, Kozakov D, Brenke R, Beglov D, Guarnieri F, Vajda S. Biophys. J. 2009; 97:2846. [PubMed: 19917240]

(29). Balannik V, Carnevale V, Fiorin G, Levine BG, Lamb RA, Klein ML, DeGrado WF, Pinto LH. Biochemistry. 2010; 49:696. [PubMed: 20028125]

(30). Tran L, Choi SB, Al-Najjar BO, Yusuf M, Wahab HA, Le L. Molecules. 2011; 16:10227. [PubMed: 22158591]

(31). Wang J, Ma C, Fiorin G, Carnevale V, Wang T, Hu F, Lamb RA, Pinto LH, Hong M, Klein ML, DeGrado WF. J. Am. Chem. Soc. 2011; 133:12834. [PubMed: 21744829]

(32). Du QS, Huang RB, Wang SQ, Chou KC. PLoS One. 2010; 5:e9388. [PubMed: 20186344]

(33). Duque MD, Ma C, Torres E, Wang J, Naesens L, Juarez-Jimenez J, Camps P, Luque FJ, DeGrado WF, Lamb RA, Pinto LH, Vazquez S. J. Med. Chem. 2011; 54:2646. [PubMed: 21466220]

(34). Balannik V, Wang J, Ohigashi Y, Jing X, Magavern E, Lamb RA, DeGrado WF, Pinto LH. Biochemistry. 2009; 48:11872. [PubMed: 19905033]

(35). Van der Goot, G., editor. Pore-forming toxins. Berlin Heidelberg New York. Springer - Verlag; 2001. p. 168

(36). Aktories K, Lang AE, Schwan C, Mannherz HG. FEBS J. 2011; 278:4526. [PubMed: 21466657]

(37). Collier RJ. Mol. Aspects Med. 2009; 30:413. [PubMed: 19563824]

(38). Sakurai J, Nagahama M, Oda M, Tsuge H, Kobayashi K. Toxins (Basel). 2009; 1:208. [PubMed: 22069542]

(39). Mueller P, Rudin DO, Tien HT, Wescott WC. Nature. 1962; 194:979. [PubMed: 14476933]
(40). White SH. Biophys. J. 1972; 12:432. [PubMed: 5019479]
(41). Montal M, Mueller P. Proc. Natl. Acad. Sci. U. S. A. 1972; 69:3561. [PubMed: 4509315]
(42). White SH, Petersen DC, Simon S, Yafuso M. Biophys. J. 1976; 16:481. [PubMed: 1276378]
(43). Thoren KL, Worden EJ, Yassif JM, Krantz BA. Proc. Natl. Acad. Sci. U. S. A. 2009; 106:21555. [PubMed: 19926859]
(44). Feld GK, Thoren KL, Kintzer AF, Sterling HJ, Tang II, Greenberg SG, Williams ER, Krantz BA. Nat. Struct. Mol. Biol. 2010; 17:1383. [PubMed: 21037566]
(45). Kintzer AF, Sterling HJ, Tang II, Williams ER, Krantz BA. PLoS One. 2010; 5:e13888. [PubMed: 21079738]
(46). Blaustein RO. J. Gen. Physiol. 2011; 137:337. [PubMed: 21402885]
(47). Basilio D, Jennings-Antipov LD, Jakes KS, Finkelstein A. J. Gen. Physiol. 2011; 137:343. [PubMed: 21402886]
(48). Brown MJ, Thoren KL, Krantz BA. J. Biol. Chem. 2011; 286:23189. [PubMed: 21507946]
(49). Basilio D, Kienker PK, Briggs SW, Finkelstein A. J. Gen. Physiol. 2011; 137:521. [PubMed: 21624946]
(50). Thoren KL, Krantz BA. Mol. Microbiol. 2011; 80:588. [PubMed: 21443527]
(51). Karginov VA, Nestorovich EM, Moayeri M, Leppla SH, Bezrukov SM. Proc. Natl. Acad. Sci. U. S. A. 2005; 102:15075. [PubMed: 16214885]
(52). Karginov VA, Nestorovich EM, Yohannes A, Robinson TM, Fahmi NE, Schmidtmann F, Hecht SM, Bezrukov SM. Antimicrob. Agents Chemother. 2006; 50:3740. [PubMed: 16982795]
(53). Karginov VA, Yohannes A, Robinson TM, Fahmi NE, Alibek K, Hecht SM. Bioorg. Med. Chem. 2006; 14:33. [PubMed: 16169738]
(54). Backer MV, Patel V, Jehning BT, Claffey KP, Karginov VA, Backer JM. Antimicrob. Agents Chemother. 2007; 51:245. [PubMed: 17074791]
(55). Karginov VA, Nestorovich EM, Schmidtmann F, Robinson TM, Yohannes A, Fahmi NE, Bezrukov SM, Hecht SM. Bioorg. Med. Chem. 2007; 15:5424. [PubMed: 17572091]
(56). Moayeri M, Robinson TM, Leppla SH, Karginov VA. Antimicrob. Agents Chemother. 2008; 52:2239. [PubMed: 18378717]
(57). Nestorovich EM, Karginov VA, Berezhkovskii AM, Bezrukov SM. Biophys. J. 2010; 99:134. [PubMed: 20655841]
(58). Nestorovich EM, Karginov VA, Bezrukov SM. Biophys. J. 2010; 99:782. [PubMed: 20682255]
(59). Ragle BE, Karginov VA, Bubeck Wardenburg J. Antimicrob. Agents Chemother. 2010; 54:298. [PubMed: 19805564]
(60). Diaz-Moscoso A, Mendez-Ardoy A, Ortega-Caballero F, Benito JM, Ortiz Mellet C, Defaye J, Robinson TM, Yohannes A, Karginov VA, Garcia Fernandez JM. ChemMedChem. 2011; 6:181. [PubMed: 21140396]
(61). Nestorovich EM, Karginov VA, Popoff MR, Bezrukov SM, Barth H. PLoS One. 2011; 6:e23927. [PubMed: 21887348]
(62). Yannakopoulou K, Jicsinszky L, Aggelidou C, Mourtzis N, Robinson TM, Yohannes A, Nestorovich EM, Bezrukov SM, Karginov VA. Antimicrob. Agents Chemother. 2011; 55:3594. [PubMed: 21555769]
(63). Kasianowicz JJ, Brandin E, Branton D, Deamer DW. Proc. Natl. Acad. Sci. U. S. A. 1996; 93:13770. [PubMed: 8943010]
(64). Braha O, Walker B, Cheley S, Kasianowicz JJ, Song L, Gouaux JE, Bayley H. Chem. Biol. 1997; 4:497. [PubMed: 9263637]
(65). Gu LQ, Braha O, Conlan S, Cheley S, Bayley H. Nature. 1999; 398:686. [PubMed: 10227291]
(66). Akeson M, Branton D, Kasianowicz JJ, Brandin E, Deamer DW. Biophys. J. 1999; 77:3227. [PubMed: 10585944]
(67). Henrickson SE, Misakian M, Robertson B, Kasianowicz JJ. Phys. Rev. Lett. 2000; 85:3057. [PubMed: 11006002]

(68). Meller A, Nivon L, Brandin E, Golovchenko J, Branton D. Proc. Natl. Acad. Sci. U. S. A. 2000; 97:1079. [PubMed: 10655487]
(69). Movileanu L, Bayley H. Proc. Natl. Acad. Sci. U. S. A. 2001; 98:10137. [PubMed: 11504913]
(70). Kasianowicz JJ, Henrickson SE, Weetall HH, Robertson B. Anal. Chem. 2001; 73:2268. [PubMed: 11393851]
(71). Meller A, Nivon L, Branton D. Phys. Rev. Lett. 2001; 86:3435. [PubMed: 11327989]
(72). Miles G, Cheley S, Braha O, Bayley H. Biochemistry. 2001; 40:8514. [PubMed: 11456489]
(73). Cheley S, Gu LQ, Bayley H. Chem. Biol. 2002; 9:829. [PubMed: 12144927]
(74). Guan X, Gu LQ, Cheley S, Braha O, Bayley H. Chembiochem. 2005; 6:1875. [PubMed: 16118820]
(75). Movileanu L, Schmittschmitt JP, Scholtz JM, Bayley H. Biophys. J. 2005; 89:1030. [PubMed: 15923222]
(76). Mathe J, Aksimentiev A, Nelson DR, Schulten K, Meller A. Proc. Natl. Acad. Sci. U. S. A. 2005; 102:12377. [PubMed: 16113083]
(77). Kang XF, Cheley S, Guan X, Bayley H. J. Am. Chem. Soc. 2006; 128:10684. [PubMed: 16910655]
(78). Wolfe AJ, Mohammad MM, Cheley S, Bayley H, Movileanu L. J. Am. Chem. Soc. 2007; 129:14034. [PubMed: 17949000]
(79). Hornblower B, Coombs A, Whitaker RD, Kolomeisky A, Picone SJ, Meller A, Akeson M. Nat. Methods. 2007; 4:315. [PubMed: 17339846]
(80). Wu HC, Bayley H. J. Am. Chem. Soc. 2008; 130:6813. [PubMed: 18444650]
(81). Mohammad MM, Prakash S, Matouschek A, Movileanu L. J. Am. Chem. Soc. 2008; 130:4081. [PubMed: 18321107]
(82). Mohammad MM, Movileanu L. Eur. Biophys. J. 2008; 37:913. [PubMed: 18368402]
(83). Stoddart D, Heron AJ, Mikhailova E, Maglia G, Bayley H. Proc. Natl. Acad. Sci. U. S. A. 2009; 106:7702. [PubMed: 19380741]
(84). Stoddart D, Heron AJ, Klingelhoefer J, Mikhailova E, Maglia G, Bayley H. Nano Lett. 2010; 10:3633. [PubMed: 20704324]
(85). Hall AR, Scott A, Rotem D, Mehta KK, Bayley H, Dekker C. Nat. Nanotechnol. 2010; 5:874. [PubMed: 21113160]
(86). Banerjee A, Mikhailova E, Cheley S, Gu LQ, Montoya M, Nagaoka Y, Gouaux E, Bayley H. Proc. Natl. Acad. Sci. U. S. A. 2010; 107:8165. [PubMed: 20400691]
(87). Wu Y, Ma L, Cheley S, Bayley H, Cui Q, Chapman ER. Biochemistry. 2011; 50:7493. [PubMed: 21815625]
(88). Li WW, Claridge TD, Li Q, Wormald MR, Davis BG, Bayley H. J. Am. Chem. Soc. 2011
(89). Hammerstein AF, Jayasinghe L, Bayley H. J. Biol. Chem. 2011; 286:14324. [PubMed: 21324910]
(90). Rotem D, Jayasinghe L, Salichou M, Bayley H. J. Am. Chem. Soc. 2012; 134:2781. [PubMed: 22229655]
(91). Bashford C. Cell. Biol. Mol. Lett. 2001; 6:328.
(92). Iacovache I, Paumard P, Scheib H, Lesieur C, Sakai N, Matile S, Parker MW, van der Goot FG. EMBO J. 2006; 25:457. [PubMed: 16424900]
(93). Lakey JH, Slatin SL. Curr. Top. Microbiol. Immunol. 2001; 257:131. [PubMed: 11417119]
(94). Zakharov SD, Cramer WA. Biochim. Biophys. Acta. 2002; 1565:333. [PubMed: 12409205]
(95). Cascales E, Buchanan SK, Duche D, Kleanthous C, Lloubes R, Postle K, Riley M, Slatin S, Cavard D. Microbiol. Mol. Biol. Rev. 2007; 71:158. [PubMed: 17347522]
(96). Gratia A, Fredericq P. C. R. Soc. Biol. (Paris). 1946; 140:1032.
(97). Lloubes R, Baty D, Lazdunski C. Nucleic Acids Res. 1986; 14:2621. [PubMed: 2421251]
(98). Kleanthous C. Nat. Rev. Microbiol. 2010; 8:843. [PubMed: 21060316]
(99). Bouveret E, Journet L, Walburger A, Cascales E, Benedetti H, Lloubes R. Biochimie. 2002; 84:413. [PubMed: 12423784]
(100). Spangler R, Zhang SP, Krueger J, Zubay G. J. Bacteriol. 1985; 163:167. [PubMed: 3891723]

(101). Vetter IR, Parker MW, Tucker AD, Lakey JH, Pattus F, Tsernoglou D. Structure. 1998; 6:863. [PubMed: 9687368]

(102). Jakes KS. Mol. Cell. 2001; 8:4. [PubMed: 11511355]

(103). James R, Penfold CN, Moore GR, Kleanthous C. Biochimie. 2002; 84:381. [PubMed: 12423781]

(104). Housden NG, Loftus SR, Moore GR, James R, Kleanthous C. Proc. Natl. Acad. Sci. U. S. A. 2005; 102:13849. [PubMed: 16166265]

(105). Ridley H, Johnson CL, Lakey JH. Adv. Exp. Med. Biol. 2010; 677:81. [PubMed: 20687482]

(106). Mosbahi K, Lemaitre C, Keeble AH, Mobasheri H, Morel B, James R, Moore GR, Lea EJ, Kleanthous C. Nat. Struct. Biol. 2002; 9:476. [PubMed: 12021774]

(107). Walker D, Mosbahi K, Vankemmelbeke M, James R, Kleanthous C. J. Biol. Chem. 2007; 282:31389. [PubMed: 17720814]

(108). Parker MW, Tucker AD, Tsernoglou D, Pattus F. Trends Biochem. Sci. 1990; 15:126. [PubMed: 2187292]

(109). Vetter, IR.; Parker, MW.; Pattus, F.; Tsernoglou, D. Insights into membrane insertion based on studies of colicins. Protein Toxin Structure; RG Landes Company; Austin, Texas and Springer: Heidelberg: 1996. p. 5-23.

(110). Parker MW, Pattus F, Tucker AD, Tsernoglou D. Nature. 1989; 337:93. [PubMed: 2909895]

(111). Wormald MR, Merrill AR, Cramer WA, Williams RJ. Eur. J. Biochem. 1990; 191:155. [PubMed: 2199197]

(112). Parker MW, Postma JP, Pattus F, Tucker AD, Tsernoglou D. J. Mol. Biol. 1992; 224:639. [PubMed: 1373773]

(113). Ghosh P, Mel SF, Stroud RM. Nat. Struct. Biol. 1994; 1:597. [PubMed: 7543362]

(114). Wiener M, Freymann D, Ghosh P, Stroud RM. Nature. 1997; 385:461. [PubMed: 9009197]

(115). Kleanthous C, Kuhlmann UC, Pommer AJ, Ferguson N, Radford SE, Moore GR, James R, Hemmings AM. Nat. Struct. Biol. 1999; 6:243. [PubMed: 10074943]

(116). Ko TP, Liao CC, Ku WY, Chak KF, Yuan HS. Structure. 1999; 7:91. [PubMed: 10368275]

(117). Soelaiman S, Jakes K, Wu N, Li C, Shoham M. Mol. Cell. 2001; 8:1053. [PubMed: 11741540]

(118). Hilsenbeck JL, Park H, Chen G, Youn B, Postle K, Kang C. Mol. Microbiol. 2004; 51:711. [PubMed: 14731273]

(119). Elkins P, Bunker A, Cramer WA, Stauffacher CV. Structure. 1997; 5:443. [PubMed: 9083117]

(120). Mel SF, Falick AM, Burlingame AL, Stroud RM. Biochemistry. 1993; 32:9473. [PubMed: 7690252]

(121). Muga A, Gonzalez-Manas JM, Lakey JH, Pattus F, Surewicz WK. J. Biol. Chem. 1993; 268:1553. [PubMed: 7678407]

(122). Wilmsen HU, Pugsley AP, Pattus F. Eur. Biophys. J. 1990; 18:149. [PubMed: 1694123]

(123). Greig SL, Radjainia M, Mitra AK. J. Biol. Chem. 2009; 284:16126. [PubMed: 19357078]

(124). Bullock JO, Kolen ER, Shear JL. J. Membr. Biol. 1992; 128:1. [PubMed: 1380089]

(125). Bullock JO. J. Membr. Biol. 1992; 125:255. [PubMed: 1372939]

(126). Bullock JO, Kolen ER. J. Membr. Biol. 1995; 144:131. [PubMed: 7541084]

(127). Krasilnikov OV, Yuldasheva LN, Nogueira RA, Rodrigues CG. Braz. J. Med. Biol. Res. 1995; 28:693. [PubMed: 8547854]

(128). Krasilnikov OV, Da Cruz JB, Yuldasheva LN, Varanda WA, Nogueira RA. J. Membr. Biol. 1998; 161:83. [PubMed: 9430623]

(129). Slatin SL, Finkelstein A, Kienker PK. Biochemistry. 2008; 47:1778. [PubMed: 18205407]

(130). Slatin SL, Duche D, Baty D. Biochemistry. 2010; 49:4786. [PubMed: 20459128]

(131). Bainbridge G, Gokce I, Lakey JH. FEBS Lett. 1998; 431:305. [PubMed: 9714531]

(132). Delcour AH. J. Mol. Microbiol. Biotechnol. 2002; 4:1. [PubMed: 11763966]

(133). Hille, B. Ion channels of excitable membranes. Siunderland; Siunderland, MA: 2001.

(134). Merrill AR, Cohen FS, Cramer WA. Biochemistry. 1990; 29:5829. [PubMed: 2200517]

(135). Qiu XQ, Jakes KS, Kienker PK, Finkelstein A, Slatin SL. J. Gen. Physiol. 1996; 107:313. [PubMed: 8868045]

(136). Jakes KS, Kienker PK, Finkelstein A. Q. Rev. Biophys. 1999; 32:189. [PubMed: 10845238]

(137). Schein SJ, Kagan BL, Finkelstein A. Nature. 1978; 276:159. [PubMed: 740032]

(138). Weaver CA, Kagan BL, Finkelstein A, Konisky J. Biochim. Biophys. Acta. 1981; 645:137. [PubMed: 6266474]

(139). Cleveland MV, Slatin S, Finkelstein A, Levinthal C. Proc. Natl. Acad. Sci. U. S. A. 1983; 80:3706. [PubMed: 6304732]

(140). Finkelstein A. Ann. N. Y. Acad. Sci. 1985; 456:26. [PubMed: 2418729]

(141). Raymond L, Slatin SL, Finkelstein A. J. Membr. Biol. 1985; 84:173. [PubMed: 2582133]

(142). Liu QR, Crozel V, Levinthal F, Slatin S, Finkelstein A, Levinthal C. Proteins. 1986; 1:218. [PubMed: 2453053]

(143). Raymond L, Slatin SL, Finkelstein A, Liu QR, Levinthal C. J. Membr. Biol. 1986; 92:255. [PubMed: 2431149]

(144). Slatin SL, Raymond L, Finkelstein A. J. Membr. Biol. 1986; 92:247. [PubMed: 2431148]

(145). Jakes KS, Abrams CK, Finkelstein A, Slatin SL. J. Biol. Chem. 1990; 265:6984. [PubMed: 1691183]

(146). Abrams CK, Jakes KS, Finkelstein A, Slatin SL. J. Gen. Physiol. 1991; 98:77. [PubMed: 1719126]

(147). Qiu XQ, Jakes KS, Finkelstein A, Slatin SL. J. Biol. Chem. 1994; 269:7483. [PubMed: 8125966]

(148). Slatin SL, Qiu XQ, Jakes KS, Finkelstein A. Nature. 1994; 371:158. [PubMed: 7521016]

(149). Kienker PK, Qiu X, Slatin SL, Finkelstein A, Jakes KS. J. Membr. Biol. 1997; 157:27. [PubMed: 9141356]

(150). Jakes KS, Kienker PK, Slatin SL, Finkelstein A. Proc. Natl. Acad. Sci. U. S. A. 1998; 95:4321. [PubMed: 9539735]

(151). Kienker PK, Jakes KS, Finkelstein A. J. Gen. Physiol. 2000; 116:587. [PubMed: 11004207]

(152). Kienker PK, Jakes KS, Blaustein RO, Miller C, Finkelstein A. J. Gen. Physiol. 2003; 122:161. [PubMed: 12860927]

(153). Kienker PK, Jakes KS, Finkelstein A. J. Gen. Physiol. 2008; 132:693. [PubMed: 19029376]

(154). Jakes KS, Finkelstein A. Mol. Microbiol. 2010; 75:567. [PubMed: 19919671]

(155). Slatin SL. Int. J. Biochem. 1988; 20:737. [PubMed: 3049178]

(156). Sobko AA, Kotova EA, Antonenko YN, Zakharov SD, Cramer WA. J. Biol. Chem. 2006; 281:14408. [PubMed: 16556601]

(157). Nassi S, Collier RJ, Finkelstein A. Biochemistry. 2002; 41:1445. [PubMed: 11814336]

(158). Neary M. Nurs. Stand. 2011; 26:57. [PubMed: 22324239]

(159). Deleo FR, Otto M, Kreiswirth BN, Chambers HF. Lancet. 2010; 375:1557. [PubMed: 20206987]

(160). Otto M. Annu. Rev. Microbiol. 2010; 64:143. [PubMed: 20825344]

(161). Otto M. Future Microbiol. 2012; 7:189. [PubMed: 22324988]

(162). Van de Velde H. La Cellule. 1894; 10:403.

(163). Denys J, Van de Velde H. La Cellule. 1895; 11:359.

(164). Otto M. Nat. Med. 2011; 17:169. [PubMed: 21297612]

(165). Gouaux JE, Braha O, Hobaugh MR, Song L, Cheley S, Shustak C, Bayley H. Proc. Natl. Acad. Sci. U. S. A. 1994; 91:12828. [PubMed: 7809129]

(166). Valeva A, Weisser A, Walker B, Kehoe M, Bayley H, Bhakdi S, Palmer M. EMBO J. 1996; 15:1857. [PubMed: 8617232]

(167). Song L, Hobaugh MR, Shustak C, Cheley S, Bayley H, Gouaux JE. Science. 1996; 274:1859. [PubMed: 8943190]

(168). Valeva A, Pongs J, Bhakdi S, Palmer M. Biochim. Biophys. Acta. 1997; 1325:281. [PubMed: 9168153]

(169). Valeva A, Palmer M, Bhakdi S. Biochemistry. 1997; 36:13298. [PubMed: 9341221]
(170). Fang Y, Cheley S, Bayley H, Yang J. Biochemistry. 1997; 36:9518. [PubMed: 9235997]
(171). Bhakdi S, Fussle R, Tranum-Jensen J. Proc. Natl. Acad. Sci. U. S. A. 1981; 78:5475. [PubMed: 6272304]
(172). Czajkowsky DM, Sheng S, Shao Z. J. Mol. Biol. 1998; 276:325. [PubMed: 9512705]
(173). Thelestam M, Olofsson A, Blomqvist L, Hebert H. Biochim. Biophys. Acta. 1991; 1062:245. [PubMed: 2004111]
(174). Krasilnikov O, Ternovsky V, Musaev Y. Dokl AN UzSSR. 1980; N7:66.
(175). Krasilnikov OV, Merzliak PG, Sabirov RZ, Tashmuk-Hamedov BA. Gen. Physiol. Biophys. 1990; 9:569. [PubMed: 1706676]
(176). Krasilnikov OV, Ternovsky VI, Merzliak PG, Zachidova LT, Hungerer KD. Biochim. Biophys. Acta. 1993; 1182:94. [PubMed: 8347691]
(177). Krasilnikov OV, Merzlyak PG, Yuldasheva LN, Azimova RK, Nogueira RA. Med. Microbiol. Immunol. 1997; 186:53. [PubMed: 9255767]
(178). Merzlyak PG, Yuldasheva LN, Rodrigues CG, Carneiro CM, Krasilnikov OV, Bezrukov SM. Biophys. J. 1999; 77:3023. [PubMed: 10585924]
(179). Krasilnikov OV, Merzlyak PG, Yuldasheva LN, Rodrigues CG, Nogueira RA. Biochim. Biophys. Acta. 1999; 1417:167. [PubMed: 10076045]
(180). Krasilnikov OV, Merzlyak PG, Yuldasheva LN, Rodrigues CG, Bhakdi S, Valeva A. Mol. Microbiol. 2000; 37:1372. [PubMed: 10998169]
(181). Krasilnikov OV, Sabirov RZ, Ternovsky VI, Merzliak PG, Tashmukhamedov BA. Gen. Physiol. Biophys. 1988; 7:467. [PubMed: 2466732]
(182). Bezrukov SM, Vodyanoy I. Biophys. J. 1993; 64:16. [PubMed: 7679295]
(183). Korchev YE, Bashford CL, Alder GM, Kasianowicz JJ, Pasternak CA. J. Membr. Biol. 1995; 147:233. [PubMed: 8558589]
(184). Bezrukov S, Vodyanoy I, Kasianowicz J. Macromolecules. 1996; 29:8517.
(185). Berestovsky GN, Ternovsky VI, Kataev AA. J. Exp. Bot. 2001; 52:1173. [PubMed: 11432935]
(186). Rostovtseva TK, Nestorovich EM, Bezrukov SM. Biophys. J. 2002; 82:160. [PubMed: 11751305]
(187). Ternovsky VI, Okada Y, Sabirov RZ. FEBS Lett. 2004; 576:433. [PubMed: 15498575]
(188). Nestorovich EM, Sugawara E, Nikaido H, Bezrukov SM. J. Biol. Chem. 2006; 281:16230. [PubMed: 16617058]
(189). Nablo BJ, Halverson KM, Robertson JW, Nguyen TL, Panchal RG, Gussio R, Bavari S, Krasilnikov OV, Kasianowicz JJ. Biophys. J. 2008; 95:1157. [PubMed: 18645196]
(190). Duret G, Delcour AH. Biophys. J. 2010; 98:1820. [PubMed: 20441745]
(191). Stojilkovic K, Berezhkovskii A, Bezrukov S. J. Chem. Phys. 2003; 119:6973.
(192). Kaneko J, Kamio Y. Biosci. Biotechnol. Biochem. 2004; 68:981. [PubMed: 15170101]
(193). Yamashita K, Kawai Y, Tanaka Y, Hirano N, Kaneko J, Tomita N, Ohta M, Kamio Y, Yao M, Tanaka I. Proc. Natl. Acad. Sci. U. S. A. 2011; 108:17314. [PubMed: 21969538]
(194). Miles G, Movileanu L, Bayley H. Protein Sci. 2002; 11:894. [PubMed: 11910032]
(195). Miles G, Jayasinghe L, Bayley H. J. Biol. Chem. 2006; 281:2205. [PubMed: 16269405]
(196). Sayeed S, Fernandez-Miyakawa ME, Fisher DJ, Adams V, Poon R, Rood JI, Uzal FA, McClane BA. Infect. Immun. 2005; 73:7413. [PubMed: 16239541]
(197). Popoff MR. FEBS J. 2011; 278:4602. [PubMed: 21535407]
(198). Bokori-Brown M, Savva CG, Fernandes da Costa SP, Naylor CE, Basak AK, Titball RW. FEBS J. 2011; 278:4589. [PubMed: 21518257]
(199). Marks JD. Anesthesiol. Clin. North America. 2004; 22:509. [PubMed: 15325716]
(200). Songer JG. Vet. Microbiol. 2010; 140:399. [PubMed: 19682805]
(201). Hunter SE, Clarke IN, Kelly DC, Titball RW. Infect. Immun. 1992; 60:102. [PubMed: 1729175]
(202). Minami J, Katayama S, Matsushita O, Matsushita C, Okabe A. Microbiol. Immunol. 1997; 41:527. [PubMed: 9272698]

(203). Gill DM. Microbiol. Rev. 1982; 46:86. [PubMed: 6806598]

(204). Cole AR, Gibert M, Popoff M, Moss DS, Titball RW, Basak AK. Nat. Struct. Mol. Biol. 2004; 11:797. [PubMed: 15258571]

(205). Miyata S, Matsushita O, Minami J, Katayama S, Shimamoto S, Okabe A. J. Biol. Chem. 2001; 276:13778. [PubMed: 11278924]

(206). Miyata S, Minami J, Tamai E, Matsushita O, Shimamoto S, Okabe A. J. Biol. Chem. 2002; 277:39463. [PubMed: 12177068]

(207). Petit L, Gibert M, Gillet D, Laurent-Winter C, Boquet P, Popoff MR. J. Bacteriol. 1997; 179:6480. [PubMed: 9335299]

(208). Petit L, Gibert M, Gourch A, Bens M, Vandewalle A, Popoff MR. Cell. Microbiol. 2003; 5:155. [PubMed: 12614459]

(209). Chassin C, Bens M, de Barry J, Courjaret R, Bossu JL, Cluzeaud F, Ben Mkaddem S, Gibert M, Poulain B, Popoff MR, Vandewalle A. Am. J. Physiol. Renal Physiol. 2007; 293:F927. [PubMed: 17567938]

(210). Borrmann E, Gunther H, Kohler H. FEMS Immunol. Med. Microbiol. 2001; 31:85. [PubMed: 11549414]

(211). Soler-Jover A, Blasi J, Gomez de Aranda I, Navarro P, Gibert M, Popoff MR, Martin-Satue M. J. Histochem. Cytochem. 2004; 52:931. [PubMed: 15208360]

(212). Lindsay CD. Hum. Exp. Toxicol. 1996; 15:904. [PubMed: 8938486]

(213). Robertson SL, Li J, Uzal FA, McClane BA. PLoS One. 2011; 6:e22053. [PubMed: 21814565]

(214). Petosa C, Collier RJ, Klimpel KR, Leppla SH, Liddington RC. Nature. 1997; 385:833. [PubMed: 9039918]

(215). Petit L, Maier E, Gibert M, Popoff MR, Benz R. J. Biol. Chem. 2001; 276:15736. [PubMed: 11278669]

(216). Knapp O, Maier E, Benz R, Geny B, Popoff MR. Biochim. Biophys. Acta. 2009; 1788:2584. [PubMed: 19835840]

(217). Nagahama M, Hara H, Fernandez-Miyakawa M, Itohayashi Y, Sakurai J. Biochemistry. 2006; 45:296. [PubMed: 16388606]

(218). Alcaraz A, Nestorovich EM, Aguilella-Arzo M, Aguilella VM, Bezrukov SM. Biophys. J. 2004; 87:943. [PubMed: 15298901]

(219). Siwy Z, Kosinska ID, Fulinski A, Martin CR. Phys. Rev. Lett. 2005; 94:048102. [PubMed: 15783605]

(220). Cervera J, Alcaraz A, Ramirez P. J. Phys. Chem. C. 2007; 111:12265.

(221). Knapp O, Popoff M. The Open Toxinology Journal. 2010; 3:53.

(222). Abrami L, Fivaz M, van der Goot FG. Trends Microbiol. 2000; 8:168. [PubMed: 10754575]

(223). Abrami L, Fivaz M, Decroly E, Seidah NG, Jean F, Thomas G, Leppla SH, Buckley JT, van der Goot FG. J. Biol. Chem. 1998; 273:32656. [PubMed: 9830006]

(224). Abrami L, Fivaz M, Glauser PE, Parton RG, van der Goot FG. J. Cell Biol. 1998; 140:525. [PubMed: 9456314]

(225). Lacy DB, Stevens RC. Curr. Opin. Struct. Biol. 1998; 8:778. [PubMed: 9914258]

(226). Howard SP, Buckley JT. J. Bacteriol. 1985; 163:336. [PubMed: 3891735]

(227). van der Goot FG, Lakey J, Pattus F, Kay CM, Sorokine O, Van Dorsselaer A, Buckley JT. Biochemistry. 1992; 31:8566. [PubMed: 1382579]

(228). Parker MW, Buckley JT, Postma JP, Tucker AD, Leonard K, Pattus F, Tsernoglou D. Nature. 1994; 367:292. [PubMed: 7510043]

(229). Wilmsen HU, Pattus F, Buckley JT. J. Membr. Biol. 1990; 115:71. [PubMed: 1692344]

(230). Wilmsen HU, Buckley JT, Pattus F. Mol. Microbiol. 1991; 5:2745. [PubMed: 1723472]

(231). Wilmsen HU, Leonard KR, Tichelaar W, Buckley JT, Pattus F. EMBO J. 1992; 11:2457. [PubMed: 1378390]

(232). Pastoriza-Gallego M, Rabah L, Gibrat G, Thiebot B, van der Goot FG, Auvray L, Betton JM, Pelta J. J. Am. Chem. Soc. 2011; 133:2923. [PubMed: 21319816]

(233). Tsitrin Y, Morton CJ, el-Bez C, Paumard P, Velluz MC, Adrian M, Dubochet J, Parker MW, Lanzavecchia S, van der Goot FG. Nat. Struct. Biol. 2002; 9:729. [PubMed: 12219082]

(234). Stefureac R, Long YT, Kraatz HB, Howard P, Lee JS. Biochemistry. 2006; 45:9172. [PubMed: 16866363]

(235). Stefureac R, Waldner L, Howard P, Lee JS. Small. 2008; 4:59. [PubMed: 18058890]

(236). Oukhaled G, Mathe J, Biance AL, Bacri L, Betton JM, Lairez D, Pelta J, Auvray L. Phys. Rev. Lett. 2007; 98:158101. [PubMed: 17501386]

(237). He Y, Olson R. J. Struct. Biol. 2010; 169:6. [PubMed: 19616104]

(238). De S, Olson R. Proc. Natl. Acad. Sci. U. S. A. 2011; 108:7385. [PubMed: 21502531]

(239). Olson R, Gouaux E. J. Mol. Biol. 2005; 350:997. [PubMed: 15978620]

(240). Krantz BA, Melnyk RA, Zhang S, Juris SJ, Lacy DB, Wu Z, Finkelstein A, Collier RJ. Science. 2005; 309:777. [PubMed: 16051798]

(241). Krasilnikov OV, Sabirov RZ, Ternovsky VI, Merzliak PG, Muratkhodjaev JN. FEMS Microbiol. Immunol. 1992; 5:93. [PubMed: 1384601]

(242). Krasilnikov OV, Muratkhodjaev JN, Zitzer AO. Biochim. Biophys. Acta. 1992; 1111:7. [PubMed: 1382601]

(243). Yuldasheva LN, Merzlyak PG, Zitzer AO, Rodrigues CG, Bhakdi S, Krasilnikov OV. Biochim. Biophys. Acta. 2001; 1512:53. [PubMed: 11334624]

(244). Krasilnikov OV, Merzlyak PG, Lima VL, Zitzer AO, Valeva A, Yuldasheva LN. Biochimie. 2007; 89:271. [PubMed: 17303303]

(245). Krasilnikov OV, Muratkhodjaev JN, Voronov SE, Yezepchuk YV. Biochim. Biophys. Acta. 1991; 1067:166. [PubMed: 1715187]

(246). Krasilnikov OV, Yuldasheva LN. Biochimie. 2009; 91:620. [PubMed: 19306957]

(247). Menzl K, Maier E, Chakraborty T, Benz R. Eur. J. Biochem. 1996; 240:646. [PubMed: 8856066]

(248). Mandal S, Mandal MD, Pal NK. Asian Pac. J. Trop. Med. 2011; 4:573. [PubMed: 21803312]

(249). Schwan C, Stecher B, Tzivelekidis T, van Ham M, Rohde M, Hardt WD, Wehland J, Aktories K. PLoS Pathog. 2009; 5:e1000626. [PubMed: 19834554]

(250). Cartman ST, Heap JT, Kuehne SA, Cockayne A, Minton NP. Int. J. Med. Microbiol. 2010; 300:387. [PubMed: 20547099]

(251). Sundriyal A, Roberts AK, Ling R, McGlashan J, Shone CC, Acharya KR. Protein Expr. Purif. 2010; 74:42. [PubMed: 20433927]

(252). Carman RJ, Stevens AL, Lyerly MW, Hiltonsmith MF, Stiles BG, Wilkins TD. Anaerobe. 2011; 17:161. [PubMed: 21376825]

(253). Shen A. J. Innate Immun. 2012; 4:149. [PubMed: 22237401]

(254). Hotze EM, Tweten RK. Biochim. Biophys. Acta. 2012; 1818:1028. [PubMed: 21835159]

(255). Heuck AP, Moe PC, Johnson BB. Subcell. Biochem. 2010; 51:551. [PubMed: 20213558]

(256). Tweten RK. Infect. Immun. 2005; 73:6199. [PubMed: 16177291]

(257). Tweten RK, Parker MW, Johnson AE. Curr. Top. Microbiol. Immunol. 2001; 257:15. [PubMed: 11417120]

(258). Heuck AP, Savva CG, Holzenburg A, Johnson AE. J. Biol. Chem. 2007; 282:22629. [PubMed: 17553799]

(259). Shatursky O, Heuck AP, Shepard LA, Rossjohn J, Parker MW, Johnson AE, Tweten RK. Cell. 1999; 99:293. [PubMed: 10555145]

(260). Shepard LA, Heuck AP, Hamman BD, Rossjohn J, Parker MW, Ryan KR, Johnson AE, Tweten RK. Biochemistry. 1998; 37:14563. [PubMed: 9772185]

(261). Tilley SJ, Orlova EV, Gilbert RJ, Andrew PW, Saibil HR. Cell. 2005; 121:247. [PubMed: 15851031]

(262). Feil SC, Rossjohn J, Rohde K, Tweten RK, Parker MW. FEBS Lett. 1996; 397:290. [PubMed: 8955365]

(263). Rossjohn J, Feil SC, McKinstry WJ, Tweten RK, Parker MW. Cell. 1997; 89:685. [PubMed: 9182756]

(264). Polekhina G, Giddings KS, Tweten RK, Parker MW. Proc. Natl. Acad. Sci. U. S. A. 2005; 102:600. [PubMed: 15637162]

(265). Rossjohn J, Polekhina G, Feil SC, Morton CJ, Tweten RK, Parker MW. J. Mol. Biol. 2007; 367:1227. [PubMed: 17328912]

(266). Xu L, Huang B, Du H, Zhang XC, Xu J, Li X, Rao Z. Protein Cell. 2010; 1:96. [PubMed: 21204001]

(267). Feil SC, Lawrence S, Mulhern TD, Holien JK, Hotze EM, Farrand S, Tweten RK, Parker MW. Structure. 2012; 20:248. [PubMed: 22325774]

(268). Law RH, Lukoyanova N, Voskoboinik I, Caradoc-Davies TT, Baran K, Dunstone MA, D'Angelo ME, Orlova EV, Coulibaly F, Verschoor S, Browne KA, Ciccone A, Kuiper MJ, Bird PI, Trapani JA, Saibil HR, Whisstock JC. Nature. 2010; 468:447. [PubMed: 21037563]

(269). Ramachandran R, Heuck AP, Tweten RK, Johnson AE. Nat. Struct. Biol. 2002; 9:823. [PubMed: 12368903]

(270). Heuck AP, Tweten RK, Johnson AE. J. Biol. Chem. 2003; 278:31218. [PubMed: 12777381]

(271). Ramachandran R, Tweten RK, Johnson AE. Proc. Natl. Acad. Sci. U. S. A. 2005; 102:7139. [PubMed: 15878993]

(272). Czajkowsky DM, Hotze EM, Shao Z, Tweten RK. EMBO J. 2004; 23:3206. [PubMed: 15297878]

(273). Sekino-Suzuki N, Nakamura M, Mitsui KI, Ohno-Iwashita Y. Eur. J. Biochem. 1996; 241:941. [PubMed: 8944786]

(274). Nakamura M, Sekino-Suzuki N, Mitsui K, Ohno-Iwashita Y. J. Biochem. 1998; 123:1145. [PubMed: 9604004]

(275). Ramachandran R, Tweten RK, Johnson AE. Nat. Struct. Mol. Biol. 2004; 11:697. [PubMed: 15235590]

(276). Dang TX, Hotze EM, Rouiller I, Tweten RK, Wilson-Kubalek EM. J. Struct. Biol. 2005; 150:100. [PubMed: 15797734]

(277). Shepard LA, Shatursky O, Johnson AE, Tweten RK. Biochemistry. 2000; 39:10284. [PubMed: 10956018]

(278). El-Rachkidy RG, Davies NW, Andrew PW. Biochem. Biophys. Res. Commun. 2008; 368:786. [PubMed: 18261465]

(279). Menestrina G, Bashford CL, Pasternak CA. Toxicon. 1990; 28:477. [PubMed: 1697105]

(280). Korchev YE, Bashford CL, Pederzolli C, Pasternak CA, Morgan PJ, Andrew PW, Mitchell TJ. Biochem. J. 1998; 329:571. [PubMed: 9445384]

(281). Palmer M, Harris R, Freytag C, Kehoe M, Tranum-Jensen J, Bhakdi S. EMBO J. 1998; 17:1598. [PubMed: 9501081]

(282). Montal M. Toxicon. 2009; 54:565. [PubMed: 19111565]

(283). Murphy JR. Toxins (Basel). 2011; 3:294. [PubMed: 22069710]

(284). Yamaizumi M, Mekada E, Uchida T, Okada Y. Cell. 1978; 15:245. [PubMed: 699044]

(285). Smith WP, Tai PC, Murphy JR, Davis BD. J. Bacteriol. 1980; 141:184. [PubMed: 6243620]

(286). Kaczorek M, Delpeyroux F, Chenciner N, Streeck RE, Murphy JR, Boquet P, Tiollais P. Science. 1983; 221:855. [PubMed: 6348945]

(287). Greenfield L, Bjorn MJ, Horn G, Fong D, Buck GA, Collier RJ, Kaplan DA. Proc. Natl. Acad. Sci. U. S. A. 1983; 80:6853. [PubMed: 6316330]

(288). Kantardjieff K, Collier RJ, Eisenberg D. J. Biol. Chem. 1989; 264:10402. [PubMed: 2732229]

(289). Choe S, Bennett MJ, Fujii G, Curmi PM, Kantardjieff KA, Collier RJ, Eisenberg D. Nature. 1992; 357:216. [PubMed: 1589020]

(290). Bennett MJ, Eisenberg D. Protein Sci. 1994; 3:1464. [PubMed: 7833808]

(291). Bell CE, Eisenberg D. Biochemistry. 1996; 35:1137. [PubMed: 8573568]

(292). Bell CE, Eisenberg D. Adv. Exp. Med. Biol. 1997; 419:35. [PubMed: 9193634]

(293). Bell CE, Eisenberg D. Biochemistry. 1997; 36:481. [PubMed: 9012663]

(294). Pohl E, Qui X, Must LM, Holmes RK, Hol WG. Protein Sci. 1997; 6:1114. [PubMed: 9144784]

(295). Kochi SK, Collier RJ. Exp. Cell Res. 1993; 208:296. [PubMed: 8359223]

(296). Collier RJ, Kandel J. J. Biol. Chem. 1971; 246:1496. [PubMed: 5545092]

(297). Gill DM, Pappenheimer AMJ. J. Biol. Chem. 1971; 246:1492. [PubMed: 5545091]

(298). Uchida T, Gill DM, Pappenheimer AMJ. Nat. New Biol. 1971; 233:8. [PubMed: 4999827]

(299). Shen WH, Choe S, Eisenberg D, Collier RJ. J. Biol. Chem. 1994; 269:29077. [PubMed: 7961874]

(300). Naglich JG, Metherall JE, Russell DW, Eidels L. Cell. 1992; 69:1051. [PubMed: 1606612]

(301). Boquet P, Silverman MS, Pappenheimer AMJ, Vernon WB. Proc. Natl. Acad. Sci. U. S. A. 1976; 73:4449. [PubMed: 63947]

(302). Sandvig K, Olsnes S. J. Cell Biol. 1980; 87:828. [PubMed: 7462324]

(303). Ratts R, Zeng H, Berg EA, Blue C, McComb ME, Costello CE, vanderSpek JC, Murphy JR. J. Cell Biol. 2003; 160:1139. [PubMed: 12668662]

(304). Ratts R, Trujillo C, Bharti A, vanderSpek J, Harrison R, Murphy JR. Proc. Natl. Acad. Sci. U. S. A. 2005; 102:15635. [PubMed: 16230620]

(305). Oh KJ, Senzel L, Collier RJ, Finkelstein A. Proc. Natl. Acad. Sci. U. S. A. 1999; 96:8467. [PubMed: 10411898]

(306). Donovan JJ, Simon MI, Draper RK, Montal M. Proc. Natl. Acad. Sci. U. S. A. 1981; 78:172. [PubMed: 6264431]

(307). Kagan BL, Finkelstein A, Colombini M. Proc. Natl. Acad. Sci. U. S. A. 1981; 78:4950. [PubMed: 6272284]

(308). Deleers M, Beugnier N, Falmagne P, Cabiaux V, Ruysschaert JM. FEBS Lett. 1983; 160:82. [PubMed: 6309569]

(309). Shiver JW, Donovan JJ. Biochim. Biophys. Acta. 1987; 903:48. [PubMed: 2443169]

(310). Misler S. Proc. Natl. Acad. Sci. U. S. A. 1983; 80:4320. [PubMed: 6308615]

(311). Kagan BL, Reich KA, Collier RJ. Biophys. J. 1984; 45:102. [PubMed: 19431527]

(312). Falnes PO, Madshus IH, Sandvig K, Olsnes S. J. Biol. Chem. 1992; 267:12284. [PubMed: 1376320]

(313). Mindell JA, Silverman JA, Collier RJ, Finkelstein A. Biophys. J. 1992; 62:41. [PubMed: 1376171]

(314). Cabiaux V, Mindell J, Collier RJ. Infect. Immun. 1993; 61:2200. [PubMed: 7683003]

(315). Mindell JA, Silverman JA, Collier RJ, Finkelstein A. J. Membr. Biol. 1994; 137:29. [PubMed: 7516433]

(316). Mindell JA, Zhan H, Huynh PD, Collier RJ, Finkelstein A. Proc. Natl. Acad. Sci. U. S. A. 1994; 91:5272. [PubMed: 7515494]

(317). Silverman JA, Mindell JA, Zhan H, Finkelstein A, Collier RJ. J. Membr. Biol. 1994; 137:17. [PubMed: 7516432]

(318). Kaul P, Silverman J, Shen WH, Blanke SR, Huynh PD, Finkelstein A, Collier RJ. Protein Sci. 1996; 5:687. [PubMed: 8845758]

(319). Oh KJ, Zhan H, Cui C, Hideg K, Collier RJ, Hubbell WL. Science. 1996; 273:810. [PubMed: 8670424]

(320). Huynh PD, Cui C, Zhan H, Oh KJ, Collier RJ, Finkelstein A. J. Gen. Physiol. 1997; 110:229. [PubMed: 9276751]

(321). Senzel L, Huynh PD, Jakes KS, Collier RJ, Finkelstein A. J. Gen. Physiol. 1998; 112:317. [PubMed: 9725891]

(322). Oh KJ, Zhan H, Cui C, Altenbach C, Hubbell WL, Collier RJ. Biochemistry. 1999; 38:10336. [PubMed: 10441127]

(323). Finkelstein A, Oh KJ, Senzel L, Gordon M, Blaustein RO, Collier RJ. Int. J. Med. Microbiol. 2000; 290:435. [PubMed: 11111923]

(324). Wu Z, Jakes KS, Samelson-Jones BS, Lai B, Zhao G, London E, Finkelstein A. Biophys. J. 2006; 91:3249. [PubMed: 16905612]

(325). Senzel L, Gordon M, Blaustein RO, Oh KJ, Collier RJ, Finkelstein A. J. Gen. Physiol. 2000; 115:421. [PubMed: 10736310]

(326). Rodnin MV, Kyrychenko A, Kienker P, Sharma O, Posokhov YO, Collier RJ, Finkelstein A, Ladokhin AS. J. Mol. Biol. 2010; 402:1. [PubMed: 20654627]

(327). Rodnin MV, Kyrychenko A, Kienker P, Sharma O, Vargas-Uribe M, Collier RJ, Finkelstein A, Ladokhin AS. Biophys. J. 2011; 101:L41. [PubMed: 22098755]

(328). Gordon M, Finkelstein A. J. Gen. Physiol. 2001; 118:471. [PubMed: 11696606]

(329). Montal M. Annu. Rev. Biochem. 2010; 79:591. [PubMed: 20233039]

(330). Flynn TC. J. Cosmet. Dermatol. 2012; 11:42. [PubMed: 22360334]

(331). Nguyen AT, Ahmad J, Fagien S, Rohrich RJ. Plast. Reconstr. Surg. 2012; 129:142e.

(332). Pickett A, Perrow K. Toxins (Basel). 2011; 3:63. [PubMed: 22069690]

(333). Dhaked RK, Singh MK, Singh P, Gupta P. Indian J. Med. Res. 2010; 132:489. [PubMed: 21149997]

(334). Bandyopadhyay S, Clark AW, DasGupta BR, Sathyamoorthy V. J. Biol. Chem. 1987; 262:2660. [PubMed: 3029090]

(335). Schiavo G, Rossetto O, Santucci A, DasGupta BR, Montecucco C. J. Biol. Chem. 1992; 267:23479. [PubMed: 1429690]

(336). Rossetto O, Montecucco C. Handb. Exp. Pharmacol. 2008; 184:129. [PubMed: 18064414]

(337). Schiavo G, Matteoli M, Montecucco C. Physiol. Rev. 2000; 80:717. [PubMed: 10747206]

(338). Simpson LL. Annu. Rev. Pharmacol. Toxicol. 2004; 44:167. [PubMed: 14744243]

(339). Schmid MF, Robinson JP, DasGupta BR. Nature. 1993; 364:827. [PubMed: 7689178]

(340). Oblatt-Montal M, Yamazaki M, Nelson R, Montal M. Protein Sci. 1995; 4:1490. [PubMed: 8520474]

(341). Montal MS, Blewitt R, Tomich JM, Montal M. FEBS Lett. 1992; 313:12. [PubMed: 1385218]

(342). Koriazova LK, Montal M. Nat. Struct. Biol. 2003; 10:13. [PubMed: 12459720]

(343). Fisher A, Montal M. Neurotox Res. 2006; 9:93. [PubMed: 16785104]

(344). Fischer A, Montal M. J. Biol. Chem. 2007; 282:29604. [PubMed: 17666397]

(345). Fischer A, Montal M. Proc. Natl. Acad. Sci. U. S. A. 2007; 104:10447. [PubMed: 17563359]

(346). Fischer A, Mushrush DJ, Lacy DB, Montal M. PLoS Pathog. 2008; 4:e1000245. [PubMed: 19096517]

(347). Fischer A, Nakai Y, Eubanks LM, Clancy CM, Tepp WH, Pellett S, Dickerson TJ, Johnson EA, Janda KD, Montal M. Proc. Natl. Acad. Sci. U. S. A. 2009; 106:1330. [PubMed: 19164566]

(348). Fischer A, Sambashivan S, Brunger AT, Montal M. J. Biol. Chem. 2012; 287:1657. [PubMed: 22158863]

(349). Chai Q, Arndt JW, Dong M, Tepp WH, Johnson EA, Chapman ER, Stevens RC. Nature. 2006; 444:1096. [PubMed: 17167418]

(350). Jin R, Rummel A, Binz T, Brunger AT. Nature. 2006; 444:1092. [PubMed: 17167421]

(351). Lacy DB, Tepp W, Cohen AC, DasGupta BR, Stevens RC. Nat. Struct. Biol. 1998; 5:898. [PubMed: 9783750]

(352). Swaminathan S, Eswaramoorthy S. Acta Crystallogr. D Biol. Crystallogr. 2000; 56:1024. [PubMed: 10944343]

(353). Swaminathan S, Eswaramoorthy S. Nat. Struct. Biol. 2000; 7:693. [PubMed: 10932256]

(354). Fischer A, Garcia-Rodriguez C, Geren I, Lou J, Marks JD, Nakagawa T, Montal M. J. Biol. Chem. 2008; 283:3997. [PubMed: 18032388]

(355). Hoch DH, Romero-Mira M, Ehrlich BE, Finkelstein A, DasGupta BR, Simpson LL. Proc. Natl. Acad. Sci. U. S. A. 1985; 82:1692. [PubMed: 3856850]

(356). Gambale F, Rauch G, Belmonte G, Menestrina G. FEBS Lett. 1992; 306:41. [PubMed: 1378409]

(357). Giesemann T, Jank T, Gerhard R, Maier E, Just I, Benz R, Aktories K. J. Biol. Chem. 2006; 281:10808. [PubMed: 16513641]

(358). Genisyuerek S, Papatheodorou P, Guttenberg G, Schubert R, Benz R, Aktories K. Mol. Microbiol. 2011; 79:1643. [PubMed: 21231971]

(359). Nagahama M, Umezaki M, Oda M, Kobayashi K, Tone S, Suda T, Ishidoh K, Sakurai J. Infect. Immun. 2011; 79:4353. [PubMed: 21911469]

(360). Fischer A, Holden MA, Pentelute BL, Collier RJ. Proc. Natl. Acad. Sci. U. S. A. 2011; 108:16577. [PubMed: 21949363]

(361). Janowiak BE, Jennings-Antipov LD, Collier RJ. Biochemistry. 2011; 50:3512. [PubMed: 21425869]

(362). Pentelute BL, Sharma O, Collier RJ. Angew. Chem. Int. Ed Engl. 2011; 50:2294. [PubMed: 21351339]

(363). Feld GK, Brown MJ, Krantz BA. Protein Sci. 2012; 21:606. [PubMed: 22374876]

(364). Feld GK, Kintzer AF, Tang II, Thoren KL, Krantz BA. J. Mol. Biol. 2012; 415:159. [PubMed: 22063095]

(365). Sterling HJ, Kintzer AF, Feld GK, Cassou CA, Krantz BA, Williams ER. J. Am. Soc. Mass Spectrom. 2012; 23:191. [PubMed: 22161509]

(366). Duesbery NS, Webb CP, Leppla SH, Gordon VM, Klimpel KR, Copeland TD, Ahn NG, Oskarsson MK, Fukasawa K, Paull KD, Vande Woude GF. Science. 1998; 280:734. [PubMed: 9563949]

(367). Vitale G, Pellizzari R, Recchi C, Napolitani G, Mock M, Montecucco C. Biochem. Biophys. Res. Commun. 1998; 248:706. [PubMed: 9703991]

(368). Leppla SH. Adv. Cyclic Nucleotide Protein Phosphorylation Res. 1984; 17:189. [PubMed: 6328915]

(369). Leppla SH. Proc. Natl. Acad. Sci. U. S. A. 1982; 79:3162. [PubMed: 6285339]

(370). Schleberger C, Hochmann H, Barth H, Aktories K, Schulz GE. J. Mol. Biol. 2006; 364:705. [PubMed: 17027031]

(371). Singh Y, Chaudhary VK, Leppla SH. J. Biol. Chem. 1989; 264:19103. [PubMed: 2509473]

(372). Klimpel KR, Molloy SS, Thomas G, Leppla SH. Proc. Natl. Acad. Sci. U. S. A. 1992; 89:10277. [PubMed: 1438214]

(373). Kintzer AF, Thoren KL, Sterling HJ, Dong KC, Feld GK, Tang II, Zhang TT, Williams ER, Berger JM, Krantz BA. J. Mol. Biol. 2009; 392:614. [PubMed: 19627991]

(374). Pimental RA, Christensen KA, Krantz BA, Collier RJ. Biochem. Biophys. Res. Commun. 2004; 322:258. [PubMed: 15313199]

(375). Friedlander AM. J. Biol. Chem. 1986; 261:7123. [PubMed: 3711080]

(376). Katayama H, Janowiak BE, Brzozowski M, Juryck J, Falke S, Gogol EP, Collier RJ, Fisher MT. Nat. Struct. Mol. Biol. 2008; 15:754. [PubMed: 18568038]

(377). Krantz BA, Finkelstein A, Collier RJ. J. Mol. Biol. 2006; 355:968. [PubMed: 16343527]

(378). Janowiak BE, Fischer A, Collier RJ. J. Biol. Chem. 2010; 285:8130. [PubMed: 20061382]

(379). Zhang S, Udho E, Wu Z, Collier RJ, Finkelstein A. Biophys. J. 2004; 87:3842. [PubMed: 15377524]

(380). Zhang S, Finkelstein A, Collier RJ. Proc. Natl. Acad. Sci. U. S. A. 2004; 101:16756. [PubMed: 15548616]

(381). Benson EL, Huynh PD, Finkelstein A, Collier RJ. Biochemistry. 1998; 37:3941. [PubMed: 9521715]

(382). Basilio D, Juris SJ, Collier RJ, Finkelstein A. J. Gen. Physiol. 2009; 133:307. [PubMed: 19204186]

(383). Kintzer AF, Sterling HJ, Tang II, Abdul-Gader A, Miles AJ, Wallace BA, Williams ER, Krantz BA. J. Mol. Biol. 2010; 399:741. [PubMed: 20433851]

(384). Blaustein RO, Lea EJ, Finkelstein A. J. Gen. Physiol. 1990; 96:921. [PubMed: 1704046]

(385). Nguyen TL. J. Biomol. Struct. Dyn. 2004; 22:253. [PubMed: 15473701]

(386). Blaustein RO, Finkelstein A. J. Gen. Physiol. 1990; 96:905. [PubMed: 1704045]

(387). Ohishi I, Odagiri Y. Infect. Immun. 1984; 43:54. [PubMed: 6197380]

(388). Aktories K, Barmann M, Ohishi I, Tsuyama S, Jakobs KH, Habermann E. Nature. 1986; 322:390. [PubMed: 3736664]

(389). Vandekerckhove J, Schering B, Barmann M, Aktories K. FEBS Lett. 1987; 225:48. [PubMed: 2891567]

(390). Aktories K, Wegner A. J. Cell Biol. 1989; 109:1385. [PubMed: 2677017]

(391). Popoff MR, Milward FW, Bancillon B, Boquet P. Infect. Immun. 1989; 57:2462. [PubMed: 2545625]

(392). Gulke I, Pfeifer G, Liese J, Fritz M, Hofmann F, Aktories K, Barth H. Infect. Immun. 2001; 69:6004. [PubMed: 11553537]

(393). Sundriyal A, Roberts AK, Shone CC, Acharya KR. J. Biol. Chem. 2009; 284:28713. [PubMed: 19692332]

(394). Chowdhury HH, Popoff MR, Zorec R. J. Physiol. 1999; 521(Pt 2):389. [PubMed: 10581310]

(395). Papatheodorou P, Wilczek C, Nolke T, Guttenberg G, Hornuss D, Schwan C, Aktories K. Infect. Immun. 2012

(396). Barth H, Blocker D, Behlke J, Bergsma-Schutter W, Brisson A, Benz R, Aktories K. J. Biol. Chem. 2000; 275:18704. [PubMed: 10749859]

(397). Nagahama M, Hagiyama T, Kojima T, Aoyanagi K, Takahashi C, Oda M, Sakaguchi Y, Oguma K, Sakurai J. Infect. Immun. 2009; 77:5139. [PubMed: 19720757]

(398). Pust S, Barth H, Sandvig K. Cell. Microbiol. 2010; 12:1809. [PubMed: 20690924]

(399). Blocker D, Behlke J, Aktories K, Barth H. Infect. Immun. 2001; 69:2980. [PubMed: 11292715]

(400). Stiles BG, Hale ML, Marvaud JC, Popoff MR. Biochem. J. 2002; 367:801. [PubMed: 12175336]

(401). Schmid A, Benz R, Just I, Aktories K. J. Biol. Chem. 1994; 269:16706. [PubMed: 7515883]

(402). Bachmeyer C, Benz R, Barth H, Aktories K, Gilbert M, Popoff MR. FASEB J. 2001; 15:1658. [PubMed: 11427518]

(403). Blocker D, Pohlmann K, Haug G, Bachmeyer C, Benz R, Aktories K, Barth H. J. Biol. Chem. 2003; 278:37360. [PubMed: 12869543]

(404). Blocker D, Bachmeyer C, Benz R, Aktories K, Barth H. Biochemistry. 2003; 42:5368. [PubMed: 12731878]

(405). Gibert M, Marvaud JC, Pereira Y, Hale ML, Stiles BG, Boquet P, Lamaze C, Popoff MR. FEBS Lett. 2007; 581:1287. [PubMed: 17350628]

(406). Kronhardt A, Rolando M, Beitzinger C, Stefani C, Leuber M, Flatau G, Popoff MR, Benz R, Lemichez E. PLoS One. 2011; 6:e23133. [PubMed: 21850257]

(407). Knapp O, Benz R, Gibert M, Marvaud JC, Popoff MR. J. Biol. Chem. 2002; 277:6143. [PubMed: 11741922]

(408). Blaustein RO, Koehler TM, Collier RJ, Finkelstein A. Proc. Natl. Acad. Sci. U. S. A. 1989; 86:2209. [PubMed: 2467303]

(409). Lang AE, Neumeyer T, Sun J, Collier RJ, Benz R, Aktories K. Biochemistry. 2008; 47:8406. [PubMed: 18636745]

(410). Neumeyer T, Schiffler B, Maier E, Lang AE, Aktories K, Benz R. J. Biol. Chem. 2008; 283:3904. [PubMed: 18077455]

(411). Orlik F, Schiffler B, Benz R. Biophys. J. 2005; 88:1715. [PubMed: 15596516]

(412). Kaiser E, Pust S, Kroll C, Barth H. Cell. Microbiol. 2009; 11:780. [PubMed: 19159389]

(413). Kaiser E, Kroll C, Ernst K, Schwan C, Popoff M, Fischer G, Buchner J, Aktories K, Barth H. Infect. Immun. 2011; 79:3913. [PubMed: 21768281]

(414). Dmochewitz L, Lillich M, Kaiser E, Jennings LD, Lang AE, Buchner J, Fischer G, Aktories K, Collier RJ, Barth H. Cell. Microbiol. 2011; 13:359. [PubMed: 20946244]

(415). Barth H. Naunyn Schmiedebergs Arch. Pharmacol. 2011; 383:237. [PubMed: 21120455]

(416). Bachmeyer C, Orlik F, Barth H, Aktories K, Benz R. J. Mol. Biol. 2003; 333:527. [PubMed: 14556742]

(417). Bezrukov SM, Kasianowicz JJ. Phys. Rev. Lett. 1993; 70:2352. [PubMed: 10053539]

(418). Kasianowicz JJ, Bezrukov SM. Biophys. J. 1995; 69:94. [PubMed: 7545444]

(419). Sakai N, Mareda J, Matile S. Acc. Chem. Res. 2008; 41:1354. [PubMed: 18590283]

(420). Finkelstein A. Toxicology. 1994; 87:29. [PubMed: 7512762]

(421). Anderson DS, Blaustein RO. J. Gen. Physiol. 2008; 132:351. [PubMed: 18725530]
(422). Rainey GJ, Young JA. Nat. Rev. Microbiol. 2004; 2:721. [PubMed: 15372082]
(423). Ivarsson ME, Leroux JC, Castagner B. Angew. Chem. Int. Ed Engl. 2012; 51:4024. [PubMed: 22441768]
(424). Bartlett JG, Inglesby TVJ, Borio L. Clin. Infect. Dis. 2002; 35:851. [PubMed: 12228822]
(425). Mock M, Fouet A. Annu. Rev. Microbiol. 2001; 55:647. [PubMed: 11544370]
(426). Gilligan PH. Curr. Opin. Microbiol. 2002; 5:489. [PubMed: 12354556]
(427). Popoff MR, Boquet P. Biochem. Biophys. Res. Commun. 1988; 152:1361. [PubMed: 2897847]
(428). Turnbull PC. Curr. Opin. Infect. Dis. 2000; 13:113. [PubMed: 11964777]
(429). Roux B, Allen T, Berneche S, Im W. Q. Rev. Biophys. 2004; 37:15. [PubMed: 17390604]
(430). Eisenberg B. J. Phys. Chem. C. Nanomater Interfaces. 2010; 114:20719. [PubMed: 21135913]
(431). Roux B. Biophys. J. 1996; 71:3177. [PubMed: 8968588]
(432). Edwards S, Corry B, Kuyucak S, Chung SH. Biophys. J. 2002; 83:1348. [PubMed: 12202360]
(433). Joseph S, Mashl RJ, Jakobsson E, Aluru NR. Nano Letters. 2003; 3:1399.
(434). Majumder M, Zhan X, Andrews R, Hinds BJ. Langmuir. 2007; 23:8624. [PubMed: 17616216]
(435). Beu TA. J. Chem. Phys. 2010; 132:164513. [PubMed: 20441294]
(436). Hilder TA, Gordon D, Chung SH. J. Chem. Phys. 2011; 134:045103. [PubMed: 21280804]
(437). De Biase PM, Solano CJ, Markosyan S, Czapla L, Noskov SY. J. Chem. Theory Comput. 2012; 8:2540. [PubMed: 22798730]
(438). Bezrukov SM, Berezhkovskii AM, Pustovoit MA, Szabo A. Journal of Chemical Physics. 2000; 113:8206.
(439). Berezhkovskii A, Pustovoit M, Bezrukov S. J. Chem. Phys. 2002; 116:9952.
(440). Berezhkovskii AM, Pustovoit MA, Bezrukov SM. J. Chem. Phys. 2003; 119:3943.
(441). Berezhkovskii AM, Bezrukov SM. Biophys. J. 2005; 88:L17. [PubMed: 15626697]
(442). Berezhkovskii A, Bezrukov S. Chemical Physics. 2005; 319:342.
(443). Bezrukov SM, Berezhkovskii AM, Szabo A. J. Chem. Phys. 2007; 127:115101. [PubMed: 17887882]
(444). Sheldon KL, Maldonado EN, Lemasters JJ, Rostovtseva TK, Bezrukov SM. PLoS One. 2011; 6:e25539. [PubMed: 22022409]
(445). Berezhkovskii AM, Pustovoit MA, Bezrukov SM. Phys. Rev. E. Stat. Nonlin Soft Matter Phys. 2009; 80:020904. [PubMed: 19792070]
(446). Berezhkovskii AM, Pustovoit MA, Bezrukov SM. Chem. Phys. 2010; 375:523. [PubMed: 21057663]
(447). Zitserman VY, Berezhkovskii AM, Pustovoit MA, Bezrukov SM. J. Chem. Phys. 2008; 129:095101. [PubMed: 19044889]
(448). Voet, D.; Voet, JG. Biochemistry. John Wiley; New York: 1995.
(449). Gordon VM, Leppla SH, Hewlett EL. Infect. Immun. 1988; 56:1066. [PubMed: 2895741]
(450). Blaustein RO, Finkelstein A. J. Gen. Physiol. 1990; 96:943. [PubMed: 1704047]
(451). Woodhull AM. J. Gen. Physiol. 1973; 61:687. [PubMed: 4541078]
(452). Tikhonov DB, Magazanik LG. J. Membr. Biol. 1998; 161:1. [PubMed: 9430616]
(453). Nestorovich EM, Danelon C, Winterhalter M, Bezrukov SM. Proc. Natl. Acad. Sci. U. S. A. 2002; 99:9789. [PubMed: 12119404]
(454). Bezrukov SM, Krasilnikov OV, Yuldasheva LN, Berezhkovskii AM, Rodrigues CG. Biophys. J. 2004; 87:3162. [PubMed: 15507690]
(455). Bezrukov SM, Winterhalter M. Phys. Rev. Lett. 2000; 85:202. [PubMed: 10991194]
(456). Nekolla S, Andersen C, Benz R. Biophys. J. 1994; 66:1388. [PubMed: 7520291]
(457). Wohnsland F, Benz R. J. Membr. Biol. 1997; 158:77. [PubMed: 9211723]
(458). Davis ME, Brewster ME. Nat. Rev. Drug Discov. 2004; 3:1023. [PubMed: 15573101]
(459). Uekama K. Chem. Pharm. Bull. (Tokyo). 2004; 52:900. [PubMed: 15304981]
(460). Szejtli J. Chem. Rev. 1998; 98:1743. [PubMed: 11848947]

(461). Crouzy S, Berneche S, Roux B. J. Gen. Physiol. 2001; 118:207. [PubMed: 11479347]
(462). Cu C, Bahring R, Mayer ML. Neuropharmacology. 1998; 37:1381. [PubMed: 9849673]
(463). Bouzianas DG. J. Med. Chem. 2010; 53:4305. [PubMed: 20102155]
(464). Beierlein JM, Anderson AC. Curr. Med. Chem. 2011; 18:5083. [PubMed: 22050756]
(465). Sawada-Hirai R, Jiang I, Wang F, Sun SM, Nedellec R, Ruther P, Alvarez A, Millis D, Morrow PR, Kang AS. J. Immune Based. Ther. Vaccines. 2004; 2:5. [PubMed: 15140257]
(466). Zhao P, Liang X, Kalbfleisch J, Koo HM, Cao B. Hum. Antibodies. 2003; 12:129. [PubMed: 15156101]
(467). Maynard JA, Maassen CB, Leppla SH, Brasky K, Patterson JL, Iverson BL, Georgiou G. Nat. Biotechnol. 2002; 20:597. [PubMed: 12042864]
(468). Wild MA, Xin H, Maruyama T, Nolan MJ, Calveley PM, Malone JD, Wallace MR, Bowdish KS. Nat. Biotechnol. 2003; 21:1305. [PubMed: 14555959]
(469). Chen Z, Moayeri M, Purcell R. Toxins (Basel). 2011; 3:1004. [PubMed: 22069754]
(470). Froude JW 2nd, Thullier P, Pelat T. Toxins (Basel). 2011; 3:1433. [PubMed: 22174979]
(471). Bradley KA, Mogridge J, Mourez M, Collier RJ, Young JA. Nature. 2001; 414:225. [PubMed: 11700562]
(472). Scobie HM, Rainey GJ, Bradley KA, Young JA. Proc. Natl. Acad. Sci. U. S. A. 2003; 100:5170. [PubMed: 12700348]
(473). Sarac MS, Peinado JR, Leppla SH, Lindberg I. Infect. Immun. 2004; 72:602. [PubMed: 14688144]
(474). Sellman BR, Mourez M, Collier RJ. Science. 2001; 292:695. [PubMed: 11326092]
(475). Bouzianas DG. Expert Rev. Anti Infect. Ther. 2007; 5:665. [PubMed: 17678429]
(476). Bouzianas DG. Trends Microbiol. 2009; 17:522. [PubMed: 19781945]
(477). Mourez M, Kane RS, Mogridge J, Metallo S, Deschatelets P, Sellman BR, Whitesides GM, Collier RJ. Nat. Biotechnol. 2001; 19:958. [PubMed: 11581662]
(478). Gujraty K, Sadacharan S, Frost M, Poon V, Kane RS, Mogridge J. Mol. Pharm. 2005; 2:367. [PubMed: 16196489]
(479). Moayeri M, Wiggins JF, Lindeman RE, Leppla SH. Antimicrob. Agents Chemother. 2006; 50:2658. [PubMed: 16870755]
(480). Singh Y, Khanna H, Chopra AP, Mehra V. J. Biol. Chem. 2001; 276:22090. [PubMed: 11278644]
(481). Yan M, Collier RJ. Mol. Med. 2003; 9:46. [PubMed: 12765339]
(482). Cao S, Guo A, Liu Z, Tan Y, Wu G, Zhang C, Zhao Y, Chen H. Infect. Immun. 2009; 77:4679. [PubMed: 19620345]
(483). Radjainia M, Hyun JK, Leysath CE, Leppla SH, Mitra AK. Proc. Natl. Acad. Sci. U. S. A. 2010; 107:14070. [PubMed: 20660775]
(484). Rubert Perez C, Lopez-Perez D, Chmielewski J, Lipton M. Chem. Biol. Drug Des. 2012; 79:260. [PubMed: 22146079]
(485). Mourez M, Collier RJ. Methods Mol. Biol. 2004; 261:213. [PubMed: 15064461]
(486). Vance D, Shah M, Joshi A, Kane RS. Biotechnol. Bioeng. 2008; 101:429. [PubMed: 18727104]
(487). Vance D, Martin J, Patke S, Kane RS. Adv. Drug Deliv. Rev. 2009; 61:931. [PubMed: 19596034]
(488). Yanjarappa MJ, Gujraty KV, Joshi A, Saraph A, Kane RS. Biomacromolecules. 2006; 7:1665. [PubMed: 16677052]
(489). Rai P, Padala C, Poon V, Saraph A, Basha S, Kate S, Tao K, Mogridge J, Kane RS. Nat. Biotechnol. 2006; 24:582. [PubMed: 16633350]
(490). Joshi A, Saraph A, Poon V, Mogridge J, Kane RS. Bioconjug. Chem. 2006; 17:1265. [PubMed: 16984137]
(491). Gujraty KV, Joshi A, Saraph A, Poon V, Mogridge J, Kane RS. Biomacromolecules. 2006; 7:2082. [PubMed: 16827573]
(492). Basha S, Rai P, Poon V, Saraph A, Gujraty K, Go MY, Sadacharan S, Frost M, Mogridge J, Kane RS. Proc. Natl. Acad. Sci. U. S. A. 2006; 103:13509. [PubMed: 16938891]

(493). Rai PR, Saraph A, Ashton R, Poon V, Mogridge J, Kane RS. Angew. Chem. Int. Ed Engl. 2007; 46:2207. [PubMed: 17310484]

(494). Rai P, Vance D, Poon V, Mogridge J, Kane RS. Chemistry. 2008; 14:7748. [PubMed: 18666271]

(495). Gujraty KV, Yanjarappa MJ, Saraph A, Joshi A, Mogridge J, Kane RS. J. Polym. Sci. A. Polym. Chem. 2008; 46:7246. [PubMed: 19855852]

(496). Joshi A, Vance D, Rai P, Thiyagarajan A, Kane RS. Chemistry. 2008; 14:7738. [PubMed: 18553325]

(497). Joshi A, Kate S, Poon V, Mondal D, Boggara MB, Saraph A, Martin JT, McAlpine R, Day R, Garcia AE, Mogridge J, Kane RS. Biomacromolecules. 2011; 12:791. [PubMed: 21302959]

(498). Christensen D, Korsholm KS, Andersen P, Agger EM. Expert Rev. Vaccines. 2011; 10:513. [PubMed: 21506648]

(499). Gonzalez-Rodriguez ML, Rabasco AM. Expert Opin. Drug Deliv. 2011; 8:857. [PubMed: 21557706]

(500). Henriksen-Lacey M, Korsholm KS, Andersen P, Perrie Y, Christensen D. Expert Opin. Drug Deliv. 2011; 8:505. [PubMed: 21413904]

(501). Muller RH, Shegokar R, Keck CM. Curr. Drug Discov. Technol. 2011; 8:207. [PubMed: 21291409]

(502). Merritt EA, Zhang Z, Pickens JC, Ahn M, Hol WG, Fan E. J. Am. Chem. Soc. 2002; 124:8818. [PubMed: 12137534]

(503). Polizzotti BD, Maheshwari R, Vinkenborg J, Kiick KL. Macromolecules. 2007; 40:7103. [PubMed: 19169374]

(504). Gargano JM, Ngo T, Kim JY, Acheson DW, Lees WJ. J. Am. Chem. Soc. 2001; 123:12909. [PubMed: 11749553]

(505). Kitov PI, Sadowska JM, Mulvey G, Armstrong GD, Ling H, Pannu NS, Read RJ, Bundle DR. Nature. 2000; 403:669. [PubMed: 10688205]

(506). Polyzos A, Alderton MR, Dawson RM, Hartley PG. Bioconjug. Chem. 2007; 18:1442. [PubMed: 17715991]

(507). Kane RS. Langmuir. 2010; 26:8636. [PubMed: 20131760]

(508). Clarkson MJ, Faull WB, Kerry JB. Vet. Rec. 1985; 116:467. [PubMed: 4002583]

(509). Harshman S, Alouf JE, Siffert O, Baleux F. Infect. Immun. 1989; 57:3856. [PubMed: 2509372]

(510). Odendaal MW, Visser JJ, Bergh N, Botha WJ. Onderstepoort J. Vet. Res. 1989; 56:251. [PubMed: 2560536]

(511). Percival DA, Shuttleworth AD, Williamson ED, Kelly DC. Infect. Immun. 1990; 58:2487. [PubMed: 1695203]

(512). Heveker N, Kiessig ST, Glaser R, Hungerer KD, Von Baehr R. Hybridoma. 1994; 13:263. [PubMed: 7528719]

(513). Heveker N, Hansen A, Hungerer KD, von Baehr R, Glaser RW. Hum. Antibodies Hybridomas. 1994; 5:18. [PubMed: 7858179]

(514). Cifrian E, Guidry AJ, O'Brien CN, Marquardi WW. Am. J. Vet. Res. 1996; 57:1308. [PubMed: 8874724]

(515). El-Enbaawy MI, Abdalla YA, Hussein AZ, Osman RM, Selim SA. Egypt. J. Immunol. 2003; 10:77. [PubMed: 15719625]

(516). McClain MS, Cover TL. Infect. Immun. 2007; 75:1785. [PubMed: 17261609]

(517). Ragle BE, Bubeck Wardenburg J. Infect. Immun. 2009; 77:2712. [PubMed: 19380475]

(518). Wang J, Qiu J, Dong J, Li H, Luo M, Dai X, Zhang Y, Leng B, Niu X, Zhao S, Deng X. J. Appl. Microbiol. 2011; 111:1551. [PubMed: 21972890]

(519). Hanada Y, Sekimizu K, Kaito C. J. Biol. Chem. 2011; 286:39360. [PubMed: 21937431]

(520). Pelish TM, McClain MS. J. Biol. Chem. 2009; 284:29446. [PubMed: 19720828]

(521). Kollef MH, Shorr A, Tabak YP, Gupta V, Liu LZ, Johannes RS. Chest. 2005; 128:3854. [PubMed: 16354854]

(522). Gu LQ, Bayley H. Biophys. J. 2000; 79:1967. [PubMed: 11023901]

(523). Lewis M, Weaver CD, McClain MS. Toxins (Basel). 2010; 2:1825. [PubMed: 20721308]
(524). Wulff H, Zhorov BS. Chem. Rev. 2008; 108:1744. [PubMed: 18476673]
(525). Zhorov BS, Tikhonov DB. J. Neurochem. 2004; 88:782. [PubMed: 14756799]
(526). Yu FH, Yarov-Yarovoy V, Gutman GA, Catterall WA. Pharmacol. Rev. 2005; 57:387. [PubMed: 16382097]
(527). Catterall WA, Goldin AL, Waxman SG. Pharmacol. Rev. 2005; 57:397. [PubMed: 16382098]
(528). Catterall WA, Perez-Reyes E, Snutch TP, Striessnig J. Pharmacol. Rev. 2005; 57:411. [PubMed: 16382099]
(529). Clapham DE, Julius D, Montell C, Schultz G. Pharmacol. Rev. 2005; 57:427. [PubMed: 16382100]
(530). Clapham DE, Garbers DL. Pharmacol. Rev. 2005; 57:451. [PubMed: 16382101]
(531). Hofmann F, Biel M, Kaupp UB. Pharmacol. Rev. 2005; 57:455. [PubMed: 16382102]
(532). Wei AD, Gutman GA, Aldrich R, Chandy KG, Grissmer S, Wulff H. Pharmacol. Rev. 2005; 57:463. [PubMed: 16382103]
(533). Gutman GA, Chandy KG, Grissmer S, Lazdunski M, McKinnon D, Pardo LA, Robertson GA, Rudy B, Sanguinetti MC, Stuhmer W, Wang X. Pharmacol. Rev. 2005; 57:473. [PubMed: 16382104]
(534). Kubo Y, Adelman JP, Clapham DE, Jan LY, Karschin A, Kurachi Y, Lazdunski M, Nichols CG, Seino S, Vandenberg CA. Pharmacol. Rev. 2005; 57:509. [PubMed: 16382105]
(535). Goldstein SA, Bayliss DA, Kim D, Lesage F, Plant LD, Rajan S. Pharmacol. Rev. 2005; 57:527. [PubMed: 16382106]
(536). Gu LQ, Shim JW. Analyst. 2010; 135:441. [PubMed: 20174694]
(537). Majd S, Yusko EC, Billeh YN, Macrae MX, Yang J, Mayer M. Curr. Opin. Biotechnol. 2010; 21:439. [PubMed: 20561776]
(538). Krasilnikov O, Ternovsky V, Tashmukhamedov B. Biofisica. 1981; 26:271.
(539). Braha O, Gu LQ, Zhou L, Lu X, Cheley S, Bayley H. Nat. Biotechnol. 2000; 18:1005. [PubMed: 10973225]
(540). Gu LQ, Dalla Serra M, Vincent JB, Vigh G, Cheley S, Braha O, Bayley H. Proc. Natl. Acad. Sci. U. S. A. 2000; 97:3959. [PubMed: 10760267]
(541). Gu LQ, Cheley S, Bayley H. Science. 2001; 291:636. [PubMed: 11158673]
(542). Gurnev PA, Harries D, Parsegian VA, Bezrukov SM. ChemPhysChem. 2009; 10:1445. [PubMed: 19504531]
(543). Gurnev PA, Harries D, Parsegian VA, Bezrukov SM. J. Phys. Condens Matter. 2010; 22:454110. [PubMed: 21339598]
(544). Kim JH, Scialli AR. Toxicol. Sci. 2011; 122:1. [PubMed: 21507989]
(545). Wnendt S, Finkam M, Winter W, Ossig J, Raabe G, Zwingenberger K. Chirality. 1996; 8:390. [PubMed: 8900028]
(546). Efcavitch JW, Thompson JF. Annu. Rev. Anal. Chem. (Palo Alto Calif). 2010; 3:109. [PubMed: 20636036]
(547). Wang HY, Ying YL, Li Y, Long YT. Chem. Asian J. 2010; 5:1952. [PubMed: 20669216]
(548). Shendure JA, Porreca GJ, Church GM, Gardner AF, Hendrickson CL, Kieleczawa J, Slatko BE. Curr. Protoc. Mol. Biol. 2011; Chapter 7(Unit7.1)
(549). Venkatesan BM, Bashir R. Nat. Nanotechnol. 2011; 6:615. [PubMed: 21926981]
(550). Luan B, Stolovitzky G, Martyna G. Nanoscale. 2012; 4:1068. [PubMed: 22081018]
(551). Deamer DW, Branton D. Acc. Chem. Res. 2002; 35:817. [PubMed: 12379134]
(552). Purnell RF, Schmidt JJ. ACS Nano. 2009; 3:2533. [PubMed: 19694456]
(553). Astier Y, Uzun O, Stellacci F. Small. 2009; 5:1273. [PubMed: 19242940]
(554). de Zoysa RS, Jayawardhana DA, Zhao Q, Wang D, Armstrong DW, Guan X. J Phys Chem B. 2009; 113:13332. [PubMed: 19736966]
(555). Manrao EA, Derrington IM, Laszlo AH, Langford KW, Hopper MK, Gillgren N, Pavlenok M, Niederweis M, Gundlach JH. Nat. Biotechnol. 2012; 30:349. [PubMed: 22446694]

(556). Halverson KM, Panchal RG, Nguyen TL, Gussio R, Little SF, Misakian M, Bavari S, Kasianowicz JJ. J. Biol. Chem. 2005; 280:34056. [PubMed: 16087661]

(557). Li J, Stein D, McMullan C, Branton D, Aziz MJ, Golovchenko JA. Nature. 2001; 412:166. [PubMed: 11449268]

(558). Fuchs H, Bachran C. Curr. Drug Targets. 2009; 10:89. [PubMed: 19199903]

(559). Panchal RG, Smart ML, Bowser DN, Williams DA, Petrou S. Curr. Pharm. Biotechnol. 2002; 3:99. [PubMed: 12022262]

(560). Panchal RG. Biochem. Pharmacol. 1998; 55:247. [PubMed: 9484789]

(561). Potala S, Sahoo SK, Verma RS. Drug Discov. Today. 2008; 13:807. [PubMed: 18678276]

(562). Mathew M, Verma RS. Cancer. Sci. 2009; 100:1359. [PubMed: 19459847]

(563). Kreitman RJ. BioDrugs. 2009; 23:1. [PubMed: 19344187]

(564). Barth H, Aktories K. Eur. J. Cell Biol. 2011; 90:944. [PubMed: 21247657]

(565). Adkins I, Holubova J, Kosova M, Sadilkova L. Curr. Pharm. Biotechnol. 2012; 13:1446. [PubMed: 22339216]

(566). Fitzgerald D, Pastan I. Ann. N. Y. Acad. Sci. 1993; 685:740. [PubMed: 8363279]

(567). Murphy JR, Lakkis FG, vanderSpek JC, Anderson P, Strom TB. Targeted Diagn. Ther. 1992; 7:365. [PubMed: 1633299]

(568). Murphy JR, vanderSpek JC. Semin. Cancer Biol. 1995; 6:259. [PubMed: 8562903]

(569). Foss FM, Saleh MN, Krueger JG, Nichols JC, Murphy JR. Curr. Top. Microbiol. Immunol. 1998; 234:63. [PubMed: 9670613]

(570). vanderSpek JC, Murphy JR. Methods Enzymol. 2000; 327:239. [PubMed: 11044987]

(571). Arora N, Klimpel KR, Singh Y, Leppla SH. J. Biol. Chem. 1992; 267:15542. [PubMed: 1639793]

(572). Arora N, Williamson LC, Leppla SH, Halpern JL. J. Biol. Chem. 1994; 269:26165. [PubMed: 7929330]

(573). Arora N, Leppla SH. Infect. Immun. 1994; 62:4955. [PubMed: 7927776]

(574). Leppla SH, Arora N, Varughese M. J. Appl. Microbiol. 1999; 87:284. [PubMed: 10475968]

(575). Liu S, Bugge TH, Leppla SH. J. Biol. Chem. 2001; 276:17976. [PubMed: 11278833]

(576). Frankel AE, Powell BL, Duesbery NS, Vande Woude GF, Leppla SH. Curr. Protein Pept. Sci. 2002; 3:399. [PubMed: 12370003]

(577). Liu S, Schubert RL, Bugge TH, Leppla SH. Expert Opin. Biol. Ther. 2003; 3:843. [PubMed: 12880383]

(578). Barth H, Hofmann F, Olenik C, Just I, Aktories K. Infect. Immun. 1998; 66:1364. [PubMed: 9529054]

(579). Barth H, Roebling R, Fritz M, Aktories K. J. Biol. Chem. 2002; 277:5074. [PubMed: 11741886]

(580). Marvaud JC, Stiles BG, Chenal A, Gillet D, Gibert M, Smith LA, Popoff MR. J. Biol. Chem. 2002; 277:43659. [PubMed: 12221101]

(581). Panchal RG, Cusack E, Cheley S, Bayley H. Nat. Biotechnol. 1996; 14:852. [PubMed: 9631009]

(582). Williams SA, Merchant RF, Garrett-Mayer E, Isaacs JT, Buckley JT, Denmeade SR. J. Natl. Cancer Inst. 2007; 99:376. [PubMed: 17341729]

(583). Goletz TJ, Klimpel KR, Arora N, Leppla SH, Keith JM, Berzofsky JA. Proc. Natl. Acad. Sci. U. S. A. 1997; 94:12059. [PubMed: 9342362]

(584). Goletz TJ, Klimpel KR, Leppla SH, Keith JM, Berzofsky JA. Hum. Immunol. 1997; 54:129. [PubMed: 9297531]

(585). Varughese M, Chi A, Teixeira AV, Nicholls PJ, Keith JM, Leppla SH. Mol. Med. 1998; 4:87. [PubMed: 9508786]

(586). Hochmann H, Pust S, von Figura G, Aktories K, Barth H. Biochemistry. 2006; 45:1271. [PubMed: 16430223]

(587). Pust S, Hochmann H, Kaiser E, von Figura G, Heine K, Aktories K, Barth H. J. Biol. Chem. 2007; 282:10272. [PubMed: 17283073]

(588). Schein SJ, Colombini M, Finkelstein A. J. Membr. Biol. 1976; 30:99. [PubMed: 1011248]

(589). Colombini M, Mannella CA. Biochim. Biophys. Acta. 2011; 1818:1438. [PubMed: 22120576]

(590). Colombini M. Biochim. Biophys. Acta. 2012

(591). Ujwal R, Cascio D, Colletier JP, Faham S, Zhang J, Toro L, Ping P, Abramson J. Proc. Natl. Acad. Sci. U. S. A. 2008; 105:17742. [PubMed: 18988731]

(592). Rostovtseva TK, Kazemi N, Weinrich M, Bezrukov SM. J. Biol. Chem. 2006; 281:37496. [PubMed: 16990283]

(593). Rostovtseva TK, Sheldon KL, Hassanzadeh E, Monge C, Saks V, Bezrukov SM, Sackett DL. Proc. Natl. Acad. Sci. U. S. A. 2008; 105:18746. [PubMed: 19033201]

(594). Rostovtseva TK, Bezrukov SM. J. Bioenerg. Biomembr. 2008; 40:163. [PubMed: 18654841]

(595). Rostovtseva TK, Bezrukov SM. Biochim. Biophys. Acta. 2012; 1818:1526. [PubMed: 22100746]

(596). Gurnev PA, Rostovtseva TK, Bezrukov SM. FEBS Lett. 2011; 585:2363. [PubMed: 21722638]

(597). Wang H, Shi H, Wang Z. Life Sci. 1999; 65:PL143. [PubMed: 10503950]

(598). Suessbrich H, Waldegger S, Lang F, Busch AE. FEBS Lett. 1996; 385:77. [PubMed: 8641472]

(599). Kang J, Chen XL, Rampe D. Biochem. Biophys. Res. Commun. 2001; 286:499. [PubMed: 11511086]

(600). Clare JJ, Tate SN, Nobbs M, Romanos MA. Drug Discov. Today. 2000; 5:506. [PubMed: 11084387]

(601). Dietrich PS, McGivern JG, Delgado SG, Koch BD, Eglen RM, Hunter JC, Sangameswaran L. J. Neurochem. 1998; 70:2262. [PubMed: 9603190]

(602). Hockerman GH, Johnson BD, Abbott MR, Scheuer T, Catterall WA. J. Biol. Chem. 1997; 272:18759. [PubMed: 9228049]

(603). Yang J, Jan YN, Jan LY. Neuron. 1995; 14:1047. [PubMed: 7748552]

(604). Sanchez M, McManus OB. Neuropharmacology. 1996; 35:963. [PubMed: 8938726]

(605). Strobaek D, Jorgensen TD, Christophersen P, Ahring PK, Olesen SP. Br. J. Pharmacol. 2000; 129:991. [PubMed: 10696100]

(606). Fanger CM, Rauer H, Neben AL, Miller MJ, Rauer H, Wulff H, Rosa JC, Ganellin CR, Chandy KG, Cahalan MD. J. Biol. Chem. 2001; 276:12249. [PubMed: 11278890]

(607). Lacy DB, Wigelsworth DJ, Melnyk RA, Harrison SC, Collier RJ. Proc. Natl. Acad. Sci. U. S. A. 2004; 101:13147. [PubMed: 15326297]

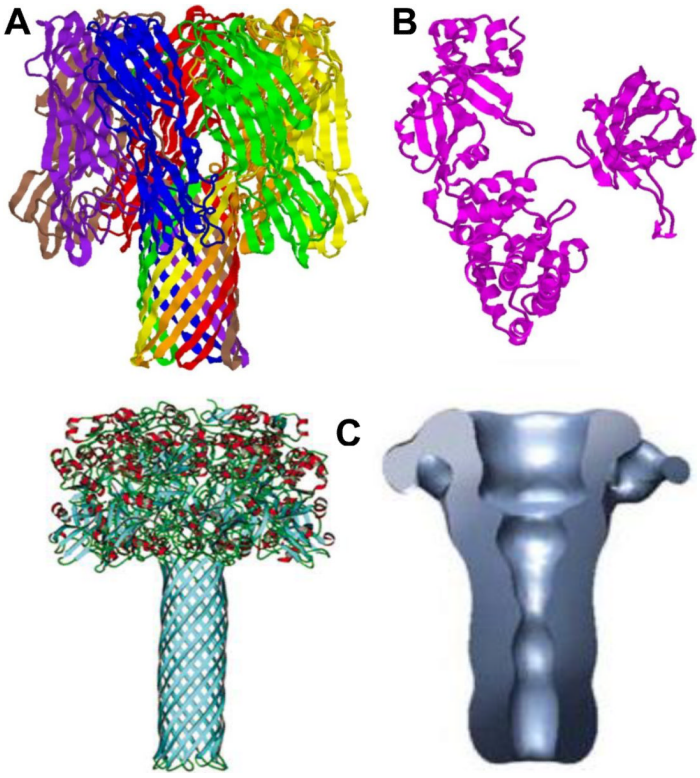

Figure 1.

Typical membrane-perforating, AB-type, and binary bacterial toxins α-hemolysin of *Staphylococcus aureus*, diphtheria toxins of *Corynebacterium diphtheriae*, and the channel-forming PA_{63} component of anthrax toxin of *Bacillus anthracis*. **A**: Ribbon representation of 1.9 Å crystal structure of heptameric α-hemolysin [167]. PDB ID: 7AHL. **B**: 2.3 Å nucleotide-free crystal structure of monomeric single-chain diphtheria toxin[292]. PDB ID: 1SGK. **C**, left: Molecular model of the heptameric PA_{63} pore. Reprinted with permission from ref[385]. Taylor & Francis Copyright 2004. **C**, right: Three-dimensional reconstruction of the PA_{63} pore based on the electron microscopy structure. Reprinted with permission from ref[376]. Copyright 2008. Nature Publishing Group.

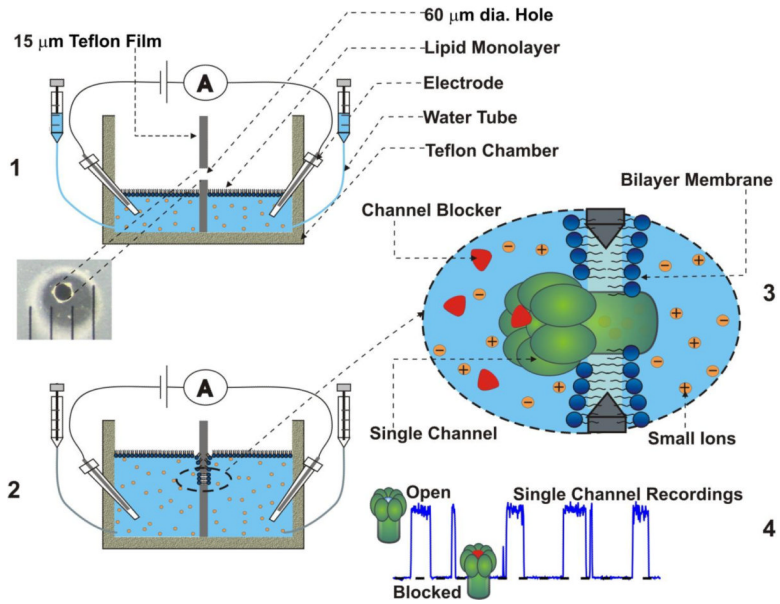

Figure 2.
Schematic illustration of planar lipid bilayer membrane formation (1, 2) and high-resolution single-channel recordings (3, 4).

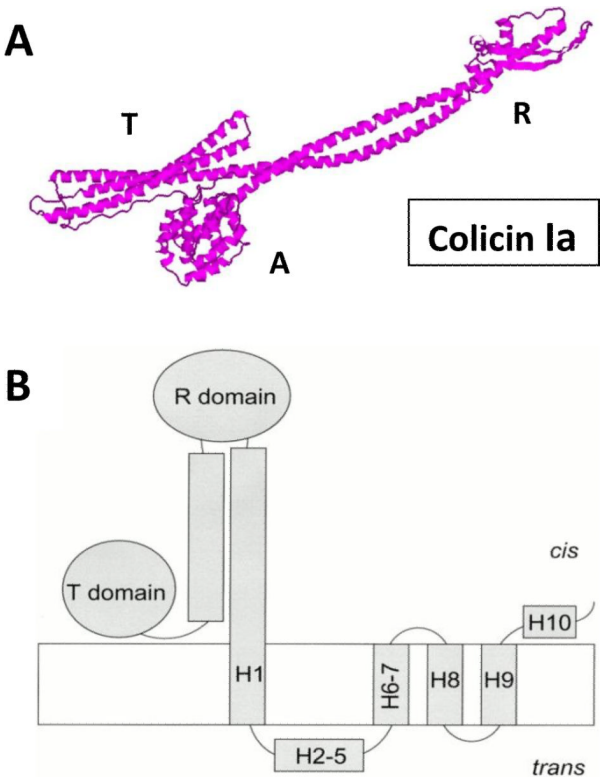

Figure 3.
Pore-forming colicin Ia. **A**: Colicin Ia crystal structure at the 3 Å resolution[114]. PDB ID: 1CII. **B**: Schematic diagram of the open state of the whole colicin Ia molecule inserted into a planar bilayer. Reprinted with permission from ref[151]. Copyright 2000. The Rockefeller University Press.

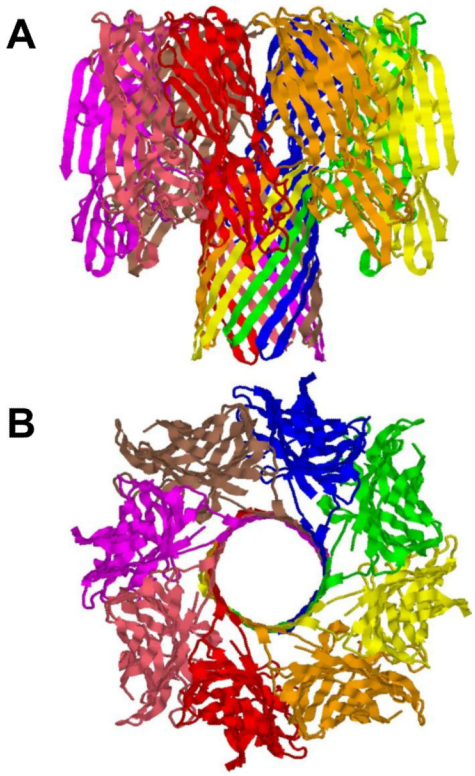

Figure 4.
Ribbon representation of the 2.5Å crystal structure of bi-component octameric γ-hemolysin[193]. PDB ID: 3B07. Side (**A**) and top (**B**) views are shown.

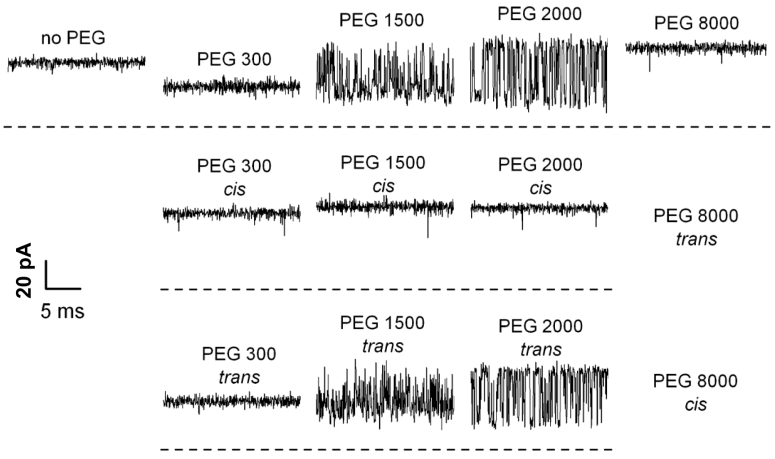

Figure 5.

A: The effect of symmetrical addition of polyethylene glycol (PEG) of different molecular weights in 15% w/w concentration on the ion current through a single ETX channel. It is seen that PEGs not only change the average conductance but, depending on molecular weight, induce significant fluctuations. **B** and **C**: Experiments performed under asymmetrical PEG additions demonstrate that these fluctuations are mostly caused by permeant PEGs added to the *trans* side of the membrane. Time resolution was 0.1 ms, transmembrane voltage −100 mV. Reprinted with permission from ref[58]. Copyright 2010. Biophysical Society.

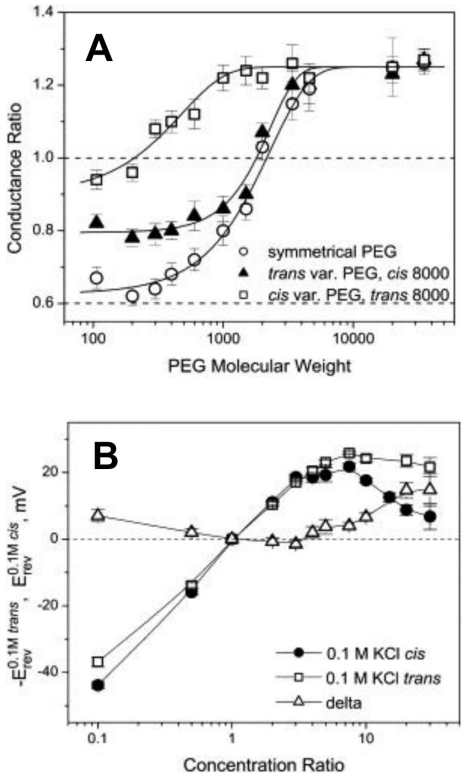

Figure 6.

A: The relative change in ETX channel conductance as a function of PEG molecular weight. The *trans* and *cis* side applications of polymers of varying molecular weights, *solid triangles* and *open squares*, respectively, have different effects on the channel conductance. The impermeant PEG 8000 was on the opposite side of the membrane. The effect of symmetrical addition of PEG is shown by *open circles*. *Dotted line* at 0.6 corresponds to the ratio of bulk solution conductivities with and without polymers. **B**: Channel reversal potential as a function of the concentration ratio for two series of measurements with the oppositely directed gradients. E_{rev} was obtained in the series of experiments where c_{cis} was kept constant at 0.1 M KCl and *ctrans* was varied from 0.01 M KCl to 3 M KCl (*solid circles*). – E_{rev} was measured in the reversed gradient where *ctrans* = 0.1 M KCl and c_{cis} was changed from 0.01 M KCl to 3 M KCl (*open squares*). The channel is asymmetric: the absolute value of the reversal potential is smaller when the more concentrated solution is on the *trans* side of the membrane. *Open triangles* show the difference. Reprinted with permission from ref[58]. Copyright 2010. Biophysical Society.

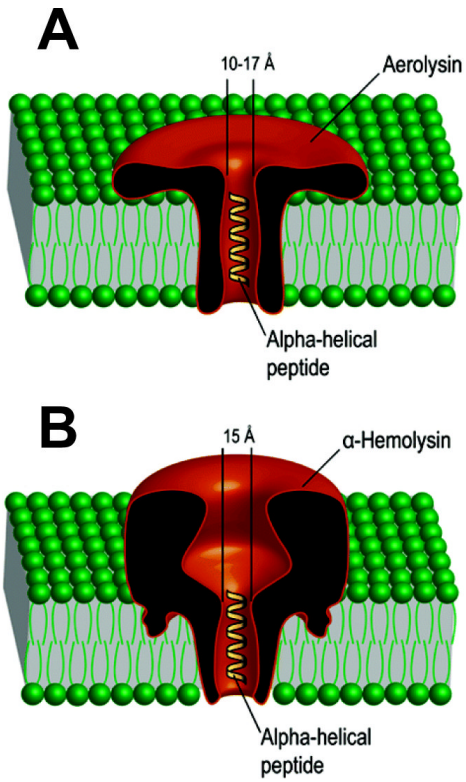

Figure 7.
Schematic representation of the single oligomeric aerolysin (left) and α-hemolysin (right) pores incorporated into planar lipid bilayers with linear α-helical peptides traversing the channels. Adapted with permission from ref[234]. Copyright 2006. American Chemical Society.

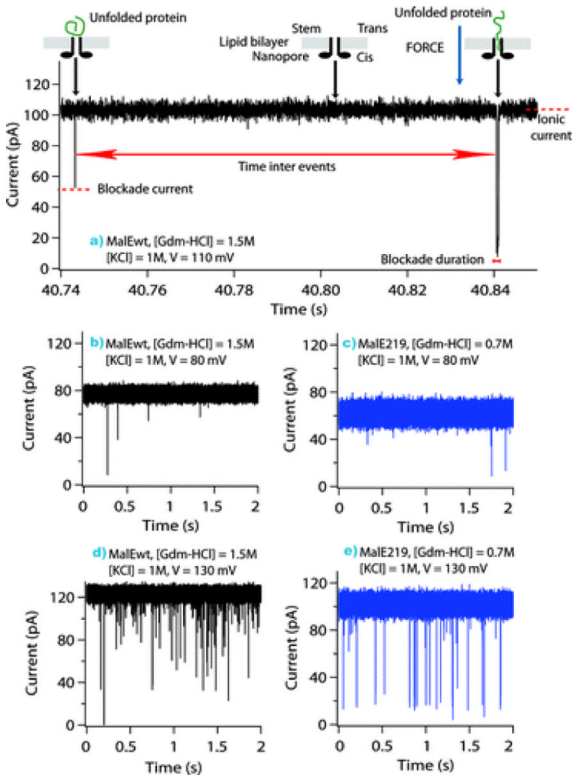

Figure 8.

Single-channel current recordings showing unfolded protein transport across the aerolysin pore as a function of applied voltage: V = 80 mV (middle), V = 110 mV (top), and V = 130 mV (bottom), for the wild-type protein MalEwt (black), and mutant protein, MalE219 (blue). The stem domain of the aerolysin pore was on the *cis* side of the lipid bilayer, and the proteins entered by the stem side. Analysis of the current tracks (top) shows the difference between bumping or translocation events. An increase in the applied voltage results in the increase of the frequency of single channel ionic current blockades (middle and bottom). Reprinted with permission from ref.[232] Copyright 2011. American Chemical Society.

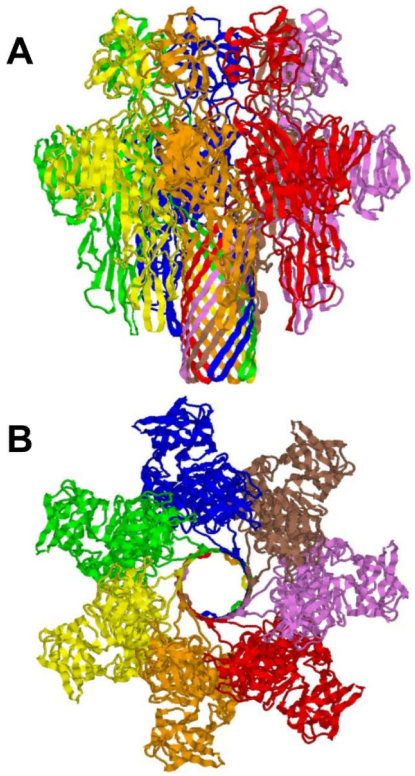

Figure 9.
Ribbon representation of the 2.88 Å crystal structure of heptameric *Vibrio cholerae* cytolysin[238]. Side (**A**) and top (**B**) views are shown. PDB ID: 3044.

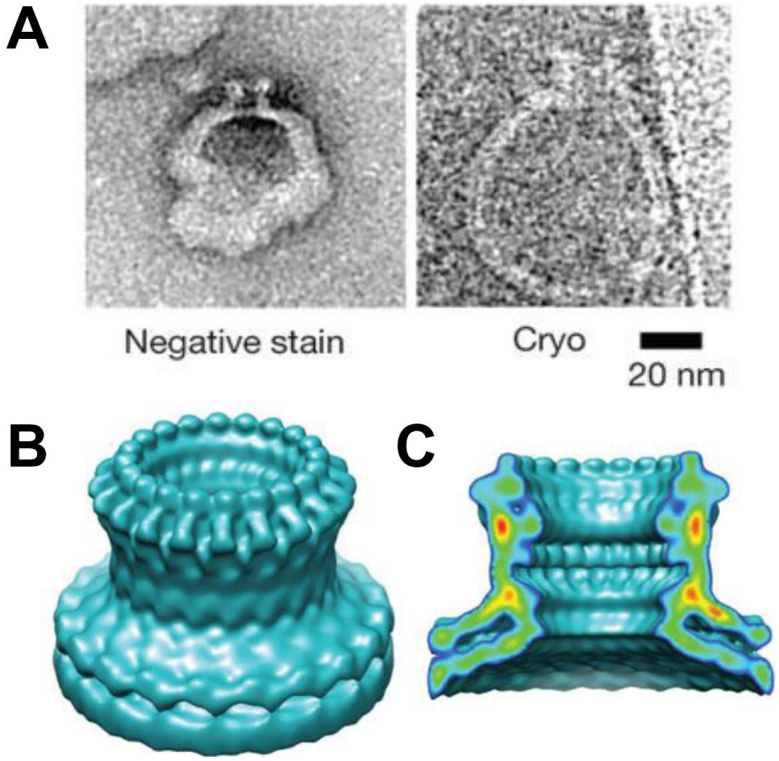

Figure 10.

Perforin pore structure. **A**: Negative stain and cryo-electron microscopy images of perforin-containing liposomes. Surface (**B**) and cut-away (**C**) views of a cryo-electron microscopy reconstruction of the perforin pore with 20-fold symmetry. The map resolution was 28.5 Å. Reprinted and modified with permission from ref[268]. Copyright 2002. Nature Publishing Group.

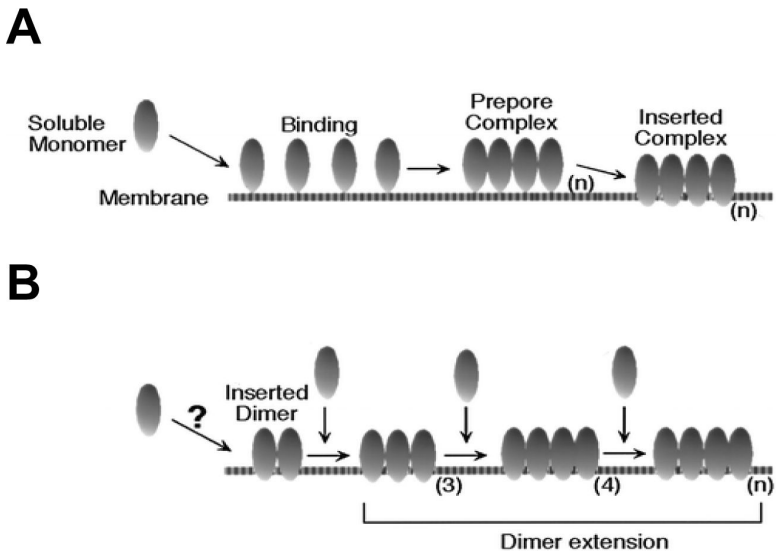

Figure 11.

Two models of membrane insertion for the cholesterol-dependent cytolysins. **A**: the prepore model[263] for the assembly and insertion of CDC. **B**: continuous growth model[281]. The number of monomers comprising the multimer is designated as (n). Reprinted with permission from ref[277]. Copyright 2000. American Chemical Society.

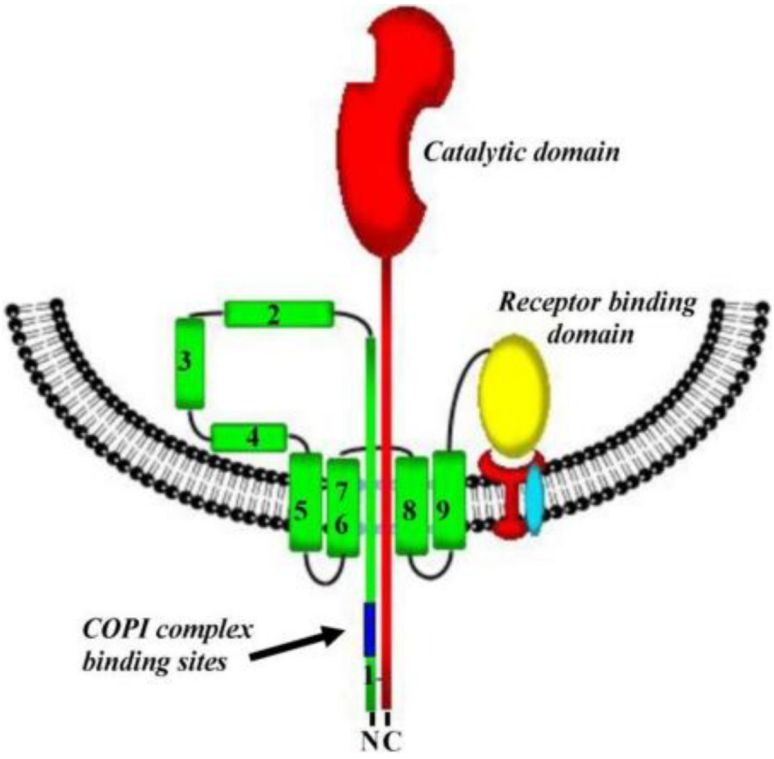

Figure 12.
Schematic representation of the diphtheria toxin transmembrane domain incorporated into the endosomal vesicle membrane, which results in the formation of a transmembrane pore. Reprinted with permission from ref[283]. Copyright 2011. MDPI AG.

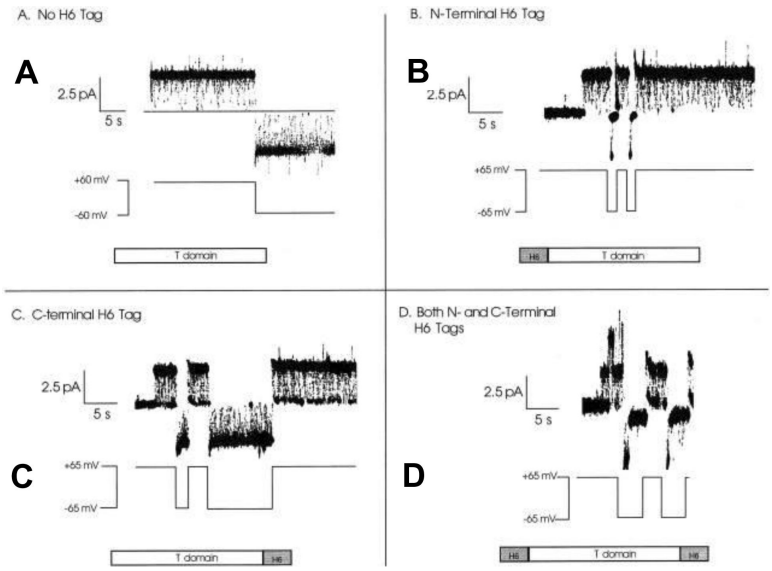

Figure 13.

Gating characteristics of the different T-domain constructs studied on a single-channel level [328]. **A**: A single channel formed by wild-type T-domain (lacking H6 tag) remains open at both +60 and −60 mV, with irresolvably brief flickerings to a zero-conductance closed state. **B**: A single channel formed by T-domain with an N-terminal H6 tag remains open at +65 mV but rapidly closes to zero conductance at −65 mV. **C**: A single channel formed by T-domain with a C-terminal H6 tag spends a good deal of time in the zero-conductance closed state at +65 mV and remains open at −65 mV like the wild-type channel. **D**: A single channel formed by T-domain with both N- and C-terminal H6 tags is blocked at both +65 and −65 mV. At positive voltages, the channel fluctuates rapidly between the open and closed states, spending about half of its time in each. At negative voltage pulses, the channel remains open briefly, before fully closing for the duration of the pulse. Reprinted with permission from ref[328]. Copyright 2001. The Rockefeller University Press.

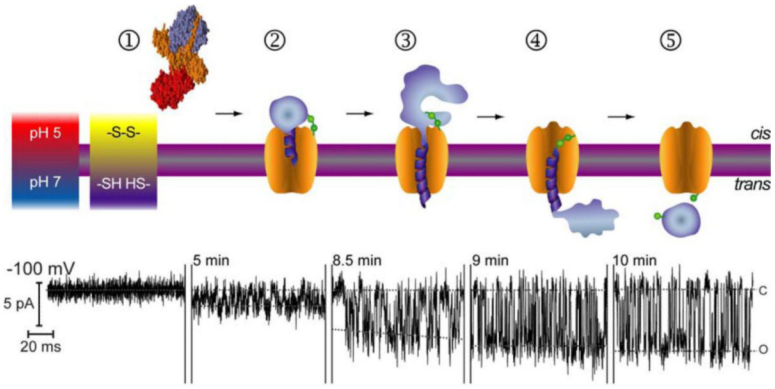

Figure 14.

Sequence of events showing BoNT light chain translocation through the heavy chain channel. Step1. BoNT/A holotoxin prior to insertion in the membrane (grey bar with magenta boundaries); BoNT/A is represented by the crystal structure rendered on YASARA using PDB accession code 3BTA[351]. Step 2. Schematic representation of the membrane inserted BoNT/A during an entry event. Steps 3 and 4. A series of transfer steps. Step 5. An exit event. Segments of typical single channel recordings are displayed under the corresponding interpretation for each step. Reprinted with permission from ref[282]. Copyright 2009. Elsevier.

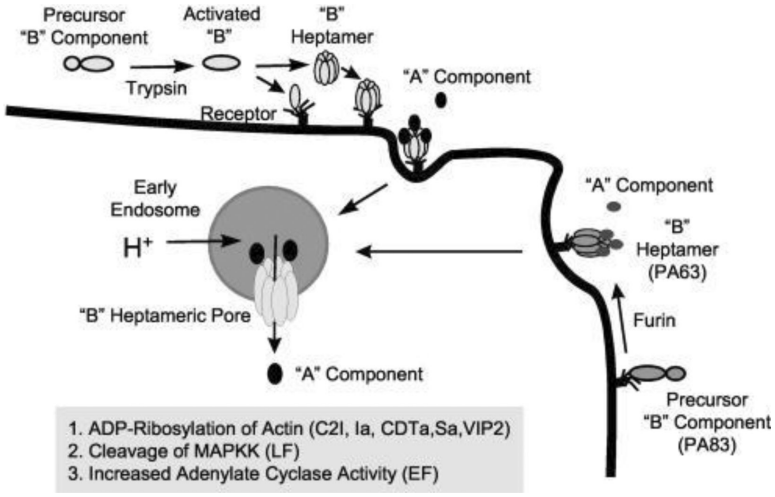

Figure 15.

Basic mechanisms of cell intoxication by *Clostridium* and *Bacillus* binary toxins. Cell-binding B-precursors are first activated by proteolytic cleavage in solution or on the cell surface (*B. anthracis* PA_{83} only). Subsequently, activated B components interact with specific cell surface receptors as either preformed ring-shaped heptamers or monomers that form heptamers on the cell surface. The enzymatic A components bind to the cell-associated B heptamer, and the receptor-toxin complex then undertakes receptor-mediated endocytosis. An acidic endosomal environment is essential for translocating the A components into the cytosol. Reprinted with permission from ref[3]. Copyright 2004. ASM Press.

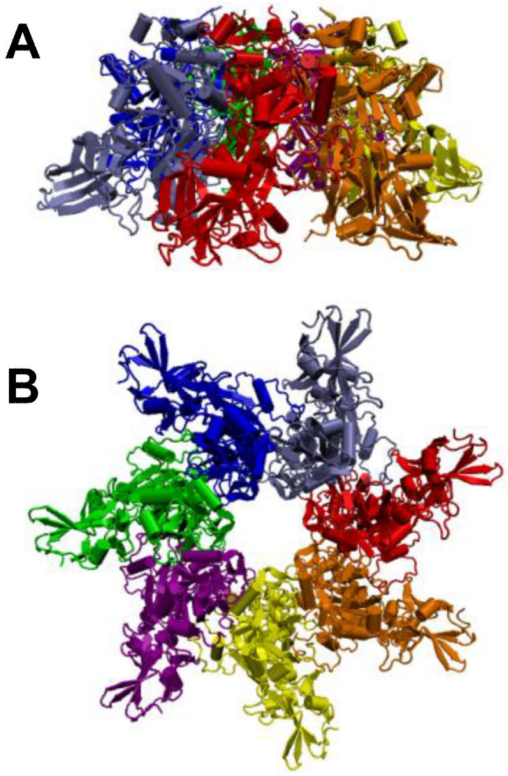

Figure 16.
Ribbon representation of 3.6 Å crystal structure of heptameric prepore of channel-forming component of anthrax toxin, PA_{63}.[607] Side (**A**) and top (**B**) views are presented. PDB ID: 1TZN.

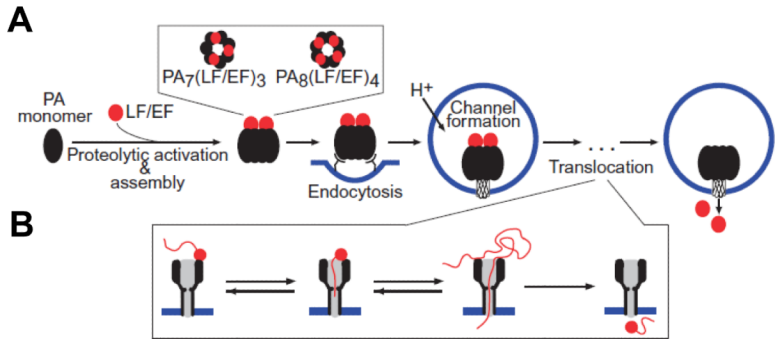

Figure 17.

A: Schematic representation for anthrax toxin receptor-mediated cell assembly and entry into a target cell[50]. First, proteolytically activated PA monomers (PA_{63}) oligomerize into the ring-shaped heptameric, $(PA_{63})_7$, or octameric, $(PA_{63})_8$, complexes, which are able to dock 3 or 4 enzymatic A components, LF and/or EF, respectively. These oligomeric prepores are then endocytosed and, under the acidic endosomal pH, converted to the transmembrane channels, which transport LF and EF into the cytosol. **B**: A possible protein unfolding and translocation pathway for anthrax toxin depicted in three successive steps: docking, protein unfolding, and translocation of the unfolded chain. Adapted with permission from ref.[50] Copyright 2011. Wiley.

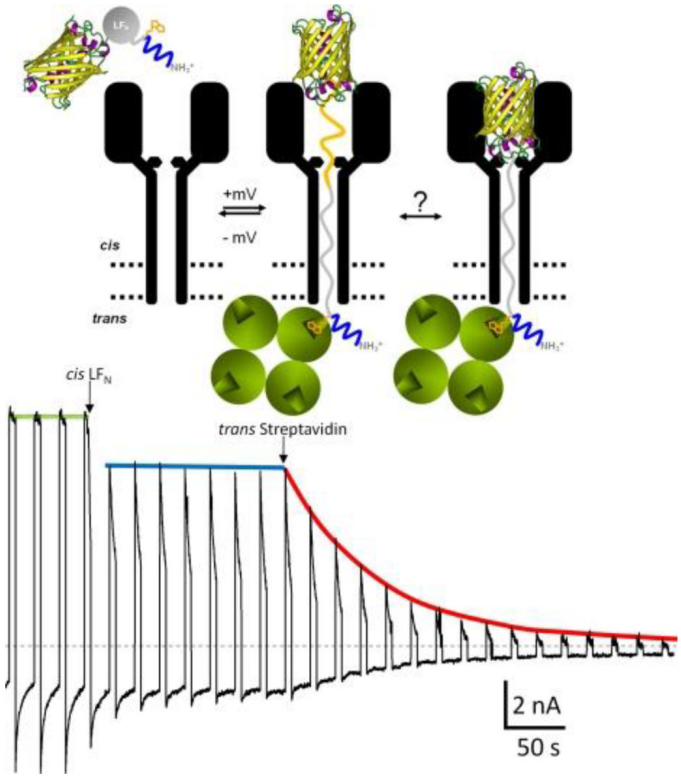

Figure 18.

Representative example of a truncated H6-LF_N construct (LF_N 1–83), whose N terminus reached the *trans* solution[47]. The N-terminal H6 tag is depicted in blue. The recording starts at the moment when an appropriate level of PA_{63}-induced current is reached and the *cis* compartment is perfused to remove the unbound $(PA_{63})_7$ from the solution. The voltage protocol of + 80 mV for 5 s and −40 mV for 15 s was then applied. At the first arrow, the LF_N (1–83), with the YFP stopper (depicted as a β barrel) attached to the C-terminus and biotin (orange) attached at residue 1, is added to the *cis* solution, and a constant level of unblocking is obtained. At the second arrow, streptavidin (four green balls) is added to the *trans* compartment. A dramatic decrease of unblocking over time is recorded, thus demonstrating that the biotin at residue 1 has reached the *trans* solution and has been grabbed by streptavidin, thereby preventing those channels from becoming unblocked at −40 mV. Reprinted with permission from ref[47]. Copyright 2011. The Rockefeller University Press.

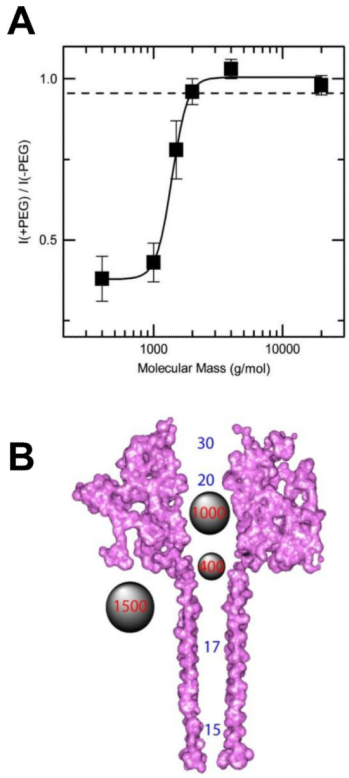

Figure 19.

A: The molecular mass cutoff of the single heptameric PA_{63} channel as estimated from the effect of differently sized PEG molecules in planar bilayers[189]. It is seen that the PEGs with MM <2000 Da are able to enter into the channel, which results in conductance decrease. The PEG concentration was 1.2% (w/w), and the applied potential was V = +70 mV. **B**: A cross-sectional view of the heptameric PA_{63} channel model[385] and spherical representations of PEG 400, 1000, and 1500 molecules. Reprinted with permission from ref[189]. Copyright 2008. Biophysical Society.

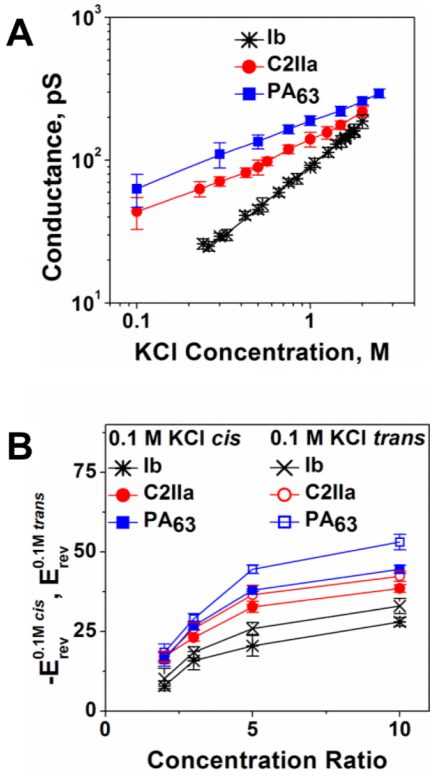

Figure 20.

A: Conductances of the PA_{63}, C2IIa, and Ib channels as functions of salt concentrations demonstrate different behaviors at small salts. The dependences are close to linear for Ib but show significant deviations from linearity for the PA_{63} and C2IIa channels. **B**: Single channel reversal potentials as functions of the ratio of salt concentrations on the different sides of the membrane for two series of measurements with oppositely directed gradients. *Open circles*: Reversal potential (E_{rev}) obtained in the series of experiments where KCl concentration in the *cis* compartment exceeds that in the *trans* compartment; at that c_{trans} = 0.1 M KCl. *Solid circles*: The values of the reversal potential ($-E_{rev}$) obtained for the reversed gradient $c_{trans} > c_{cis}$ = 0.1 M KCl. The sign of the reversal potential is inverted in the latter case to facilitate comparison; the selectivity stays cationic in both cases. The channels are asymmetric because the absolute value of the reversal potential is greater when the more concentrated solution is on the *cis* side of the membrane. Membranes were formed from the DPhPC at pH 6.

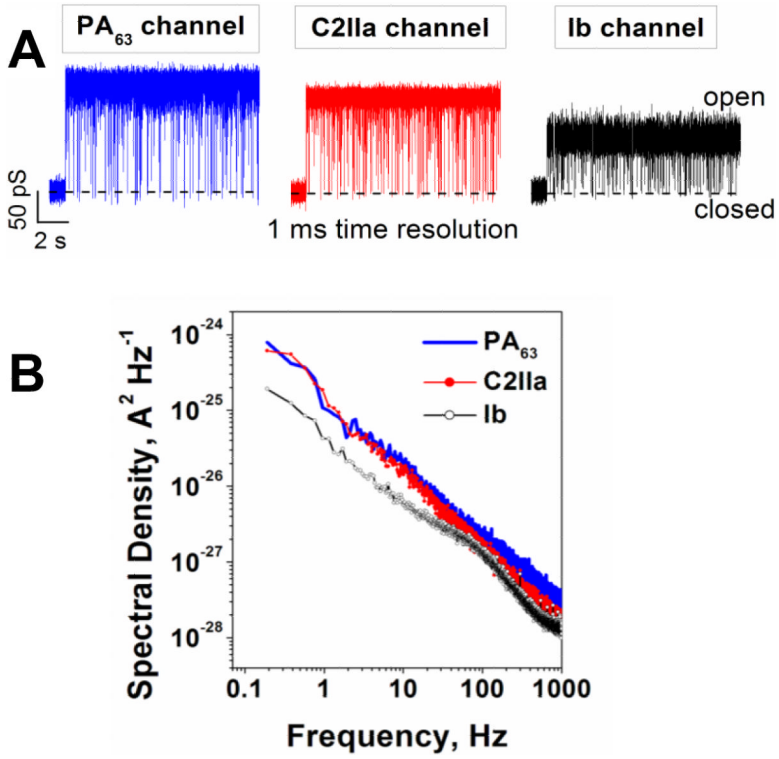

Figure 21.

A: In the absence of blockers, ion currents through the PA_{63}, C2IIa, and Ib single channels reconstituted into planar lipid membranes demonstrate fast flickering between the open and closed states. The currents are given at 1 ms time resolution. **B**: Power spectral densities of the currents shown in panel A display 1/*f* behavior. Measurements were taken in 1 M KCl solutions at pH 6 buffered by 5 mM MES. The applied voltage was 50 mV.

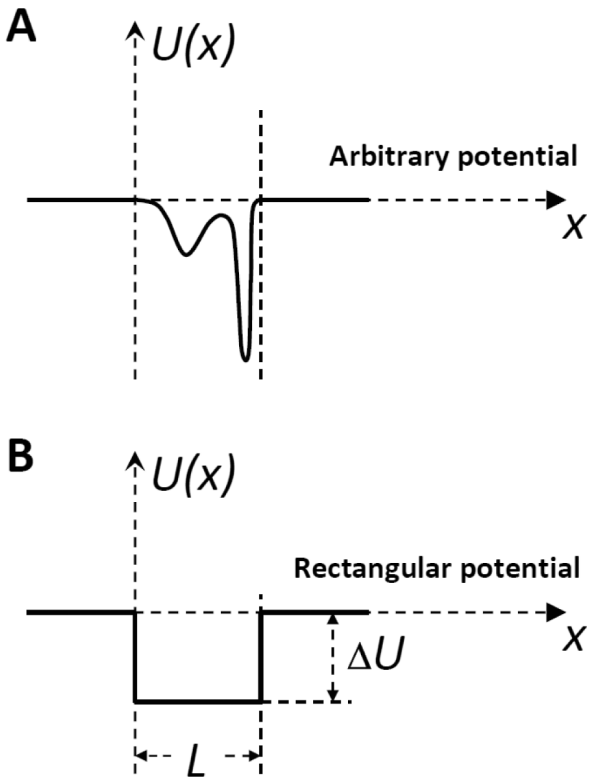

Figure 22.
Schematic view of the particle's potential of mean force in a membrane channel. **A**: An arbitrary potential demonstrating different level of interaction with different parts of the channel along its axis (*x* coordinate). **B**: A hypothetical square-well potential.

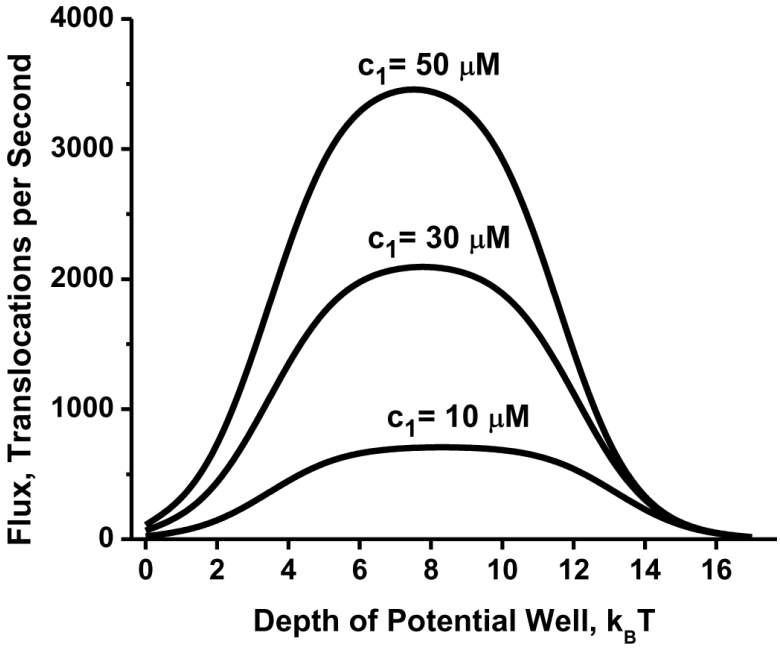

Figure 23.

Non-monotonic behavior of the flux given by Eq. (6) as a function of potential well depth at three different concentrations of translocating molecules and = 0. Reprinted with c_2 permission from ref[441]. Copyright 2005. Biophysical Society.

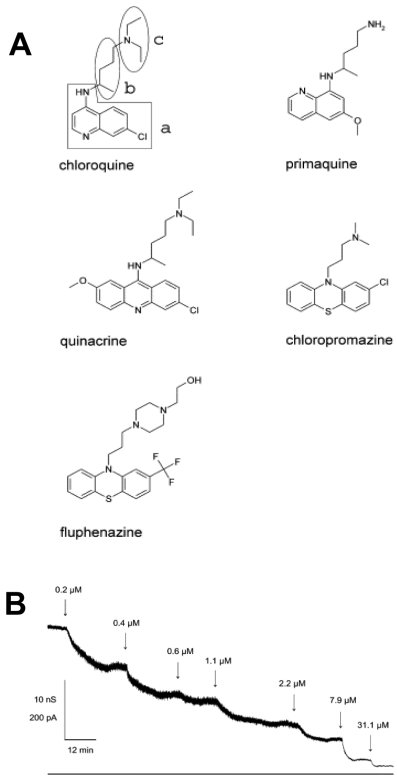

Figure 24.

A: Structures of chloroquine and related compounds, which are able to block channel-forming B components of the binary toxins in the planar bilayers. **B**: Titration of membrane conductance induced by C2II with fluphenazine in 1 M KCl at the applied voltage of 20 mV. Reprinted with permission from ref[416]. Copyright 2003. Elsevier.

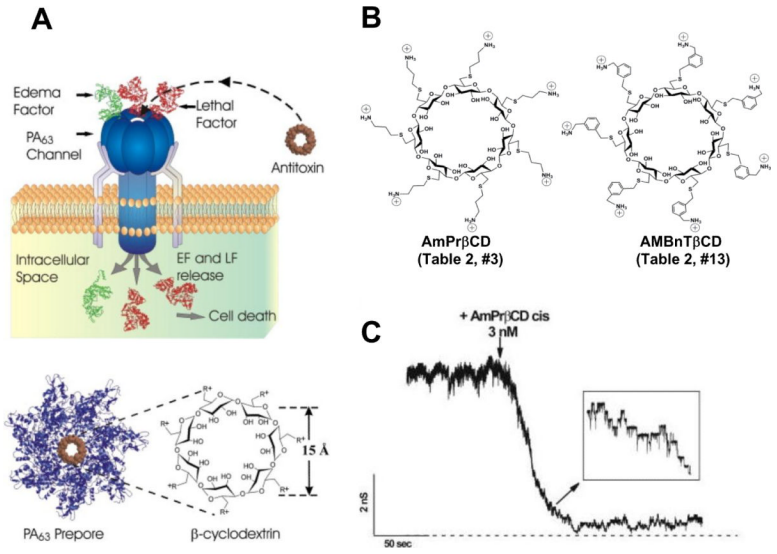

Figure 25.

A, top: Blocking anthrax on a single-channel level. A heptameric mushroom-like channel of PA_{63} produced by *Bacillus anthracis* believed to be a translocation pathway for lethal and edema factor, LF and EF, inside the cell under attack. The idea is to design complementary heptameric low-molecular weight compounds – cationic cyclodextrins (A, *bottom*) that enter the pore and block it as molecular plugs. Note that the cartoon is a simplified illustration of the LF and EF penetration into the mammalian cell. In reality, the process is much more complex (Figs. 15 and 17). Adapted with permission from ref[57]. Copyright 2010. Ciophysical Society. **B**: Two 7-fold symmetrical synthetic molecules, per-6-S-(3-aminomethyl)thio-β-cyclodextrin (AMBnTβCD), left panel, and per-6-S-(3-amino)propylthio-β-cyclodextrin (AmPrβCD), right panel, were used as blockers of the PA_{63}, C2IIa, and Ib pores. **C**: Planar lipid bilayer membrane containing about 60 PA_{63} channels in 0.1 M KCl. The downward arrow indicates the addition of AmPrβCD to the *cis* side of the membrane (side of PA addition). The dashed line shows zero current level. Adopted with permission from ref[51]. Copyright 2005. National Academy of Sciences.

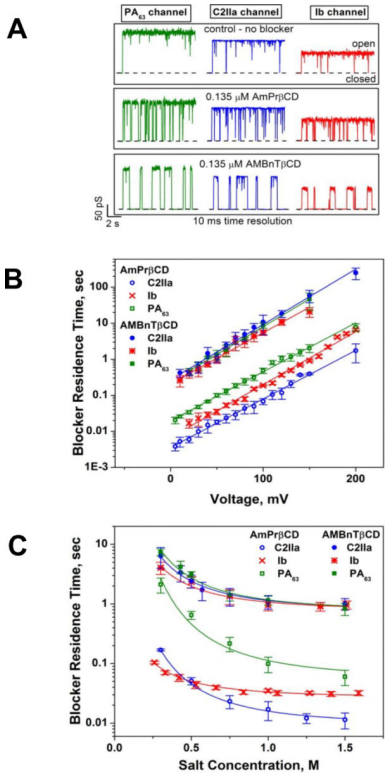

Figure 26.

A: Ion currents through single PA_{63}, C2IIa, and Ib channels in the absence (upper row of tracks) and in the presence of 0.135 μM AmPrβCD (middle row) and AMBnTβCD (bottom row) blockers in the *cis* side of the chamber. Measurements were taken in 1 M KCl solutions at pH 6 and 50 mV applied voltage. Recordings are shown at 10 ms time resolution. AMBnTβCD displays a significantly longer binding lifetime with all channels compared with AmPrβCD, whereas the time between the blockage events, characterizing the on-rate of the binding reaction, seems to be practically unchanged. **B**: Residence times of blocker binding to the channels plotted as functions of the transmembrane voltage reveal exponential voltage dependence. **C**: Residence times of blocker binding to the channels as functions of bulk salt concentration show different degrees of salt dependence for the three channels and two blockers. The salt dependence is most pronounced for AmPrβCD interacting with the PA_{63} pore. For the more efficient AMBnTβCD, the dependence is weaker.

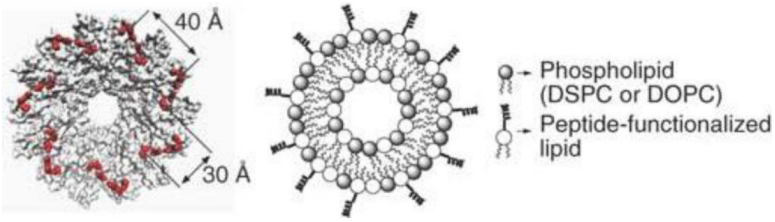

Figure 27.

Neutralization of the PA_{63} heptameric complexes by peptide-functionalized liposomes of about 50 nm in size[489]. Left: The structure of the enzyme-binding face of heptameric PA_{63}. Residues 197, 200, 207, 210 and 214, which form part of the LF-binding site, are highlighted in red. Approximate distances between residues 200 (30 Å) on adjacent monomers and residues 210 (40 Å) on adjacent monomers are indicated. Right: A schematic representation of a liposome-based anthrax toxin inhibitor. Reprinted with permission from ref[489]. Copyright 2006. Nature Publishing Group.

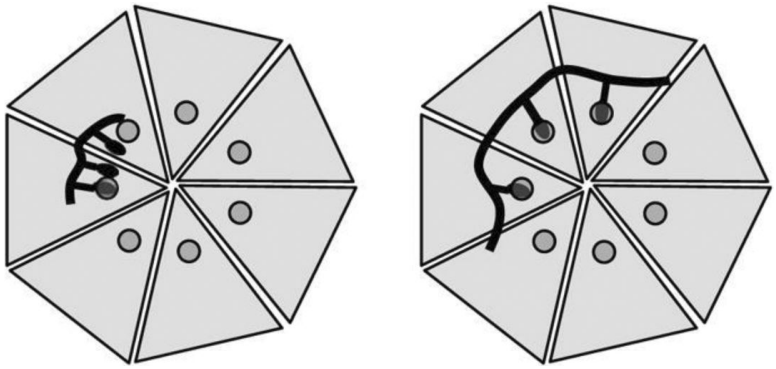

Figure 28.
Design of polyvalent inhibitors with control over the molecular weight and ligand spacing[491]. The linear polyvalent inhibitors displaying peptides (black ovals) are shown bound to the PA_{63} heptamer at the peptide-binding sites (circles). The spacing between peptides on the linear scaffold is either too short (left panel) or is sufficient (right panel) to allow a polyvalent interaction. Reprinted with permission from ref[491]. Copyright 2006. American Chemical Society.

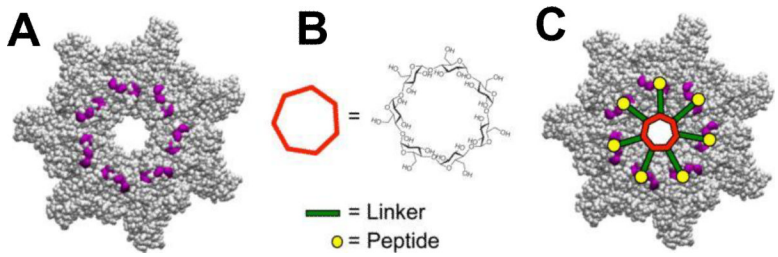

Figure 29.

Structure-based design of the heptavalent anthrax toxin inhibitors[497]. **A**: The structure of the LF-binding face of heptameric PA_{63}. Residues 184, 187, 197, and 200, which form part of the peptide-binding site are shown in purple. **B**: The structure of 7-fold symmetrical β-cyclodextrin, which was used as a scaffold for the heptameric inhibitor. **C**: A scheme illustrating the binding of a heptavalent inhibitor, synthesized by the attachment of seven inhibitory peptides to the β-cyclodextrin via an appropriate PEG linker, to heptameric PA_{63}. Reprinted with permission from ref[497]. Copyright 2011. American Chemical Society.

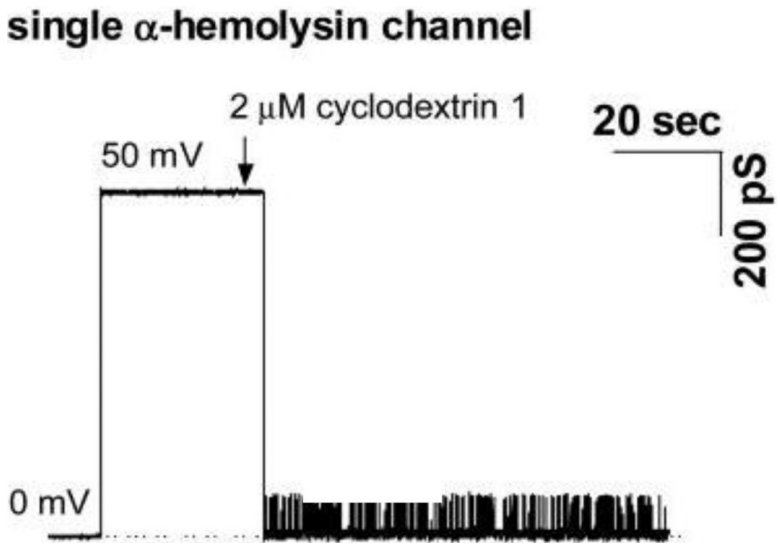

Figure 30.

Modulation of the ion current through a single α-HL channel by 7-fold symmetrical βCD IB201 (Table 2, compound 31). In the absence of βCD, the current through the single α-HL channel is rather stable (no significant current fluctuations at 10 ms time resolution are seen). IB201 addition leads the channel to switch to a weakly conductive blocked sub-state. Reprinted with permission from ref[55]. Copyright 2007. Elsevier.

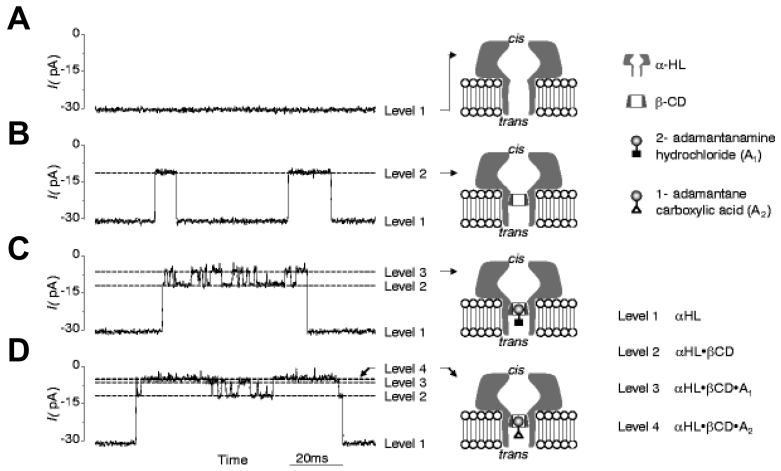

Figure 31.

Bilayer recordings showing the interaction of a single α-HL pore with βCD and the model analytes 2-adamantanamine (A1) and 1-adamantanecarboxylic acid (A2) at −40 mV applied voltage[65]. α-HL was added to the *cis* compartment of the chamber and βCD and the adamantine derivatives were in the *trans* compartment. **A**: Control, single α-HL pore is unblocked (level 1). **B**: 20 mM *trans*-addition of βCD generates transient partial blockages of the channel (level 2). **C**: 80 mM *trans*-addition of 2-adamantanamine does not affect the fully open channel (level 1), but produces an additional block of α-HL- βCD complex (level 3). **D**: 20 mM *trans*-addition of 1-adamantanecarboxylic acid produces additional blockades (level 4), of the longer duration than those produced by 2-adamantanamine (level 3). Reprinted with permission from ref[65]. Copyright 1999. Nature Publishing Group.

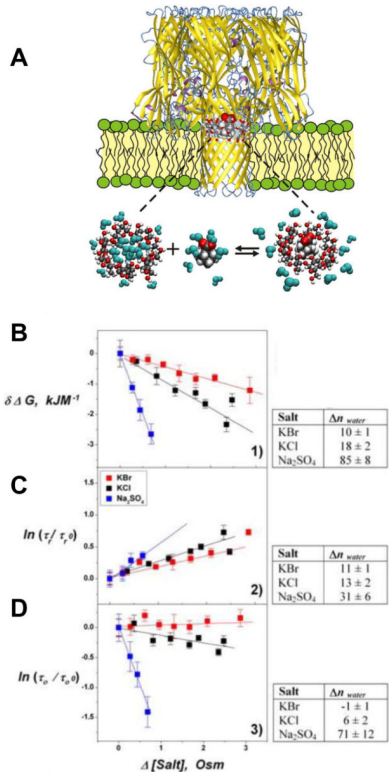

Figure 32.

The single-molecule nanopore approach illustrated in Fig. 31 was used to study the dynamic side of the Hofmeister effect[542]. **A**: Cartoon of the complexation process between the cyclodextrin hosted by the α-HL pore and adamantane carboxylate. **B**: Changes in the free energy of cyclodextrin– adamantane complexation, δΔG, versus changes in salt osmolarity. **C**: Effect of increasing osmolarity on the average residence time of adamantane in the channel-bound cyclodextrin, τ_r. **D**: Effect on the average time between the successive complexation events, τ_o. Both times are normalized by their values measured prior to extra salt addition. Tables on the right show the effective numbers of excluding water molecules. It is seen that not only the complex stability, as measured by the average adamantane residence time, but also the on-rates, represented by inverse τ_o, are influenced by salt addition and thus contribute to the changes in the complexation free energy. Reprinted with permission from ref[542]. Copyright 2009. Wiley.

Table 1

PA_{63} conductance block by small cationic compounds

#	Cationic Compounds	Structure	IC_{50}
1	Tetramethylammonium	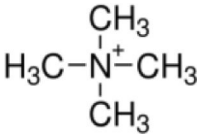	1.6 mM
2	Tetraethylammonium	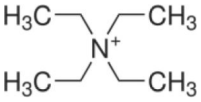	224 μM
3	Tetrapropylammonium	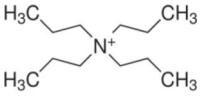	350 ± 10 nM
4	Tetrabutylammonium	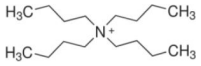	7.3 ± 0.2 μM
5	Tetrapentylammonium	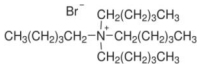	2 μM
6	Tetrahexylammonium	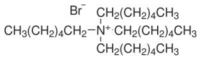	3.8 ± 0.3 μM
7	(2-acetylamino-2,2-bis-ethoxycarbonyl-ethyl)-trimethyl-ammonium	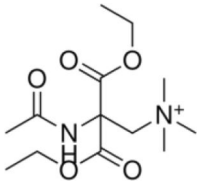	1 ± 0.1 mM
8	Tetraphenylphosphonium	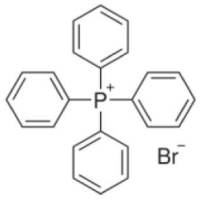	46 ± 2 nM
9	Chloroquine	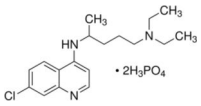	510 ± 30 nM

#	Cationic Compounds	Structure	IC_{50}
10	Quinacrine	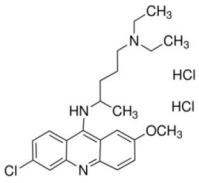	60 ± 5 nM
11	Benzyltriphenylphosphonium	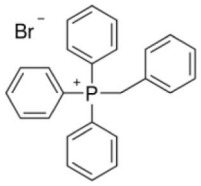	110 ± 30 nM
12	Butyltriphenylphosphonium	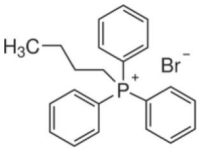	88 ± 5 nM
13	Isoamyltriphenylphosphonium	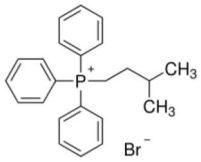	35 ± 6 nM
14	Methyltriphenylphosphonium	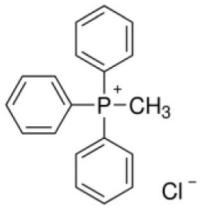	370 ± 60 nM

Table 2

PA_{63} conductance block and cytotoxicity inhibition by cationic cyclodextrins

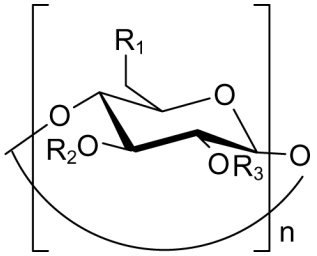

#	n	R_1	R_2, R_3	Inhibition of conductance IC_{50}, nM	Inhibition of cytotoxicity IC_{50}, μM
I. Hepta-6-aminoalkyl β-cyclodextrin derivatives [52]					
1	7	$-NH_2$	-H	140 ± 90	20 ± 9
2	7	$-S(CH_2)_2NH_2$	-H	3.5 ± 0.9	7.8 ± 2.4
3	7	$-S(CH_2)_3NH_2$	-H	0.57 ± 0.39	2.9 ± 1.0
4	7	$-S(CH_2)_4NH_2$	-H	1.1 ± 0.5	5.1 ± .2.4
5	7	$-S(CH_2)_5NH_2$	-H	3.8 ± 1.0	7.5 ± 2.4
7	7	$-S(CH_2)_6NH_2$	-H	0.97 ± 0.38	0.6 ± 0.3
8	7	$-S(CH_2)_7NH_2$	-H	4.6 ± 3.2	1.9 ± 1.1
9	7	$-S(CH_2)_8NH_2$	-H	2.4 ± 0.95	0.3 ± 0.1
10	7	$-S(CH_2)_{10}NH_2$	-H	27.0 ± 17.0	2.6 ± 0.1
II. Hepta-6-guanidinealkyl β-cyclodextrin derivatives [52]					
11	7	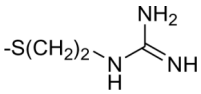	-H	5.3±3.2	8.9±6.0
12	7	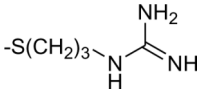	-H	12.6±9.0	12.2±2.9
III. Hepta-6-arylamine β-cyclodextrin derivative [52,62]					
13	7	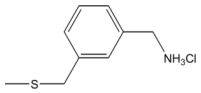	-H	0.13±0.10	0.8±0.5
IV. Cationic α- and γ cyclodextrin derivatives [62]					
14	6	$-NH_2$	-H	1200 ± 300	>100
15	8	$-NH_2$	-H	170 ± 50	12 ± 3
16	6	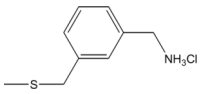	-H	29±5	45±13

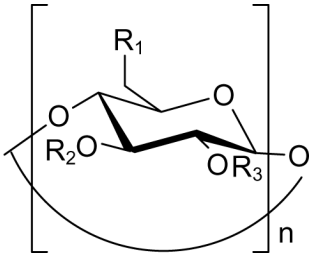

#	n	R_1	R_2, R_3	Inhibition of conductance IC_{50}, nM	Inhibition of cytotoxicity IC_{50}, μM
17	8	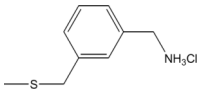	-H	2.8±1.3	5.4±0.8
V. Novel β-cydodextrin derivatives [60]					
18	7	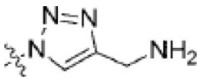	-H	n/a	>100
19	7	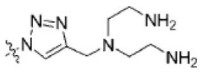	-H	n/a	>100
20	7	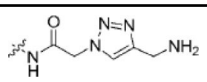	-H	n/a	>100
21	7	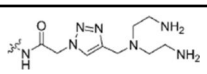	-H	n/a	>100
22	7	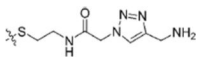	-H	n/a	>100
23	7	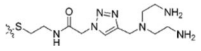	-H	n/a	>100
24	7	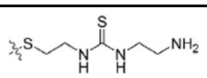	-H	n/a	26 ± 21
25	7	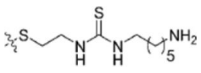	-H	n/a	3.2 ± 1.9
26	7	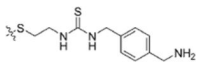	-H	n/a	20 ± 14
27	7	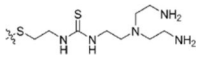	-H	n/a	>100
28	7	-H	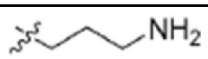	n/a	4.1 ± 0.4

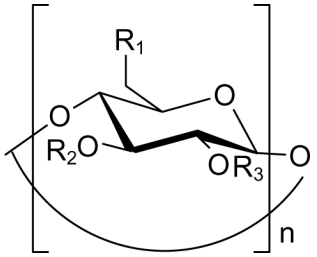

#	n	R_1	R_2, R_3	Inhibition of conductance IC_{50}, nM	Inhibition of cytotoxicity IC_{50}, μM
29	7	-H	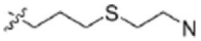	n/a	2.1 ± 0.2
VI. α-, β-, and γ-cyclodextrin derivatives tested against α-hemolysin [62]					
30	6	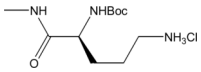	-H	>5000	>100
31	7	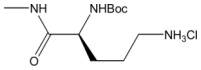	-H	~50	3.3±2.3
32	8	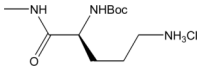	-H	>5000	>100

TABLE 3

Some of the most potent non-peptide blockers of classical ion-selective channels

Channel	Compound	IC_{50}	Comments
Potassium, $K_V4.3$	Nicotine	34 nM	ref.[597]*
Potassium, $K_V11.1$	Astemizole	48 nM	ref.[598]*
Potassium, $K_V11.3$	Sertindole	43 nM	ref.[599]*
Sodium, $Na_V1.1$	Tetrodotoxin	6 nM	ref.[527,600]
Sodium, $Na_V1.6$	Tetrodotoxin	1 nM	ref. [527,601]
Calcium, $Ca_V1.2$	Devapamil	50 nM	ref.[528,602]
Inwardly Rectifying Potassium, $K_{ir}2.1$	Spermine	0.9 nM	ref.[534,603]
Calcium-Activated Potassium, $K_{Ca}1.1$	Paxilline	1.9 nM	ref.[532,604]
Calcium-Activated Potassium, $K_{Ca}2.1$	UCL1684	0.8 nM	ref.[532,605]
Calcium-Activated Potassium, $K_{Ca}2.2$	UCL1684	0.28 nM	ref.[532,606]

*Additional information can be found in a recent review[533]; however, it has to be used with caution as is contains a number of confusing misprints. The original papers cited there should be consulted to avoid misleading conclusions.